ASPECTS OF THE ATMOSPHERIC ENERGY BUDGET OVER SOUTH-EAST AUSTRALIA

by

T.L. Hart B.Sc. (Hons.)

submitted in fulfilment of the requirements for the degree of

Master of Science

UNIVERSITY OF TASMANIA

HOBART

May 1981

I declare that this thesis contains no material which has been accepted for the award of any other degree or diploma in any university, and that, to the best of my knowledge and belief, this thesis contains no copy or paraphrase of material previously published or written by any other person, except when due reference is made in the text of the thesis.

(T.L. Hart)

May, 1981

CONTENTS

Page

ABSTRACT

LIST OF RECURRING SYMBOLS

CHAPTER

1. INTRODUCTION 1

2. REVIEW : THE EARTH-ATMOSPHERE ENERGY BUDGET

2.1 The global scale earth-atmosphere energy budget

2.1.1 Energy budget of an atmospheric column 3
2.1.2 Energy storage 7
2.1.3 Atmospheric energy flux 10
2.1.4 Net radiant flux at the top of the atmosphere 13
2.1.5 Overall energy balance 18

2.2 Regional scale energy budget studies

2.2.1 Tropical studies 19
2.2.2 Mid-high latitude studies 22
2.2.3 Water vapour budget studies 25

3. ANALYSIS METHODS AND RESULTS

3.1 Data sources and quality

3.1.1 Data sources 27
3.1.2 Data quality 28

3.2 Method

3.2.1 Evaluation of energy fluxes 36
3.2.2 Evaluation of flux divergences 38
3.2.3 Treatment of water vapour measurements 39
3.2.4 Adjustment of wind data for mass balance 44

3.3 Results

3.3.1 Satellite radiation observations 48
3.3.2 Atmospheric and ground storage 53
3.3.3 Energy fluxes and flux divergence 56
3.3.4 Sampling errors 72

4. DISCUSSION

4.1 Synoptic situations and their relation to the measured energy fluxes 79

4.2 Contribution of the various energy types to the overall flux and flux divergence

4.2.1 Total Flux 85
4.2.2 Eddy Flux 86
4.2.3 Flux Divergence 88

4.3 Vertical profiles of flux and flux divergence 91

4.4 Comparison of measured fluxes and flux divergences with zonal averages 94

Page

CHAPTER

5. CONCLUSIONS 98

ACKNOWLEDGEMENTS

REFERENCES

APPENDICES

A1. Energy budget equations for the atmosphere

A2. Further details on procedures for the mass balance adjustment

LIST OF RECURRING SYMBOLS

Roman small letters		Units
C_p	specific heat of air at constant pressure	$J\ Kg^{-1}\ K^{-1}$
C_s	specific heat of soil	
C_v	specific heat of air at constant volume	
g	acceleration due to gravity	$m\ s^{-2}$
i	unit vector directed eastwards	
j	unit vector directed northwards	
l	length	m
$\underline{n}$	unit vector normal to a given line	
p	atmospheric pressure	mb
q	specific humidity/mixing ratio	$g\ Kg^{-1}$
r	correlation coefficient	
s	distance	m
t	time	s
u	zonal velocity component, positive eastwards	$m\ s^{-1}$
v	meridional velocity component, positive northwards	$m\ s^{-1}$
x	distance measured in east-west direction, positive eastwards	m
y	distance measured in north-south direction, positive northwards	m
z	distance measured vertically	m

Roman capital letters		
A	area	m^2
D	frictional force per unit mass	$m\ s^{-2}$
F	energy flux	$W\ m\ Kg^{-1}/W\ m^{-1}$
F_H	sensible energy flux	
F_O	oceanic energy flux	
F_Q	latent energy flux	
I	enthalpy ($= C_p T$)	$J\ Kg^{-1}$
K	kinetic energy per unit mass	$J\ Kg^{-1}$

L	latent heat of vaporisation	$J\ Kg^{-1}$
P	pressure of a given level in the atmosphere	mb
	period of oscillation	s
Q_D	rate of energy supplied non-adiabatically	$W/W\ Kg^{-1}/W\ m^{-2}$
Q_E	rate of energy supplied by latent heat transfer	
Q_H	rate of energy supplied by sensible heat transfer	
Q_R	rate of energy supplied by rainfall	
Q^*	net radiant flux (density)	
$Q\downarrow$	absorbed short wave radiant flux (density)	
$Q\uparrow$	outgoing long-wave radiative flux (density)	
R	gas constant	$286\ J\ Kg^{-1}\ K^{-1}$
S	rate of energy storage	$W/W\ m^{-2}$
	solar constant	$1360\ W\ m^{-2}$
T	temperature	K
$\underline{V}$	velocity	$m\ s^{-1}$

Greek capital letters

Φ	geopotential energy per unit mass	$J\ Kg^{-1}$

Greek small letters

$\alpha\ (= {}^1/\rho)$	specific volume	$m^3\ Kg^{-1}$
α	albedo	
λ	thermal conductivity	$W\ m^{-1}\ K^{-1}$
ρ	density	$Kg\ m^{-3}$
σ	a closed line enclosing a given area	
ω	vertical velocity in pressure co-ordinates	$mb\ s^{-1}$

Subscripts

A	atmosphere
BA	bottom of the atmosphere (surface)
G	ground
H	sensible energy
O	ocean
Q	latent energy

TA	top of the atmosphere
s	soil

Abbreviations

NEA	Newell et al. (1974) (see list of references)
NOAA/NESS	National Oceanic and Atmospheric Administration/National Environmental Satellite Service
OR	Oort and Rasmusson (1971) (see list of references)

ABSTRACT

This study presents measurements of the atmospheric energy fluxes over south-east Australia and discusses the role of these fluxes and their divergence in the regional scale atmospheric energy budget.

Monthly averages of quasi-horizontal energy fluxes were calculated from daily observations at six upper air stations for the period 1974-1976. The relative contributions of the mean and eddy fluxes were considered.

Energy flux divergences were computed for four months of 1975 and compared with independent estimates derived from (a) satellite radiant flux data (in the case of the overall energy flux divergence), and (b) a regional moisture budget (for the latent energy term). Adjustments of the raw wind data to ensure mass balance were found to be necessary and objective techniques for this purpose are discussed. Although exact balance of the energy budget was not obtained, the contribution of the different energy types (enthalpy, potential, latent, kinetic) consistently showed counteraction among the various terms and between their mean and eddy resolutions. For each of the four months considered, the total energy flux divergence showed zonal convergence and meridional divergence. Vertical profiles of the energy flux divergence are also presented.

The net radiant flux density at the top of the atmosphere, closely related to the atmospheric energy flux divergence over the region, showed small interannual variations. Analysis of the short and long wave satellite radiation data showed that these variations, due mainly to changes in cloudiness, were dominated by the fluctuations in the short wave term.

The relation between the surface synoptic weather pattern and atmospheric energy transport was investigated by correlating the monthly average mean and eddy fluxes with the frequency of different wind

directions and isobaric curvatures. Useful relations were found except for the zonal eddy flux. The meridional fluxes were most closely related to the frequency of northerly surface winds over the region.

The study incorporates a review of the global scale earth-atmosphere energy budget and also of other regional scale investigations. Some differences between results for south-east Australia and the zonal average are noted.

CHAPTER 1

INTRODUCTION

The net poleward energy transport by the atmospheric general circulation has been the subject of several major observational studies, but increasing attention is also being given to longitudinal variations. It is now possible to combine satellite data with aerological observations in investigations into the atmospheric energy flows of regional scale weather systems. The present study uses this combination to investigate monthly averages of the atmospheric energy flux and flux divergence over south-eastern Australia during a three year period.

For considerations of the energy budget of the earth-atmosphere system the only significant source of energy is solar radiation, and on a climatic time scale the inward flux of solar radiation is almost, and perhaps exactly, balanced by the radiation reflected and emitted from the earth-atmosphere system. However not all points on the earth's surface or in the atmosphere are themselves in radiation balance. Almost all of the atmosphere suffers a net radiative loss, but at the earth's surface a radiative surplus in equatorial regions gives way to a deficit in polar regions. This differential heating, with a radiative surplus in warmer regions and a deficit in the cooler regions, maintains available potential energy which drives the atmospheric and oceanic circulations. These circulations transport energy on average from the earth's surface to the atmosphere (principally in the form of latent heat due to evaporation but also as sensible heat) and from atmospheric regions of total energy surplus to those experiencing a deficit. The flow of energy within the atmosphere is simultaneously a cause and a result of the "weather" and moderates the temperatures that would occur if all parts of the earth had a locally balanced radiative budget.

Although the terms of the earth's radiation budget and the consequent poleward energy flow were first evaluated by Sir George Simpson in 1928, the past thirty years have produced a series of studies on the global scale using the increased network of aerological stations. The most complete of these observational studies of the atmospheric general circulation are those of Oort and Rasmusson (1971) for the Northern Hemisphere and of Newell et al (1972, 1974) which were concerned principally with the tropics. No equally extensive studies have been made for the whole of the Southern Hemisphere, due mainly to data scarcity.

During the 1960's photographic and radiometric data from satellites provided independent and authoritative measurements of the radiative properties of the earth-atmospheric system. In some cases these determinations differed significantly from pre-satellite estimates. For example, Vonder Haar and Suomi (1971) reported an observed mean planetary albedo of 0.29 compared with the earlier theoretical estimate of 0.35. Most of the error was due to an overestimate of tropical cloudiness. The new results suggest a greater absorption of solar radiation in the tropical oceans with a consequent increase in the required oceanic energy flow.

Studies based on both aerological and satellite data have revealed significant regional scale variations. Newell et al (1972, 1974) demonstrated marked longitudinal variations in many of the fluxes and, in their conclusions, anticipated studies on the regional scale based on and adding to their findings on the general circulation scale. Vonder Haar (1972), making use of the early satellite data, noted that in the case of the annual average of net radiation at the top of the atmosphere "the magnitude of intrazonal net radiation gradients is as strong in some sectors as the more well-known north-south gradients", and he suggested that intrazonal circulations may arise. His results

show a strong gradient of net radiation between a maximum over the Bay of Bengal and a minimum over eastern Australia.

Further investigation of such regional scale variations has been facilitated by the fact that radiation measurements are now available from satellites on a routine basis. High resolution radiometric observations have been made by the NOAA series of near-polar orbiting satellites since June 1974. One of the stated aims of the NIMBUS 6 Earth Radiation Budget Experiment was "to provide direct measurements of the radiation budget on regional scales (500km) on a monthly basis, for climate monitoring and prediction." (Smith et al, 1977). A study of the Asian summer monsoon has been made based on the NOAA data (Winston and Krueger, 1977). Further studies on this scale should assist in the formulation of theories on the atmospheric energy flux and in the development and validation of numerical climate models.

Holopainen (1977) uses satellite net radiant flux data to show that there must be a net energy transport in the atmosphere from the oceans to the continents, but recognizes that more needs to be known about the net radiation than simply its magnitude. He concludes:

> "An important future investigation must be to study on the basis of aerological observations, in what form and by what mechanism this net energy transport is accomplished. This kind of study would seem particularly interesting and feasible for the Australian area which, in the light of satellite observations is an anomalous region and has a good network of aerological stations".

Concern with regional scale variations provides the motivation for the present study. The atmospheric energy budget over South Eastern Australia is considered for the three year period 1974-1976, by combining satellite observations of net radiation at the top of the atmosphere with determinations of the energy flux within the atmosphere using aerological observations. The objectives of the study are:

1. The calculation of the monthly averages of the atmospheric flux components at individual stations for the three year period.

2. To calculate the total energy flux divergence, using satellite net radiant flux measurements as verification and to assess the relative contributions of

   (a) the mean and eddy fluxes

   (b) the zonal and meridional fluxes, and

   (c) the individual energy types (sensible, latent) to the regional energy budget.

3. To consider variations of the fluxes and radiation components in relation to the prevailing synoptic weather patterns.

Chapter 2 gives a brief review of energy budget measurements on the global and regional scales. In Chapter 3 an outline is given of the method employed in the research together with the results obtained. The results are discussed further in Chapter 4 and conclusions are presented in Chapter 5.

CHAPTER II
REVIEW
THE EARTH-ATMOSPHERE ENERGY BUDGET

2.1 *The Global Scale Earth-Atmosphere Energy Budget*

Comprehensive reviews of the atmospheric energy budget are given by Lorenz (1967) and Newell et al. (1969), while the studies of Newell et al. (1972, 1974) and Oort and Rasmusson (1971) present detailed analyses of the energy transport by the general circulation of the atmosphere. Investigations of the energy budget using satellite data (e.g. Oort and Vonder Haar, 1976) provide a useful check on such studies.

Recent estimates of the terms involved in the global scale energy budget are discussed briefly in this section, based mainly on the results presented by Newell et al. (1974) and Oort and Rasmusson (1971) hereafter referred to as NEA and OR respectively.

2.1.1 *Energy Budget of an Atmospheric Column*

The energy equations for an earth-atmosphere column are derived in Appendix A1, and for a column extending from the top of the atmosphere to below the level at which significant energy exchanges occur, can be written symbolically (Eq. A1.14) as

$$Q^*_{TA} = \nabla.(F_A + F_O) + S_A + S_G + S_O \qquad \ldots (2.1)$$

where Q^*_{TA} is the net radiant flux at the top of the atmosphere, F_A is the vertically integrated energy flux (sensible and latent energy) in the atmosphere, F_O is the oceanic energy flux and S_A, S_O and S_G represent the rate of energy storage in the atmosphere, ocean and ground respectively. The flux of sensible energy includes the enthalpy (= CpT), potential energy and kinetic energy terms (see Appendix A1). The budget of Eq. 2.1 is shown schematically

in Fig. 2.1. The energy flux terms involve covariances of the form $\overline{vh}$ where v represents a velocity component, h some atmospheric or oceanic property, and the overbar denotes a time average. Such terms are called the average total transfer of the property h.

Expressing v and h in terms of their mean and a deviation (denoted by a prime)

$$v = \bar{v} + v' \qquad h = \bar{h} + h' \qquad \ldots (2.2)$$

then $$\overline{vh} = \overline{(\bar{v} + v')\ (\bar{h} + h')}$$

$$= \bar{v}\bar{h} + \overline{v'\ h'} \qquad \ldots (2.3)$$

By definition $\bar{v}'$ is zero. The first term on the right side $\bar{v}\bar{h}$ is called the mean transfer and $\overline{v'\ h'}$ the transient eddy term.

For energy budget studies on a global scale zonal averages are often considered. Denoting the zonal averages of A and its deviation from the zonal average by [A] and A^* respectively, the average total transfer can be expanded as:

$$[\overline{vh}] = [\bar{v}]\,[\bar{h}] + [\,\bar{v}^*\,\bar{h}^*\,] + [\overline{v'h'}] \qquad \ldots (2.4)$$

The terms on the right hand side represent the transport by the mean motion, standing eddies and transient eddies respectively.

Rasmusson (1972) stresses that the transient eddy terms represent contributions from the entire temporal spectrum between the response time of the radiosonde and the period over which the data are averaged. Annual averages include seasonal variations as transient eddies, while in averages over more than one year inter-annual variations would also contribute.

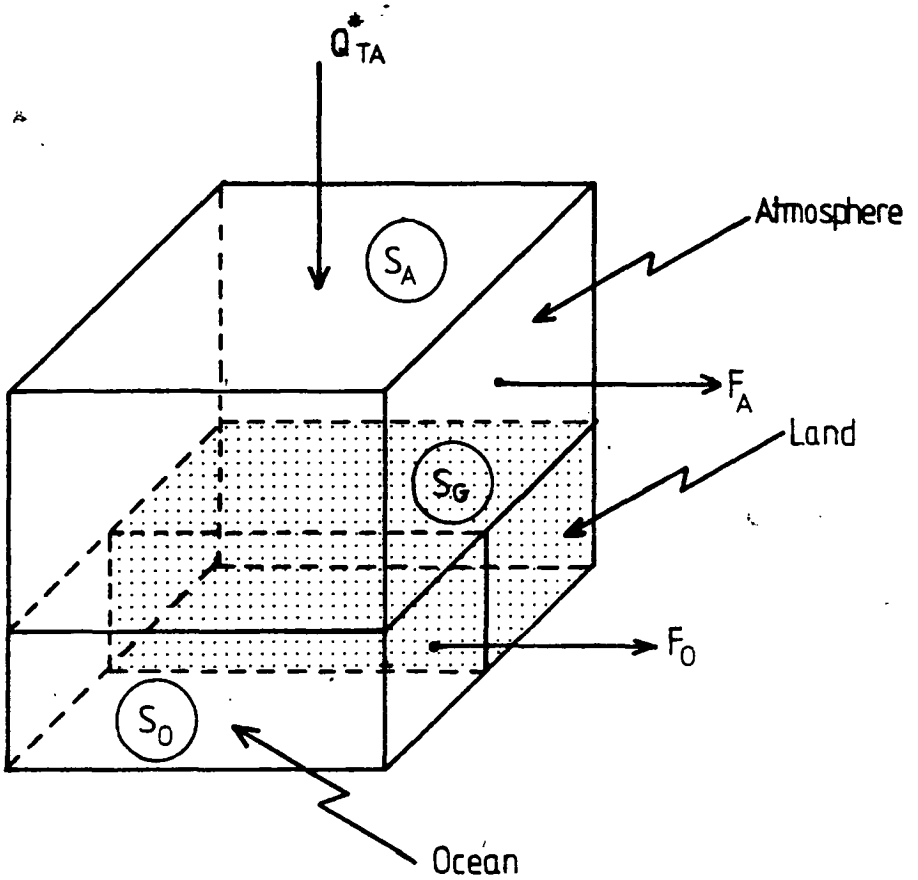

Fig. 2.1 Schematic representation of the energy budget in an earth–atmosphere column. Q^*_{TA} represents the net radiant flux at the top of the atmosphere, F_A the vertically integrated energy flux (sensible and latent) in the atmosphere, F_O the vertically integrated oceanic flux and S_A, S_G and S_O the rates of energy storage in the atmosphere, ground and ocean respectively.

2.1.2 Energy Storage

(a) Energy Storage in the Atmosphere

Rates of energy in the atmosphere as a function of latitude and season are listed in Table 2.1 using the northern hemisphere results of Oort and Vonder Haar (1976) and the global value as presented by NEA. The storage rates show a maximum exceeding 20 W m^{-2} in high latitudes during late spring and a minimum below -20 W m^{-2} in early autumn. The two sets of values show the same basic pattern but there are significant differences particularly at high latitudes. This may be due to the more detailed calculations of Oort and Vonder Haar. Contributions to the total storage from individual energy terms are discussed by Oort (1971).

(b) Heat Storage in Land

The rate of heat storage (S_G) in the land is dealt with in standard texts such as Sellers (1965) and Monteith (1973). A brief summary is given in Appendix A1. The values used by NEA in their global energy budget study are listed in Table 2.1. These values have been weighted by the percentage of land in each latitude zone giving low values in the southern hemisphere due to the large fraction of the surface that is ocean. Even in the northern hemisphere the rate of energy storage in the land has a smaller amplitude than that for the atmosphere. The atmospheric and land storage terms also differ in phase, with the land values having their greatest magnitude in summer and winter.

Table 2.1

Rate of Energy Storage in the Atmosphere (S_A) and Land (S_G) ($W\ m^{-2}$)

Latitude	December - February			March - May			June - August			September - November		
	S_A (1)	S_A (2)	S_G	S_A (1)	S_A (2)	S_G	S_A (1)	S_A (2)	S_G	S_A (1)	S_A (2)	S_G
80-90°N	-4	-3	0	11	19	0	5	2	1	-11	-18	0
70-80	-5	-3	-2	12	19	1	6	2	2	-13	-18	-1
60-70	-5	-2	-3	14	17	1	7	3	3	-16	-19	-2
50-60	-6	-2	-3	16	15	1	7	4	3	-17	-18	-1
40-50	-5	-3	-2	15	15	1	7	5	3	-16	-18	-1
30-40	-4	-3	-2	11	13	1	6	6	2	-13	-16	-1
20-30	-3	-2	-1	8	10	1	4	4	1	- 9	-11	-1
10-20	-2	-2	-1	4	5	0	2	1	1	- 4	- 5	0
0-10	-1	-1	0	1	2	0	0	-1	0	0	1	0
0-10°S	1		0	- 2		0	-1		0	2		0
10-20	3		0	- 6		0	-2		0	5		0
20-30	4		0	-11		-1	-2		-1	7		0
30-40	5		0	-12		0	-1		0	9		0
40-50	4		0	-10		0	-1		0	8		0
50-60	4		0	-10		0	-1		0	7		0
60-70	5		0	-14		-1	-2		-1	11		0
70-80	7		1	-19		-1	-2		-2	14		1
80-90	8		2	-21		-2	-3		-2	16		1
Northern Hemisphere	-4	-2	-1.5	10	10	0.5	5	3	2	-11	-11	-1
Southern Hemisphere	4		0.5	-12		-0.5	-2		-1	9		0
Globe	0		-0.5	- 1		0	1.5		0.5	- 1		-0.5
Globe (3)	0.5			1.5			0.5			-2.5		

References: (1) Newell et al. (1974)
(2) Oort and Vonder Haar (1976)
(3) Ellis et al. (1978)

(c) Heat Storage in the Ocean

The rate of heat storage in oceans can be calculated from sea surface temperature data using the same approach as for storage in land. NEA briefly review early efforts at evaluating this term but express strong reservations about the accuracy of the estimates.

Ellis et al (1978) and Oort and Vonder Haar (1976) present estimates based on oceanographic soundings to a depth of 275 metres, below which temperature variations were small. The main energy storage was found to occur in the first 100 metres. Details of the analysis are described by Levitus and Oort (1977). Sampling problems were encountered with considerable areas of sparse data in the southern hemisphere. The results of Oort and Vonder Haar for the northern hemisphere are shown in Fig. 2.2. In mid-latitudes the values agree reasonably well with those of NEA but significant differences are revealed in the tropical oceans, with the more recent results showing a more pronounced annual variation. There are also large differences near the North Pole, but the values for that region are considered unreliable due to scarcity of data.

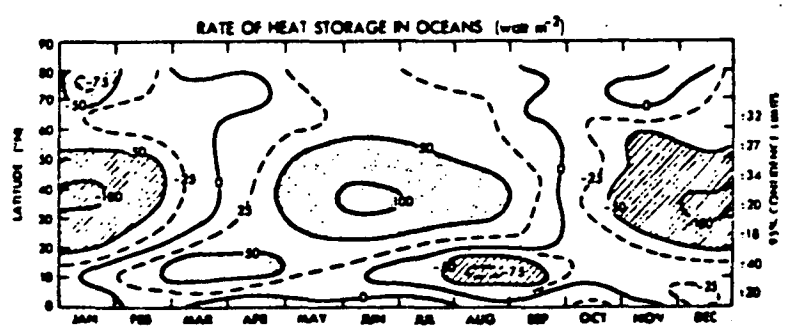

Fig. 2.2 Rate of heat storage in the northern hemisphere oceans as a function of latitude and month of year. Units are W m^{-2}. To obtain typical oceanic values divide by the percentage of the horizontal area covered by oceans (61 per cent for the northern hemisphere as a whole). (After Oort and Vonder Haar, 1976).

Comparison with Table 2.1 shows that the heat storage in the ocean is nearly an order of magnitude greater than in the land or atmosphere. The highest oceanic values occur in mid-latitudes and have an amplitude exceeding 100 W m^{-2}. Oort and Vonder Haar point out that most of the northern hemisphere storage occurs east of North America over the Gulf Stream region and east of Asia over the Kuroshio area.

2.1.3 Atmospheric Energy Flux

The studies of OR and NEA concentrate mainly on horizontal transports although also considering vertical fluxes. OR used once daily (00 GMT) observations between the surface and 75mb from about 700 northern hemisphere stations for the five year period May 1958 to April 1963. The data were objectively analysed and grid point values extracted.

NEA used data from 330 tropical radiosonde and radar wind stations for the period July 1957 to December 1964 with supplementary extratropical data. Most analyses were carried out subjectively.

OR present results for the northern hemisphere of the mean and eddy poleward fluxes of enthalpy, potential energy, latent energy and kinetic energy. For the mean fluxes the individual terms, especially the potential energy and enthalpy fluxes, are large in magnitude but partially compensate so that the total transport is much smaller than the individual terms. The mean transport in the tropics (Hadley Cell) is smaller than the eddy transport of mid-latitudes. The sign of the transport at low latitudes is determined by the potential energy transport. Oort (1971) describes the processes that transform latent energy into potential energy through condensation and upward vertical motion in the inter-tropical convergence zone (ITCZ). The conversion of potential to internal energy takes place in the subsiding air of the sub-tropical ridge.

The minor role of eddies in the horizontal energy transport of the tropics reflects the uniformity of the temperature and moisture fields in the region rather than the absence of eddies. Eddy transfer of potential energy is small due to the almost geostrophic nature of observed winds outside the tropics.

The results of OR, while confirming the findings of earlier studies that the maximum flux of sensible energy occurs in winter and that it is accomplished mainly by large scale eddies, also found that at mid-latitudes the standing eddies had a greater effect in mid-winter than the transient waves. Vertical cross-sections of the poleward energy transport by eddies show two maxima, one at about 850mb and the other near the tropopause at about 200mb.

The eddy flux of latent energy is an important term in the overall budget especially between 20 and 40^{o}N where, in some months, due to the strong standing eddy term associated with the Asian monsoon, it exceeds the eddy sensible energy flux. However, Rasmusson (1972) cautions that the latent energy flux measurements are likely to have significant errors due to limited vertical sampling in routinely available radiosonde reports. The kinetic energy flux is very small relative to the other terms. Oort (1971) found that the annual cycle in the standing waves contributes about 15 per cent of the annual poleward energy transport by the standing eddies but inter-annual variability did not contribute significantly to the eddy fluxes for the northern hemisphere. Inter-annual variations in latent energy flux have been discussed more recently by Rosen et al. (1979).

The divergence of the atmospheric flux ($\nabla.F_A$ in Eq. 2.1) over the northern hemisphere taken from Oort and Vonder Haar (1976) is presented in Fig. 2.3. There is a region of energy convergence in polar latitudes with a smaller region of weak convergence at about 15^{o}N in the first eight months of the year. A zone of strong divergence persists in the sub-tropical latitudes of 20-30^{o}N with a secondary area

of divergence in the 40-50° belt between late autumn and early spring. The values differ slightly from divergences calculated using the flux estimates of OR, particularly for winter where the results of OR indicate only a single area of divergence at low latitudes giving way to convergence at high latitudes.

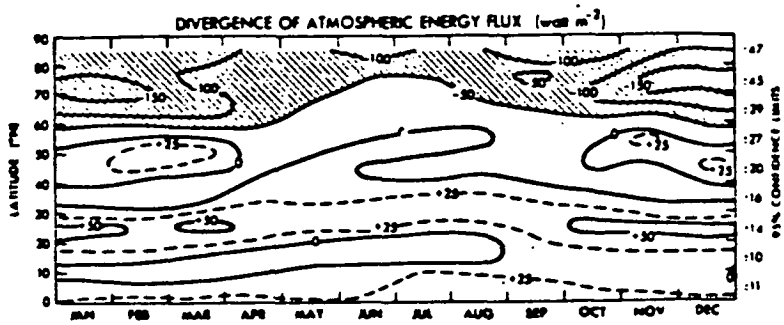

Fig. 2.3 Atmospheric energy flux divergence based on radiosonde data as a function of latitude and month of the year for the northern hemisphere. Units are W m^{-2}. (After Oort and Vonder Haar, 1976).

OR concentrated almost exclusively on the northern hemisphere due to the paucity of data in the southern hemisphere, but some results to 40°S are presented by NEA. These reveal significant differences between the fluxes at similar latitudes in each hemisphere. Comparison of the two sets of results also indicates a degree of uncertainty in the flux estimates as there are considerable differences in areas where the results overlap, especially for the mean fluxes. While these discrepancies may reflect real differences between the two periods studied, they may also be due to different analysis techniques or inadequate data fields. Oort (1978) concludes from a numerical simulation study in which some data were omitted that the present network is inadequate for the determination of atmospheric transports. He found that although the transient eddy terms were well-defined in both hemispheres, the standing eddy terms were significantly in error in the northern hemisphere and highly unreliable, although a minor term, in the southern hemisphere.

The accuracy of the results presented by both NEA and OR has also been questioned by Mak (1978) as a result of his estimates of the northern hemisphere standing eddy momentum flux at 500mb. His study used geostrophic winds determined from analysed height fields, rather than

interpolated station data as used by OR and NEA. He found a larger standing eddy flux than in the earlier studies and also systematic differences in the fluxes over ocean and continental areas with the zonal average being a small residual of large compensating terms. As found by Oort (1978) the transient eddy term agreed with earlier estimates.

The contributions of the different energy components to the atmospheric flux divergence in the northern hemisphere are shown for summer and winter in Fig. 2.4. The divergence of the mean flux is a small residual of large terms with the enthalpy and latent energy flux divergences having opposite phase to the potential energy flux divergence. The mean and eddy flux divergences are about the same magnitude as far north as 60^{o}N even in winter. The eddy flux divergences of enthalpy and latent energy tend to be out of phase between 30 and 70^{o}N in winter and equatorward of 60^{o}N in summer. All the mid-latitude flux divergences are small in summer. Poleward of 60^{o}N in winter and 70^{o}N in summer, the sign of the total energy convergence in the atmosphere is due to the eddy flux.

2.1.4 Net Radiant Flux at the Top of the Atmosphere

Estimates of the net radiant flux at the top of the atmosphere can be made with radiative transfer models using climatological data. NEA present several estimates of the global distribution and annual cycle of this term, while Sasamori and London (1972) present results with special emphasis on the southern hemisphere.

Apart from theoretical limitations these model results suffer from a lack of data, especially on cloud cover over the oceans. Independent measurements of the earth-atmosphere radiation budget from satellites have been made since a preliminary experiment performed on Explorer 7 in 1959. Early results were presented by Winston (1967), Winston and Taylor (1967) and Raschke and Bandeen (1970). Estimates based on five years' data using mainly low resolution radiometers

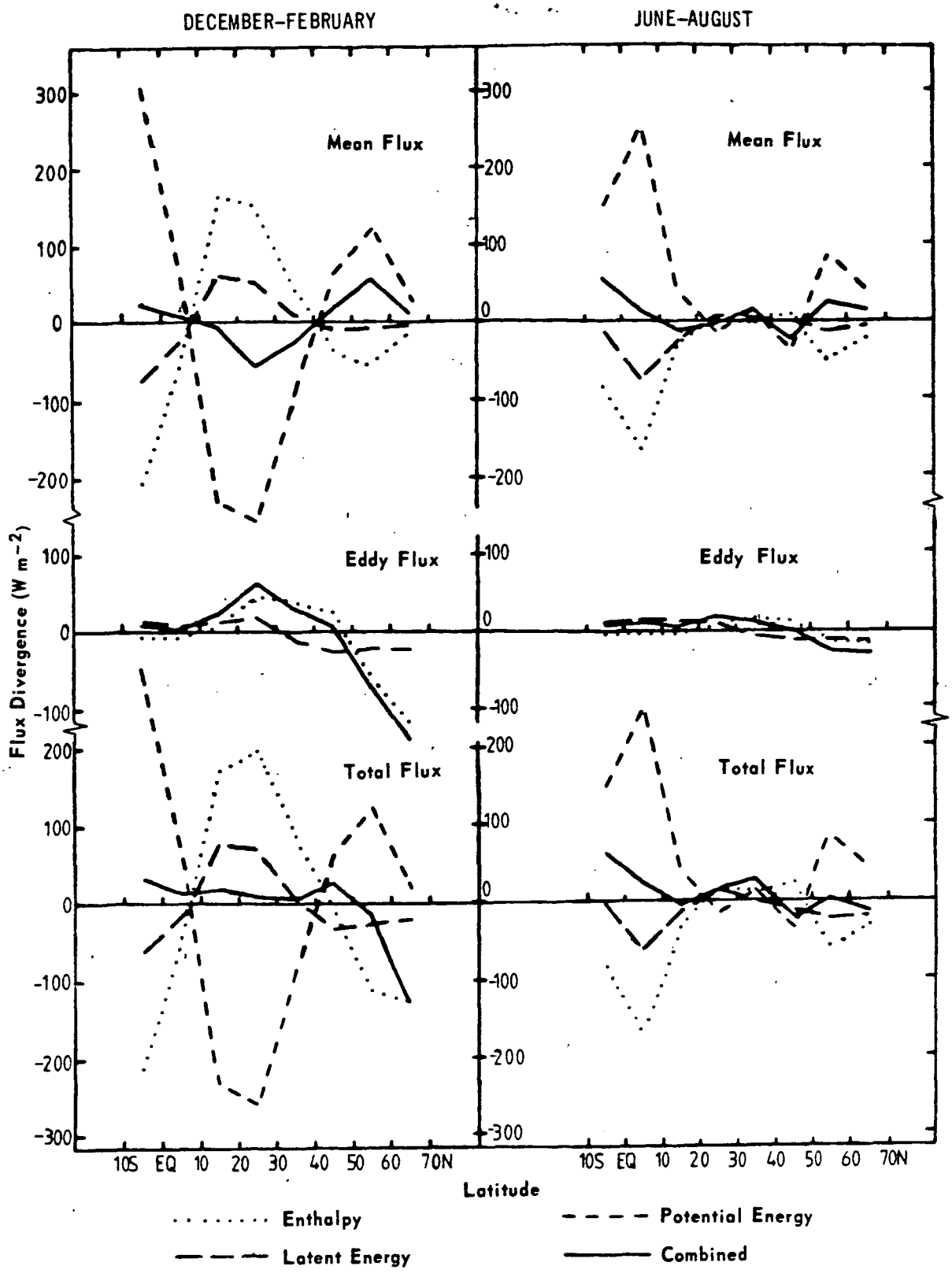

Fig. 2.4 Mean, eddy and total atmospheric flux divergences of individual energy forms for two seasons (after Oort and Rasmusson, 1971). Units are Wm^{-2}.

were published by Vonder Haar and Suomi (1971), and data from Nimbus 3, the first satellite with synoptic scale resolution (10^4 - 10^6 km^2) coverage over the entire globe were presented by Raschke et al. (1973). Zonal and global averages of these studies were in good agreement, but a study by Winston et al. (1972) found significant differences in the longitudinal distribution of long wave radiation and albedo between their results and those of Vonder Haar and Suomi.

Subsequent results have been published by Oort and Vonder Haar (1976) using data from a variety of satellites between 1964 and 1971, Jacobowitz et al. (1979) using 18 months' data from the Earth Radiation Budget (ERB) Experiment on the Nimbus 6 satellite and Winston et al. (1979), analysing 1974-1978 data from the operational NOAA series of satellites.

While offering the possibility of continuously and accurately monitoring the earth-atmosphere radiant flux, satellite data have their own problems of acquisition and interpretation. These problems will be discussed at some length because of the use made of satellite data in this study.

Yates (1977) summarises the main instrumental characteristics required as a flat, stable and known spectral response with known angular properties. The short wave instrument should also be calibrated by a sun view with the same instrumentation as the earth view.

In practice these requirements can only be partially met. The energy spectrum is usually sampled at discrete channels with one channel normally sufficient to cover the short solar wavelengths (0.2-4μm) but several channels for the earth's thermal radiation. Theoretical calculations of radiative transfer show that about 98 per cent of the variance in the spectrally integrated radiance can be accounted for by using the water vapour window (10.5-12.5μm) radiance alone (Winston et al. 1979). Significant reductions of standard error occur when the 13.3μm carbon dioxide and 14.5μm water vapour radiances are also included.

The short wave radiometers on board the NOAA series of operational satellites had no in-flight calibration, and there has been questioning of some albedo measurements (Gruber, 1977). The ERB Experiment and the instruments on present Japanese and American geostationary satellites are calibrated by viewing the sun.

One of the stated aims of the ERB Experiment was to measure the angular characteristics of the earth's radiative fluxes which present problems in interpreting the measured radiances. Four narrow angle telescope channels were able to scan along and across the sub-satellite track. The operational NOAA satellites only scanned cross-track. In their radiation budget study Raschke et al. (1973) used an empirical model relating reflectance to the solar zenith angle to compute flux densities of reflected solar radiation and to average them over the daylight period, while in the treatment of NOAA data the reflected radiative flux is assumed to be isotropic. Similarly, in the interpretation of the long wave radiative flux measurements some limb darkening corrections are required.

Observations from a single satellite in a sun-synchronous orbit suffer from a sampling problem in that daily averages are based on the assumption that each day-time (night-time) measurement is representative of the whole day (night) period. Diurnal variations of temperature and cloudiness are not monitored. This problem is ameliorated where data from satellites having different observation times are amalgamated, although this introduces difficulties due to differences in the type, viewing geometries and resolutions of the sensors.

A comparison of results from sensors having different resolutions is given by Smith et al. (1977) who present concurrent results from an omnidirectional and a narrow angle scanning radiometer. Such significant features as the inter-tropical convergence zone (ITCZ) are not resolved by the low resolution instrument.

Except for the ERB Experiment, direct measurements have not been made of the solar constant and a value is adopted for computing the albedo and the net radiant flux, Q^*_{TA}, the latter being derived from the formula:

$$Q^*_{TA} = S(1-\alpha) - Q\uparrow \qquad \ldots(2.10)$$

where S represents the solar constant, α albedo and $Q\uparrow$ the outgoing long wave radiant flux from the top of the atmosphere.

Because the net radiant flux is a small difference of two large terms, small relative errors in either α, $Q\uparrow$ or the assumed solar constant can lead to significant absolute errors in Q^*_{TA}.

Data from the NOAA satellites and ERB experiment are compared on a global scale by Gruber (1977). Except for the outgoing long wave radiation in which a systematic error occurred in the uncorrected NOAA results, the agreement between the two sets of data was good, even though the NOAA satellites had been developed primarily as operational satellites and were not ideally suited for a radiation budget study.

Global maps of NOAA data (Winston et al., 1979) and Nimbus 3 results (Raschke et al., 1973) are also generally similar, but with some notable differences. Commenting on the Nimbus 3 results Holopainen (1977) notes that the departures of net radiant flux from the zonal average tend to be positive over the oceans and negative over the land. The NOAA data do show negative anomalies over the north African region but the main anomalies within mid-latitude zones in the southern hemisphere are relative deficits to the west and a surplus over and to the east of the South American and African continents. This pattern is also evident to a lesser extent over Australia which generally has a net radiant flux above the zonal average. These disagreements may be due to the difference in observation times of the satellites, about 1130 and 2330 local time for Nimbus 3 and 0900 and 2100 for the NOAA satellites.

Seasonal values of the net radiant flux taken from Gruber (1977) are presented in Table 2.2. The mean annual meridional energy transports (ocean and atmosphere) derived from the results obtained from several satellites show good agreement. Except for the values of Raschke et al. (1973) these satellite studies confirm the finding of Vonder Haar and Suomi (1971) that there is no annual inter-hemispheric energy transport despite the asymmetries in geophysical and meteorological properties of the hemispheres.

Table 2.2

Seasonal Values of Net Radiative Flux based on one year of data from the NOAA satellites.

(Taken from Gruber, 1977)

Net radiant flux ($W\ m^{-2}$)

Latitude	Dec - Feb	Mar - May	Jun - Aug	Sep - Nov
80°N	-175	-125	-100	-180
70	-180	-115	- 20	-170
60	-170	- 52	12	-142
50	-145	- 17	27	-102
40	-112	10	43	- 65
30	- 80	18	47	- 39
20	- 45	32	45	- 7
10	+ 10	52	48	30
Equator	35	45	30	45
10	58	25	- 10	43
20	70	- 5	- 47	40
30	73	- 40	- 80	35
40	53	- 60	-125	10
50	30	-118	-162	- 20
60	5	-147	-180	- 60
70	- 63	-163	-175	-132
80°S	-120	-150	-150	-129

Inter-annual variations of satellite-derived radiative parameters are considered for the monsoon area by Winston and Krueger (1977) and their use as a diagnostic tool in circulation studies suggested.

2.1.5 Overall Energy Balance

In the energy budget equations in the form of Eq. 2.1 there is still one unknown, $\nabla \cdot F_O$ the divergence of the oceanic energy flux. Oort and Vonder Haar (1976) consider that direct measurements of this term are not feasible and calculate the term as a residual from known values of the other terms. The results reveal a more major role of the oceanic flux in transporting energy from the tropics than had been expected before satellite-derived estimates. An area of divergence in the tropics gives way to convergence at high latitudes where the atmospheric flux becomes the dominant energy transporter. In the tropics the results suggest a large oceanic flux from the summer to the winter hemisphere.

Although the atmospheric fluxes are poorly known in the southern hemisphere due to lack of data, Trenberth (1979) has applied the same method. For mean annual conditions his results show that the oceanic and atmospheric fluxes are approximately equal between 0^0 and 30^0S. Even as far south as 60^0S the oceanic flux still transports about one third of the total flux, in contrast to the northern hemisphere where the oceanic flux is negligible at 60^0N. He attributes this to the different land-sea distribution of the two hemispheres and the absence of significant atmospheric standing eddy flux in high southern latitudes.

The budget of the atmospheric column alone can be considered. This is described by Eq. A1.12, expressing the sensible and latent energy fluxes as a combined atmospheric flux F_A.

$$Q_{TA}^{*} - Q_{BA}^{*} = \nabla \cdot F_A + S_A - (Q_H + Q_E) \qquad \ldots(2.11)$$

This approach requires an estimation of the net radiational cooling of the atmosphere ($Q_{TA}^{*} - Q_{BA}^{*}$) and the sensible and latent energy fluxes (Q_H, Q_E) from the surface to the air. Oort (1971) combines available estimates of these terms with his estimates of $\nabla \cdot F_A$ and S_A to

test whether all the terms balance. He finds fair agreement considering the assumptions used in the determination of all the terms. Oort and Vonder Haar (1976) use satellite radiation data and measured values of $\nabla \cdot F_A$ and S_A to estimate the term $Q_{BA}^* - Q_H - Q_E$, the net energy flux from the atmosphere to the earth, as a residual.

2.2 *Regional Scale Energy Budget Studies*

The energy transformations taking place on a regional scale and the role of such scales in the general circulation have been the subject of studies by a number of investigators. This section briefly reviews these studies starting with early tropical results and leading on to mid-latitude reports.

2.2.1 *Tropical Studies*

The earliest regional scale energy studies investigated the dynamics of tropical areas. A study of the inter-tropical convergence zone (ITCZ) over several months led Riehl and Malkus (1958) to suggest that individual cumulonimbus clouds were responsible for the vertical energy transport in the ascending arm of the Hadley Cell.

Berson (1961) investigated the summer monsoon in the northwest Australia-Indonesian region to focus attention on the role of longitudinal asymmetries in the tropical circulation. He found a more vigorous circulation in the monsoon regime than had been found in reports of studies on the winter side of the ITCZ. The dominant energy flux terms were the import of latent energy and export of sensible energy by the monthly mean wind with the latter term dominating. The eddy flux of latent energy was about 25 per cent of the mean latent energy flux and counteracted the mean latent energy flux divergence, a trend attributed by Berson to ocean land moisture gradients in the area.

The meridional sensible and latent energy flux divergences were about 150 W m^{-2} while the divergence of the individual zonal fluxes was generally less than 50 W m^{-2}. The overall energy flux divergence was a small residual in which both meridional and zonal terms were significant.

While the meridional winds in all cases showed latent energy import and sensible energy export the reverse was generally true for the zonal winds during the monsoon months.

Berson considered an upper layer bounded by the 550mb level and found a large potential energy divergence with smaller enthalpy convergence. In the lower layer (pressures exceeding 550mb) the reverse was true with both terms smaller in magnitude.

Hastenrath (1966) discusses the energy budget of two areas, one over the Caribbean Sea and the other over the Gulf of Mexico, based on one year's aerological data. Although classed as trade wind areas Hastenrath found that the Caribbean Sea showed marked seasonal variation. In the dry (winter) season its energetical behaviour was that of a classical trade wind zone with latent energy export and sensible energy import. This pattern was reversed in the wet (summer) season with latent energy import and sensible energy export so that the region behaved like ITCZ regions. The Gulf of Mexico also showed this reversal in mid-summer. For both areas the divergence of the energy flux was found to be associated principally with the mean poleward transport. The vertical structure, however, was more complex than the two layer division of Berson. Alternating layers of inflow and outflow were found with the summer values dominated by a flux divergence from the 300-100mb layer of 1300 W m^{-2}. The individual sensible energy flux divergences were an order of magnitude greater than the radiative terms. Vertical transfer of energy was carried out mainly by the mean motion, but the eddy (convective) terms were also significant, especially in summer.

Gruber (1970) considered the energy budget of the Florida Peninsula during summer months to ascertain the role played by convective processes in the vertical transport of energy for that region. A diurnal variation of the flux divergences was found even as high as the 200mb level, related to the sea-breeze circulation, and the measured flux divergences were adjusted according to an idealised model to obtain a daily average value. The wind data were objectively adjusted to ensure mass balance over the area.

Gruber found that the Peninsula represented a potent energy source for the atmosphere, calculating the net transfer of energy at the air-surface boundary as about 210 W m^{-2} compared with estimates of 150 and 120 W m^{-2} for the Caribbean and Gulf of Mexico respectively in Hastenrath's study. About 80 per cent of this transfer over Florida was in the form of latent energy.

A schematic version of the energy budget as discussed by Gruber is given in Fig. 2.5. Alternating layers of import and export were observed with energy convergence in the lowest layer and export at the top. The export of sensible energy by the upper layer is again the major term and although less than the export from this level over the Caribbean it is almost twice the corresponding value of 430 W m^{-2} from the adjacent Gulf of Mexico during the summer of 1960 (Hastenrath, 1966).

Vertical energy fluxes were calculated by Gruber as residuals after estimating the non-adiabatic terms of net radiant flux and latent energy release by precipitation for each layer. Mean and turbulent processes were both significant in the vertical transfer of energy, with turbulent processes (convection) dominating the transfer of latent energy.

The potential energy and enthalpy flux divergences over the Florida Peninsula in summer are an order of magnitude greater than the zonally averaged values at the same latitude (cf. Fig. 2.4). The latent energy flux divergence is less than the zonal but the total atmospheric energy flux divergence is still about 120 W m^{-2} compared with an average value for the 20-30^{0}N latitude belt of about 20 W m^{-2}. Gruber suggests that the mean circulation was primarily responsible for the atmospheric flux divergence over Florida, while in the zonal average for summer the total eddy flux divergence appears to dominate.

In summer the Caribbean Sea also appears to export more sensible energy (53 W m^{-2}, Hastenrath, 1966) than the zonal average (14 W m^{-2}) but its latent energy flux convergence, and both forms of energy for the Gulf of Mexico are close to the zonal averages. In winter the Caribbean

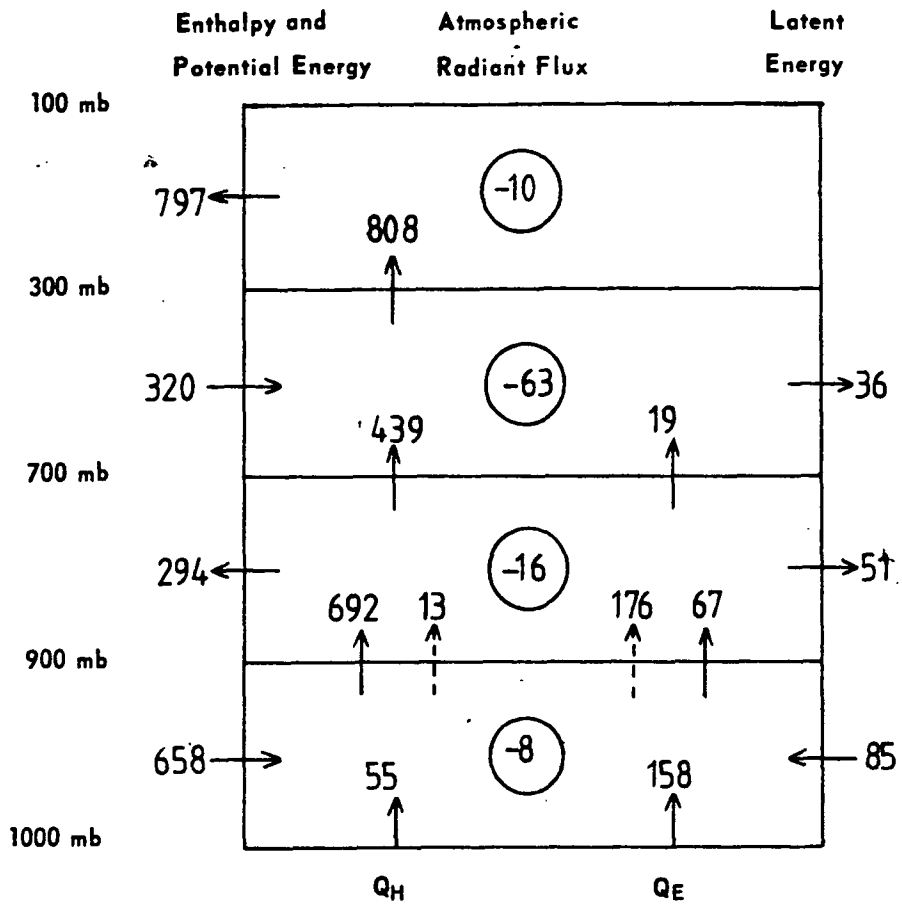

Fig. 2.5 Schematic representation of the energy sources and sinks for summer over the Florida Peninsula (after Gruber, 1970). Vertical arrows represent transfer by mean motion (solid) and turbulent motion (dashed). Circled values denote net radiant cooling and horizontal arrows represent flux divergences. Units are Wm^{-2}.

also exports slightly more than the zonal average with an above average convergence of sensible energy more than compensated by a large latent energy flux divergence (126 W m^{-2} compared to a zonal average of 77 W m^{-2}). The Gulf of Mexico, in contrast, appears as an area of strong energy import (-154 W m^{-2}) in a weakly exporting latitude belt (+11 W m^{-2}) due mainly to strong sensible energy convergence.

2.2.2 Mid-high latitude studies

A study of the energetics of the region surrounding the Baltic Sea was carried out by Behr and Speth (1977) using seven years of records. Energy equations of the form Eq. A1.18 were used so that latent energy is only considered when condensation occurs. The non-adiabatic energy sources for the atmospheric column were taken as the release of latent energy by condensation and the net long wave radiation as well as heat transfer from the surface. Short wave absorption in clouds or air seems to have been neglected.

Horizontal flux divergences of enthalpy and potential energy were computed by Behr and Speth, including a breakdown into mean and eddy components. The mean fluxes were generally greatest in October and least in July in line with the mean wind field, but the eddy fluxes showed no marked annual cycle. Although the mean fluxes were several orders of magnitude greater than the eddy fluxes, the divergences of each were comparable in magnitude. The individual flux divergences varied markedly in sign and magnitude over the four sub-areas. The overall energy flux divergence was generally a small residual of large counteracting terms with individual enthalpy flux divergencess as large as 2000 W m^{-2}. Among the non-adiabatic terms the sensible energy transfer from the surface and the latent energy released by precipitation were an order of magnitude less than the net long wave radiation which ranged from -165 to -220 W m^{-2}.

While the divergence of the eddy potential energy flux was generally of the same sign as the eddy enthalpy flux divergence this was not true for the respective mean flux divergences. There was also marked counteraction between the mean and eddy terms of enthalpy flux divergence.

The individual flux divergences, especially the sensible energy terms, are at least one order of magnitude greater than the zonal average values (cf. Fig. 2.4) where the greatest flux divergence at these latitudes was about 120 W m^{-2} for the mean potential energy flux divergence at 55°N in winter. Summing the individual components shows that the region generally has sensible energy convergence of between 100 and 150 W m^{-2}. For the north and east of the study area in winter this rate of import is only slightly greater than the zonal average, but otherwise this strong convergence is in contrast to a zonal average of weak divergence.

The variation in the pattern of flux divergences over the study area expresses the importance of regional scale variations in the earth-atmosphere energy budget and reveals an even more complex structure than is suggested by zonal averages.

Gallardo et al. (1977) performed energy budget calculations for the western Mediterranean area based on two years' data. In the overall energy budget several options for the net atmospheric radiant flux and condensational heating were used as exact balance of all the terms was not obtained.

A latent energy budget for the area was also attempted by Gallardo et al using climatic rainfall and evaporation data combined with the computed latent energy flux divergences. Precipitation was calculated as a residual and gave reasonable agreement with observed values except for spring. The latent energy flux divergence was found to be dominated by the mean flow. Latent energy import occurred between the surface and 850mb in all seasons except summer when there was strong export up to the 700mb level.

The mean flux divergences of sensible energy (enthalpy and potential energy) at individual levels were generally an order of magnitude greater than those of the eddy flux, but both components were of comparable magnitude in the vertical integral due to alternating layers of opposite sign in the vertical profiles of mean flux divergence. There was considerable variation between the two years studied. Average vertical profiles of the total and eddy sensible energy flux divergences are shown in Fig. 2.6. The mean flux divergence shows a layer of strong convergence in the middle and upper troposphere with divergence in the lower stratosphere. A layer of convergence occurs near the surface in winter. The eddy flux divergence is essentially of the same sign in the vertical with summer divergence and winter convergence. Strongest eddy convergence in winter occurs near the jet stream level but the strongest summer divergence occurs near the surface.

The eddy and mean flux divergences of sensible energy counteracted, as also found in the study of Behr and Speth. The eddy term dominated in winter leading to overall convergence, but the mean term in summer was almost twice the eddy term, again producing overall convergence. Sensible energy divergence occurred in winter and spring.

Relative to the zonal average (a mean of the values for 35°N and 45°N in Fig. 2.4) the western Mediterannean appears to be an energy exporter in summer with a total flux divergence of 47 W m^{-2} compared to a zonal average of 3 W m^{-2}. The reverse is true in winter with a net import (-44 W m^{-2}) in a belt of average divergence (17 W m^{-2}). The component mean and eddy terms are at least an order of magnitude greater than the corresponding zonal averages, and the distribution between latent and sensible energy is different from the zonal norm. The zone as a whole has sensible energy divergence and latent energy convergence in both summer and winter, while the western Mediterranean has convergence of both terms in winter, and in summer has strong sensible energy convergence (-80 W m^{-2}) more than compensated by latent energy divergence

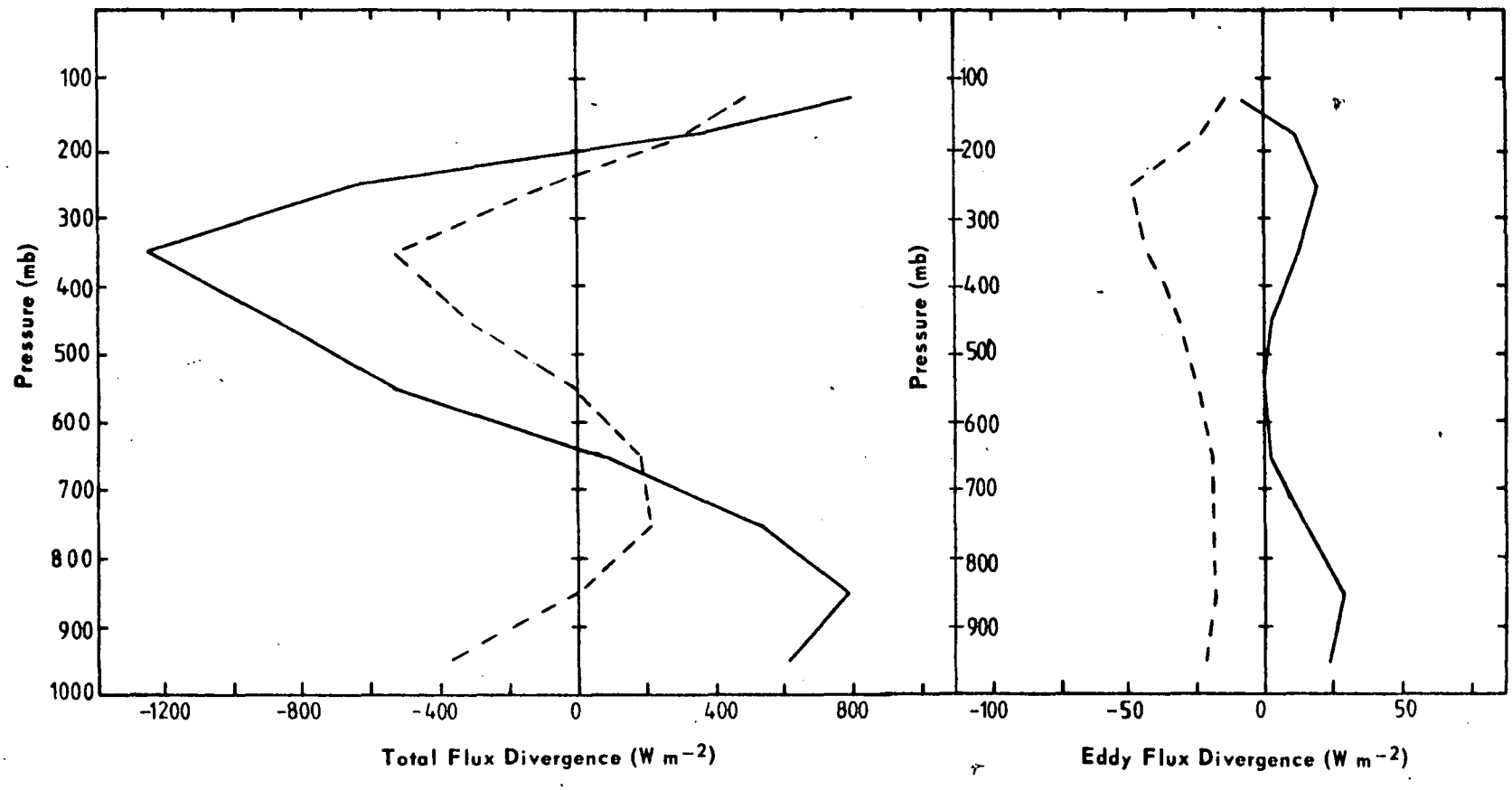

Fig. 2.6 Vertical profiles of the total and eddy sensible energy flux divergences (Wm^{-2}) for summer (solid) and winfer (dashed) over the western Mediterranean (after Gallardo et al., 1977).

(127 W m^{-2}). In summer, then, the area seems to act as a strong moisture source using imported sensible energy (mainly from the mean flow) to drive evaporation from the surface.

2.2.3 Water Vapour Budget Studies

In addition to the results quoted above information on the latent energy component of the energy budget can be obtained from water vapour budget studies which have been carried out as part of more general water budget investigations. Many are principally hydrological studies concerned with computing net rainfall runoff, but some describe the atmospheric processes involved in the water vapour transport.

Such studies have been reviewed by Rasmusson (1977) who discusses the methods used and likely sources of error. Rasmusson questions the accuracy of studies carried out for areas less than about 10^6 km^2 using the routine upper air network, not only because of errors in the radiosonde observations but also because of the inadequate spatial and temporal resolution possible with the existing upper air network. In earlier work Rasmusson (1967) found a significant diurnal variation in water vapour fluxes on even the continental scale (the United States in this case), especially in summer. An intensive study for the Baltic Sea region (Baese and Liebing, 1977) of evaporation minus precipitation obtained realistic results only for the larger sub-regions (of the order of 10^5 km^2).

Palmen (1967) also discusses the reliability of water vapour budget analyses and quotes the results of a study over northern Africa (including the Sahara desert) which revealed a strong excess of evaporation over precipitation, which would seem unlikely according to present hydrological knowledge.

One of the earliest studies was that of Hutchings (1957) who studied a 9 x 10^4 km^2 area over southern England for the three summer months of 1954 using twice daily rawinsonde observations at four stations. He found reasonable agreement between the net convergence and storage of

water vapour calculated from the upper air data and the difference between observed precipitation and computed evapotranspiration. Both the mean and eddy terms of the water vapour flux divergence changed sign in the vertical with convergence in the lowest layers (1000-850mb) and divergence above. Although the magnitudes of the mean terms were greater at individual levels than the eddy terms, both terms were comparable in the vertical integral and opposite in sign. Hutchings found that the vertical transport of water vapour was due more to the small-scale convective and turbulent flux than transport by the mean vertical mass flux.

A study by the same author for the Australian region (Hutchings, 1961) based on one year's once daily upper air data found reasonable agreement in eastern Australia on an annual basis but not on a monthly basis. Hutchings attributed some of the disagreement to the computed evapotranspiration which represented potential rather than actual values. Rasmusson (1968) used three year's twice daily data to calculate the pattern of water vapour flux divergence over North America. Although in general agreement with independent hydrological data, Rasmusson was not confident about the fine structure of the results. The sign of the total water vapour flux divergence over the continent again varied in the vertical in summer with low level convergence and upper level divergence. In winter there was convergence at most levels. The central American Sea was portrayed as a strong source area with the continent acting as a sink, particularly near the north Pacific Coast and the south-east coast.

None of the studies appears to adjust the upper air data for overall mass balance, although Rasmusson (1968) suggests that some of the errors may be due to mass imbalance. Considering the compensation between mean and eddy terms and among different layers and the need found in total energy budget studies for an adjustment of the data to obtain mass balance, it would seem that a similar procedure to ensure mass balance would be desirable for latent energy budget studies even though the water vapour transport is confined mainly to the lower troposphere.

CHAPTER III

ANALYSIS METHODS AND RESULTS

3.1 Data Sources and Quality

3.1.1 Data Sources

The data used in the present study are of two main types - standard climatic data and satellite radiometric observations. The climatic data were mainly routine daily upper wind and radiosonde observations over south-east Australia for the period 1 January 1974 to 31 December 1976, supplied on magnetic tape by the Australian Bureau of Meteorology. Details of the reporting stations used are listed in Table 3.1 and the locations of the stations are shown in Fig. 3.1. The radiosonde records included values of the mixing ratio of water vapour, defined as the mass of water vapour per unit mass of dry air. Energy flux computations require values of specific humidity (defined as the mass of water vapour per unit mass of the air-water vapour mixture). The two terms are approximately equal numerically because of the small quantities of water vapour in the air under normal conditions. Values of mixing ratio were treated in the computations as being equivalent to values of specific humidity.

Long term averages of the upper air observations were taken from Maher and Lee (1977) except for the total water vapour content for which the results of Pierrehumbert (1972) were used. Where required, long term or monthly averages of surface climatic data were taken from Bureau of Meteorology publications. The area studied was the hexagon bounded by a line joining the stations Adelaide, Cobar, Williamtown, Wagga Wagga, Laverton and Mt Gambier. The area of this hexagon was measured planimetrically as 4.30×10^5 km^2.

Monthly mean satellite radiation data were obtained on microfilm from the United States National Oceanic and Atmospheric Administration - National Environmental Satellite Service (NOAA/NESS) covering the period from June 1974, when the observations commenced, to February 1978.

Table 3.1

Details of Rawinsonde Stations Used

Station	WMO Number	Latitude (°S)	Longitude (°E)	Elevation (Metres)	Wind Finding Equipment	Observation Times (GMT)*	
						Upper Wind	Radiosonde
Adelaide	94672	34° 57'	138° 32'	7.6	WF44	0500, 1100, 1700, 2300	1100, 2300
Mildura	94693	34° 14'	142° 05'	50.3	WF2	0500, 1100, 1700, 2300	
Cobar	94711	31° 32'	145° 49'	243.8	WF2	0500, 1100, 1700, 2300	2300
Williamtown	94776	32° 49'	151° 50'	4.0	WF44	0500, 1100, 1700, 2300	1100, 2300
Wagga Wagga	94910	35° 06'	147° 30'	214.3	WF3	0500, 1100, 1700, 2300	2300
Laverton	94865	37° 53'	144° 45'	14.3	WF44	0500, 1100, 1700, 2300	1100, 2300
Mt Gambier	94821	37° 49'	140° 46'	64.9	WF44	0500, 1100, 1700, 2300	2300

* One hour earlier when Daylight Saving Time in operation

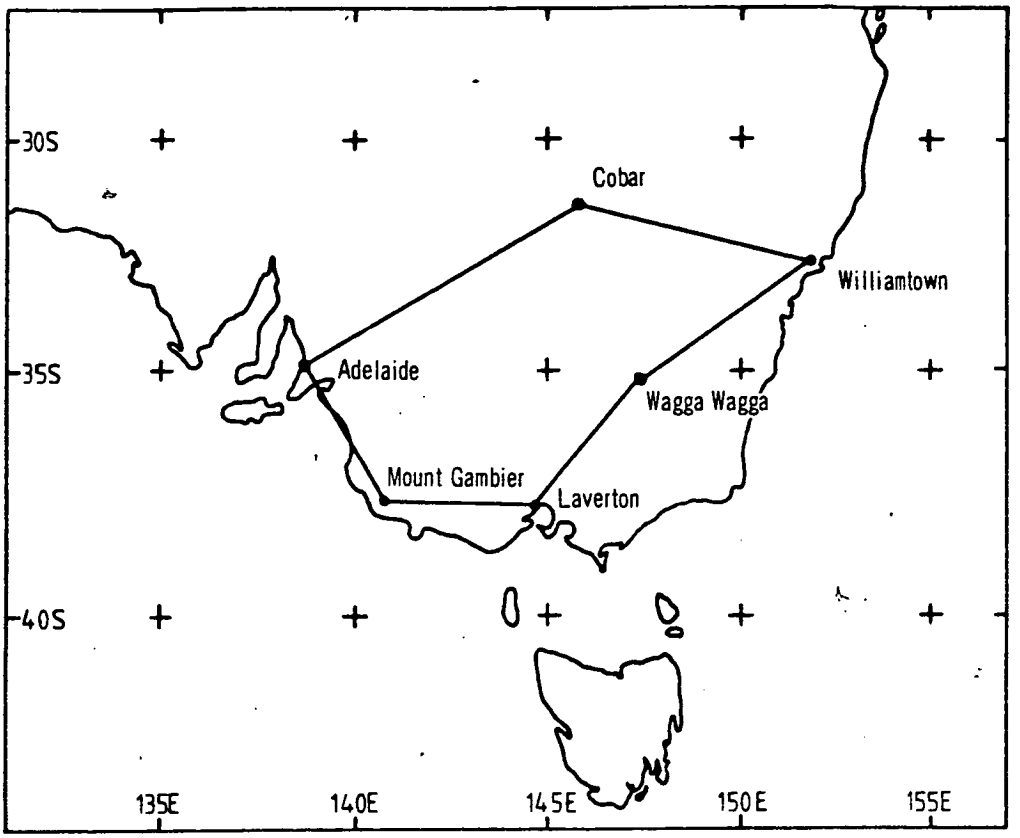

Fig. 3.1 Location diagram showing reporting stations used and the irregular hexagonal study area.

The radiation budget parameters (absorbed solar radiation, albedo, outgoing long-wave radiation, net radiation) are given at grid points with 2.5 degree latitude-longitude spacing for the whole globe. The data were acquired from the 2-channel scanning radiometers on the operational satellites NOAA-2 to NOAA-5, which had a near polar sun-synchronous orbit at an altitude of approximately 1100km. Gray (1978) stated that the measurement of each parameter was based on one "look" per day with an adjustment to the local vertical. As a day-time and a night-time value of long wave radiation are measured, the average of these two values was used in this study as representative of the twenty-four hour period. Gray also states that limitations on computer processing time did not permit the averaging of measurements from successive orbits in areas of overlap. Gruber (1977) gives details of methods and approximations used in deriving the radiation budget values. Reflected energy was sensed in the 0.5 - 0.7 μm range of the visible spectrum and spot measurements of the albedo were assumed to represent average daily values. Emitted energy was measured in the infrared water vapour window 10.5 - 12.5 μm, and a non-linear regression equation used to determine the total outgoing longwave radiation flux (4 - 50 μm) from measurements in the window region. (Abel and Gruber, 1979).

3.1.2 Data Quality

(a) Radiosonde and Upper Wind Data

The data supplied on magnetic tape had previously been subjected to the Bureau of Meteorology's routine quality control, aimed at eliminating transmission and processing errors and ensuring internal self-consistency of the records. These tests included hydrostatic checks of the radiosonde records and limitations on the vertical wind shear in the upper wind data. Between the surface and 100mb the radiosonde data were available at thirteen levels and the upper wind measurements at fourteen levels.

Most of the pressure levels in the two data sets were coincident, although the 750mb level is used for upper winds and the 800mb level in the radiosonde data. Mixing ratio measurements were not given above the 400mb level.

Errors in Australian upper air observations are discussed in *The Laverton Serial Sounding Experiment* (Bureau of Meteorology, 1968). The errors in wind estimates increase with height due to uncertainty in determining the position of the balloon. For the WF44 radar system the maximum root mean square (rms) vector error expected in the upper troposphere was less than 5 m s^{-1} for 95 per cent of flights. For the Laverton system studied the actual random errors were approximately half the maximum specified by the manufacturers, implying an actual maximum rms vector error of about 2.5 m s^{-1}. Figures presented for the Laverton WF2 radar were similar to the maximum errors expected on the WF44 system. However, the manual calculations required in the processing of WF2 reports add further errors of the same order of magnitude (Spillane, 1969).

The rms errors for the temperature and pressure were found to be less than 0.8 K and 1.0 mb respectively. Humidity measurements in the absence of cloud are estimated to be accurate to within five per cent at temperatures above 0°C. No estimate of the error was given for temperatures below 0°C although Oort (1978) quotes a figure of ten per cent. The measured values within clouds may be too low by up to twenty-five per cent.

The humidity sensing elements used in the radiosondes have a threshold value of mixing ratio dependent on pressure and temperature, below which humidity is not recorded. (See Table 3.2). Values of mixing ratio below the threshold value are treated as zero in the radiosonde records. The treatment of values below the threshold in the flux computations is discussed in the next section.

The effect of these instrumental errors on flux values can be considered using the formula for the propagation of errors (Young, 1965). The variance σ_y^2 of a quantity y(a,b) calculated from the observed quantities a and b is given by

$$\sigma_y^2 = (\partial y/\partial a)^2 \ \sigma_a^2 + (\partial y/\partial b)^2 \ \sigma_b^2 \qquad \ldots(3.1)$$

Table 3.2

Minimum Relative Humidity and corresponding mixing ratio (g Kg^{-1}) that can be normally measured by the radiosondes currently used in Australia.

Temperature (^{0}C)	Limiting Relative Humidity	Limiting Mixing Ratio (g/Kg) for given Pressure (mb)							
		1000	900	850	800	700	600	500	400
30	14%	3.7	4.1	4.4	4.6	5.3			
20	15	2.2	2.4	2.6	2.7	3.1	3.7		
10	18	1.4	1.5	1.7	1.8	2.0	2.3	2.8	
0	21	0.8	0.9	1.0	1.0	1.1	1.3	1.6	1.9
-10	24	0.4	0.5	0.5	0.5	0.6	0.7	0.9	1.0
-20	26	0.2	0.2	0.2	0.3	0.3	0.3	0.4	0.5
-30	29	0.1	0.1	0.1	0.1	0.2	0.2	0.2	0.2
-40	32					0.1	0.1	0.1	0.1

(i) Total enthalpy flux

The variance σ_1^2 of the enthalpy flux (C_pTV) is then

$$\sigma_1^2 = (CpV)^2 \ \sigma_T^2 + (C_pT)^2 \ \sigma_V^2 \qquad \ldots (3.2)$$

where σ_T and σ_V are the variance of temperature and wind velocity respectively.

Taking typical values of 25 m s^{-1} and 250 K for V and T respectively, and using σ_V = 2.5 m s^{-1} and σ_T = 0.8 K gives a value of 6.2 x 10^5 W m Kg^{-1} for σ_1 in a flux of 6.2 x 10^6 W m Kg^{-1}. Because of the large magnitude of the temperature, the contribution of the first term on the right hand side of Eq. 3.2 is negligible, and the errors are dominated by the uncertainty in the wind measurements.

(ii) Latent energy flux

For latent energy flux LqV the variance σ_2^2 is

$$\sigma_2^2 = (LV)^2 \ \sigma_q^2 + (Lq) \ \sigma_V^2 \qquad \ldots (3.3)$$

Using σ_q = 0.05q and v = 2.5 m s^{-1} the standard deviation σ_2 represents 25 per cent of the latent heat flux for V = 10 m s^{-1} but only eight per cent of the flux for V = 40 m s^{-1}. The partial contribution to σ_2 of the specific humidity errors (found by inserting σ_V = 0 in Eq. 3.3) is five per cent, but the partial contribution of wind errors (σ_q = 0) decreases from 25 per cent at V = 10 m s^{-1} to 6 per cent at V = 40 m s^{-1}. In contrast to the enthalpy flux the contributions of errors in specific humidity are comparable with those in wind measurements, especially at high wind speeds.

(iii) Eddy enthalpy flux

The variance σ_3^2 of the eddy enthalpy flux $C_p T'V'$ (defined in Chapter 2) can be found by applying the formula for the propagation of errors to the expression

$$y\ (T, \overline{T}, V, \overline{V}) = CpT'V' = Cp(T-\overline{T})\ (V-\overline{V}) \qquad \ldots\ (3.4)$$

Then

$$\sigma_3^2 = (Cp(T-T))^2\ (\sigma_v^2 + \sigma_{\overline{v}}^2) + (Cp(v-\overline{v}))^2\ (\sigma_T^2 + \sigma_{\overline{T}}^2) \qquad \ldots\ (3.5)$$

The variance of the mean of a set of n measurements is given by the variance of the individual measurements divided by the number of measurements.

Then $$\sigma_{\overline{T}}^2 = \sigma_T^2/n \quad \text{and} \quad \sigma_{\overline{v}}^2 = \sigma_v^2/n \qquad \ldots\ (3.6)$$

where n is the number of observations.

For monthly averages $\sigma_{\overline{T}}^2$ and $\sigma_{\overline{v}}^2$ will be small compared with σ_T^2 and σ_v^2 so that σ_3^2 is given approximately by

$$\sigma_3^2 \simeq (CpV')^2\ \sigma_T^2 + (CpT')^2\ \sigma_v^2 \qquad \ldots\ (3.7)$$

Values of σ_3 expressed as a percentage of the eddy flux are given in Table 3.3 for a range of T' and V' using $\sigma_T = 0.8K$ and $\sigma_V = 2.5\ m\ s^{-1}$. Also given are the contributions of each term to the total percentage. The percentage error decreases from near 50 per cent at low values of T' and V' to about ten per cent for high values. Again, in contrast to the total enthalpy flux, the errors from temperature measurements are comparable with those from wind measurements, except for low values of V'.

The above considerations refer to root mean square (rms) errors in individual observations. For monthly averages, assuming the instrumental errors are random rather than systematic, the rms errors will be reduced by the factor $1/\sqrt{30}$, and for vertical integrals a further reduction of $1/\sqrt{m}$ will occur where m is the number of levels used.

Table 3.3

RMS instrumental error in eddy enthalpy flux measurements, for a range of wind and temperature deviations, using σ_T = 0.8K and σ_V = 2.5 m s^{-1}, expressed as a percentage of the eddy flux. The partial contribution for instrumental errors in temperature alone (σ_V=0) or wind alone (σ_T=0) are given in lines a and b respectively, with the combined percentage error derived from Eq. 3.3 in line c.

		V' (ms^{-1})			
T^1 (K)		5	10	20	40
5	a.	16	16	16	16
	b.	50	25	13	6
	c.	53	30	20	17
10	a.	8	8	8	8
	b.	50	25	13	6
	c.	51	26	15	10
15	a.	5	5	5	5
	b.	50	25	13	6
	c.	50	25	14	8

Spillane (1969) and Oort (1978) point out that mesoscale and microscale variations may add further errors of the same order of magnitude as the instrumental errors. Missing data, especially wind observations at high levels, are another source of error. The tendency for reports to be missing during high

wind shear conditions, or lost in rain echoes for some radar systems (e.g. WF2), may produce a bias in mean wind or flux values. A quantitative study of this problem was made for momentum fluxes by Priestley and Troup (1964). They found that the omission of as few as ten per cent of observations caused significant errors in the eddy momentum flux $\overline{u' v'}$, in some cases even causing a reversal of sign.

Systematic diurnal variations in the wind and energy fields will also lead to errors as energy fluxes representing a daily average are calculated from once or at most twice daily rawinsonde flights. On the small-scale the fluxes at coastal stations will be affected by land-sea contrasts and local sea-breeze circulations, but there is evidence that diurnal variations also occur on a large scale. Rasmusson (1967) found a significant diurnal variation in the water vapour flux field over North America, especially south of 50^0N in summer, as part of a broad-scale diurnal circulation that could be detected at pressures as low as 500mb. He found that diurnal variations in the water vapour flux divergence were comparable with the computed mean flux divergence itself.

(b) Satellite Data

Difficulties in satellite radiometric observations in general have been discussed briefly in Chapter II. The accuracy of the NOAA data is discussed qualitatively by Gruber (1977) who states that systematic noise characteristics of the system and the lack of onboard calibration for the visible radiometer compounded uncertainty due to the narrow spectral intervals of the equipment and the assumptions used in reducing the raw data to estimates of radiance.

Oort and Vonder Haar (1976) present estimates of the standard error of the mean in seasonal and annual net radiation measurements for ten degree latitude zones. The standard error was generally less than 7 W m^{-2} in low and middle latitudes but increased to between 10 and 15 W m^{-2} poleward of 70^0. These estimates were based on measurements from a variety of satellites and equipment over 29 months of records. The authors suggest that the natural temporal variability dominates their error estimate. The difficulties of intercomparison are reduced when data from only one series of satellites are used, but the temporal sampling problem is accentuated as the NOAA satellites cross the Equator at approximately 0900 and 2100 local time. This limited sampling will introduce errors due to the diurnal variation of albedo (variations of cloudiness as well as solar zenith angle) and long wave radiation.

In a comparison of the early NOAA measurements with results from the Nimbus 6 Earth Radiation Budget Experiment, Gruber (1977) found that NOAA long wave radiation fluxes were consistently 10 W m^{-2} higher. As measurements reported by Gruber imply an annual net radiation deficit for the earth of 12 W m^{-2} it seemed that the NOAA long wave data were systematically too high. The linear regression used to derive the long wave radiant flux from the measured radiances was replaced by a non-linear regression and the archive values corrected (Winston et al. 1979). The corrected results were used in this study. Gruber also reports

that between December 1975 and September 1976 measured albedo values appear to be too low by about three per cent in albedo units due to instrument degradation.

3.2 *Method*

3.2.1 *Evaluation of Energy Fluxes*

The equations for the energy balance of an atmospheric column and for the breakdown of fluxes into mean and eddy terms have been outlined in Chapter 2 and Appendix A1. The products of daily values of the wind components with each of the energy terms (enthalpy, potential energy, latent energy and kinetic energy) were averaged over a month at each of the six radiosonde stations to obtain the mean monthly total flux at a given pressure level. The mean flux for each month was calculated from only those observations used in calculating the total transfer. The eddy flux was then obtained by subtracting the mean from the total flux. Generally only 2300 GMT data were used, although the results at 1100 GMT are presented for several months.

Trapezoidal integration was used to obtain the vertical integral at each station, with the daily surface pressure used as the lower limit of integration. The upper limit of integration was taken as 100 mb because of the increase in the proportion of missing observations at pressures below this value. It was assumed that the net vertical flux of mass or energy through the 100 mb level averaged over the area in question is zero, although not necessarily requiring the vertical velocity or vertical energy flux at each station to be zero.

The net radiation measurements are taken from outside the atmosphere, so that for comparison between the net radiation and energy flux divergence measurements, it was assumed that the satellite measurements could be regarded as representative of the radiation at the 100 mb level. This is not unreasonable as:

(a) 90 per cent of the mass of the atmosphere is below the 100 mb level, and

(b) the region above 100 mb is close to radiative balance in mid-latitudes (Dopplick 1974).

For the 950, 750 and 250 mb levels, upper wind but not radiosonde measurements were available. Interpolation from adjoining levels was used to obtain the temperature, geopotential and mixing ratio at these levels. In the case of 750 and 250 mb the mean of the measurements at adjacent levels was used, but for the 950 mb level the surface and 900 mb values were weighted according to the difference in pressure of each from 950 mb. Otherwise, no attempt was made to interpolate missing observations, except for several months treated in detail and discussed in Section 3.3.

3.2.2 *Flux Divergences*

The divergences of the winds and energy fluxes were calculated by evaluating line integrals round the polygon joining the reporting stations using the method outlined by Gruber and O'Brien (1968).

Consider a hexagon with sides of length S_1, S_2, ... S_6 and unit outward normal vectors $\underline{n}_1$, $\underline{n}_2$, ... $\underline{n}_6$ as shown in Fig. 3.2 The line integral of the normal wind component V_n round the hexagon is given by:

$$\oint V_n \, ds = \sum_{i=1}^{6} \int_i^{i+1} \underline{V} \cdot \underline{n}_i \, ds_i \qquad \ldots (3.8)$$

(Note: when i = 6, i+1 refers to Vertex 1)

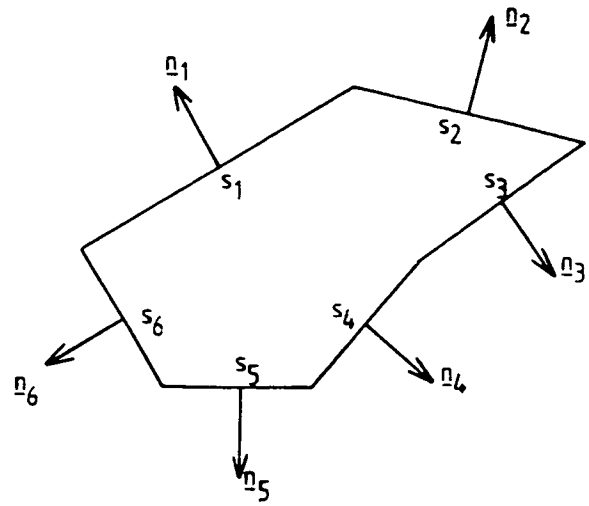

Fig. 3.2 Irregular hexagon with stations at the vertices, sides s_1, ..., s_6 and unit normal vectors n_1, ..., n_6 directed outwards.

Using trapezoidal integration, which effectively assumes a linear variation of the normal wind component between successive integration points,

$$\oint V_n \, ds = \sum_{i=1}^{6} \frac{1}{2} \left(\underline{V}_i + \underline{V}_{i+1} \right) \cdot s_i \underline{n}_i \qquad \ldots (3.9)$$

Expanding the brackets and collecting coefficients of the $\underline{Vi}$ gives

$$\oint V_n \, ds = \sum_{i=1}^{6} \underline{V}_{i+1} \cdot \frac{1}{2} \left(S_i \, \underline{n}_i + S_{i+1} \, \underline{n}_{i+1} \right) \qquad \ldots (3.10)$$

The wind vector at each station i is weighted by a vector $\underline{W}_i = \frac{1}{2} (S_i \underline{n}_i + S_{i+1} \, \underline{n}_{i+1})$ which has magnitude equal to, but direction normal to the line joining the mid-points of the sides adjacent to the station. So the line integral can be simply evaluated from the values at each station, and if integrals over different polygens are desired, these can be achieved by merely altering the factors applied to the value at each station.

The bearings and magnitudes of the vectors $\underline{W}_i$ for the hexagon being considered were calculated using standard spherical trigonometrical techniques and are listed in Table 3.4. Due to the curvature of the earth, the bearing of the outward normals varies slightly along the line joining each station, so that an average value was used. The values in Table 3.4 were verified by calculating the divergence of uniform westerly and southerly winds over the hexagon.

Table 3.4

Bearing and Magnitude of the Weighting Vectors used in the Calculation of Energy Flux Divergence.

STATION	MAGNITUDE (Km)	BEARING (Degrees clockwise from north)
Adelaide	420.8	303.7
Cobar	633.2	349.5
Williamtown	213.2	67.7
Wagga	425.8	138.5
Laverton	333.3	153.0
Mt Gambier	320.2	211.1

3.2.3 Treatment of Water Vapour Measurements

(a) Correction for Values of Specific Humidity below the Threshold Values

Two sets of figures are often given in the presentation of precipitable water data. In one set, observations of specific humidity below the threshold are assigned the threshold value and in the other set these are treated as zero. It was decided that in presenting flux measurements this was too cumbersome and that

some averaging was necessary. Actual values will be between these extreme values. Assuming that the frequency distribution of specific humidity on a monthly basis is reasonably well-behaved (e.g. is a single-humped distribution) then the expected value of a given measurement below the threshold should be a function of the proportion of observations below the threshold.

$$\text{i.e. } q^* = f(m/n)B \qquad \ldots (3.11)$$

where q^* represents the adopted value of the specific humidity, B is the threshold mixing ratio and f is a factor less than unity dependent on the ratio of the number of observations below the threshold m to the total number of measurements n.

The two limiting cases used to choose a value for f are shown in Fig. 3.3.

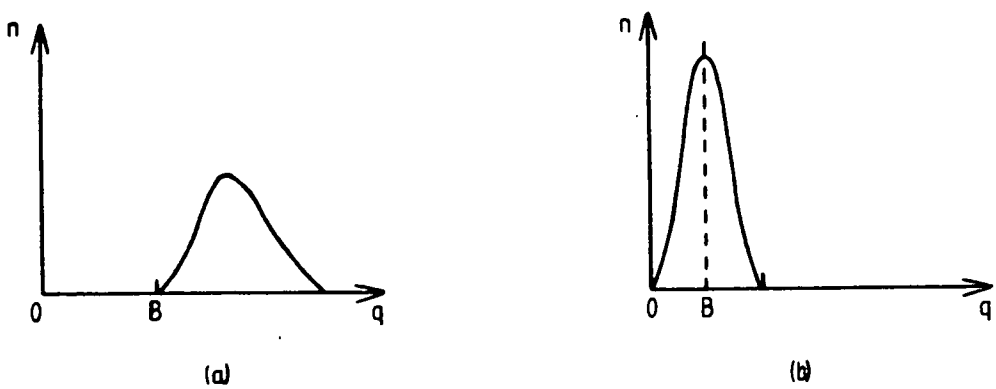

Fig. 3.3 Limiting frequency distributions used to suggest values for the factor f (see text)

In case (a) all the observations are above the threshold, and in (b) all are below the threshold. If the distribution

in (a) is moved slightly towards lower values of q, so that one observation is below the threshold value, the expected value of that observation would be close to B. In this case, then, f is chosen to be unity.

If all the observations are below the threshold, a value of B/2 is chosen as the mean value of mixing ratio expected, giving f=1/2. Then equation (3.11) becomes

$$q^* = (0.5 + 0.5(m/n))B \qquad \ldots (3.12)$$

This selection, in particular case (b) is rather arbitrary, but as most below threshold observations occur at high levels where the water vapour content is low, the procedure is not critical.

In the flux calculations the ratio m/n was determined on a monthly basis. A quadratic equation had been derived for each pressure level from the values in Table 3.2 to express the threshold value B in terms of the temperature at that level. The appropriate value of B was determined on a daily basis from the observed temperature.

(b) Correlation of Mean and Median Specific Humidity

In the publication of mixing ratio data (treated as specific humidity in this study) the Bureau of Meteorology presents median rather than mean data because of the above-mentioned threshold limitation. To enable comparison of the monthly mean values obtained as outlined above with Bureau of Meteorology median data, the relation between the two was investigated over 32 months for which concurrent

data were available. A linear least squares regression technique was used to obtain a relation of the form

$$q_{mean} = b + a^* q_{median} \quad \ldots (3.13)$$

where a and b are constants.

Results obtained from the combined data at the 6 radiosonde stations are given in Table 3.5.

Table 3.5

Regression of mean on median specific humidity $q_{mean} = b + a^* q_{median}$ based on 32 months combined data of the six radiosonde stations.

Level (mb)	Regression Coefficient (a)	Intercept (b)	Standard error of regression coefficient	Correlation Coefficient
Surface	0.98	0.2	0.011	0.99
900	0.95	0.3	0.012	0.99
850	0.93	0.3	0.014	0.98
800	0.83	0.6	0.014	0.97
700	0.79	0.7	0.025	0.92
600	0.93	0.4	0.041	0.90
500	0.87	0.3	0.051	0.89
400	0.80	0.1	0.084	0.87

The regression equations were applied to the long term median values of mixing ratios presented by Maher and Lee (1977) for the period 1957-1975 to calculate long term averages of total water vapour content. If the median value was not given, half the threshold limit was used. The regression coefficients derived from single station data were

used where the standard error was less than 0.05. Otherwise the results of all stations combined were used, (generally at or below 700 mb). A comparison of the results for Laverton with the average of the two sets of precipitable water figures obtained by Pierrehumbert (1972) for the period 1958-1969 is presented in Table 3.6. The greatest difference in the two sets is about 5 per cent.

Table 3.6

Total water vapour content for Laverton (2300 GMT) derived by regression from median mixing ratios for 1957-1975 (Maher and Lee, 1977) compared with monthly mean values for the period 1958-1969 (Pierrehumbert, 1972). Units are MJ m^{-2}.

Month	Water vapour content (MJ m^{-2}) derived by regression from median mixing ratios	Monthly mean water vapour content (MJ m^{-2}) from Pierrehumbert (1972)*
January	47.6	48.6
February	48.1	50.2
March	46.2	47.9
April	42.1	40.3
May	37.8	36.5
June	34.5	32.4
July	32.2	30.2
August	32.2	30.8
September	34.3	32.7
October	37.7	37.5
November	39.8	41.3
December	43.6	45.1
Year	39.7	39.5

* The average of the "exclusive" and "inclusive" values of Pierrehumbert (1972) were used.

3.2.4 Adjustment of Wind data for Mass Balance

As in the studies of Gruber (1970) and Behr and Speth (1977) the mass flux integrated over the total atmospheric column was found to be significantly different from zero, even for monthly mean winds. For example mean winds for January, 1974 showed a mean convergence of 6.5×10^{-3} Kg $m^{-2}s^{-1}$ implying an unrealistic surface pressure rise of 55 millibars per day. Observed pressure changes between successive months are generally less than 5 millibars or less than 0.5 per cent of the total mass. Assuming a typical value for the total atmospheric energy content of 2500 MJ m^{-2}, the maximum expected energy flux averaged over one month due to the surface pressure change alone is about 5 W m^{-2}, which is less than the standard error of the net radiation measurements. So for monthly mean conditions it is reasonable to assume that the integrated mass divergence should be zero.

On a daily basis the surface pressure change averaged over the total area could be as much as 10mb, and the corresponding energy flux associated with such a pressure change averaged over one day is about 300 W m^{-2}. This makes it unreasonable to assume zero mass divergence on a daily basis, although Behr and Speth (1977) appear to make this assumption. In the present study the required integrated mass divergence for a given day was calculated from the surface pressure change which occurred between the preceding and succeeding days.

Several objective techniques have been used to adjust for mass balance in energy budget studies. Gruber and O'Brien (1968) describe a technique for least squares minimisation with constraints. Using a Lagrangian undetermined multiplier the procedure chooses a least-squares smoothing of the wind components normal to the perimeter of the atmospheric box while requiring the winds to satisfy mass balance. The procedure considers an arbitrary atmospheric volume, round the perimeter of which are M sounding stations, each providing data at L levels. The total mass flux divergence α is assumed to be known from independent physical considerations.

$$\int_{P_t}^{P_b} \phi V_n \, ds \, dP/g = \alpha \qquad \ldots (3.14)$$

The wind data at each level are represented by a polynomial of degree N-1 where $N \leq M$. The stations are numbered from 1 to M and the one-dimensional space co-ordinate x_j of station j is the fractional distance round the perimeter (i.e. $x_j \leq 1$).

The appropriate polynomial for each level l is given by

$$_lP_n(x_j) = \sum_{i=1}^{n(l)} a_{il} x_j^{n-1} \qquad \ldots (3.15)$$

It is not necessary for the degree of the polynomial to be the same at all levels. The coefficients a_{il} are chosen by a least squares minimisation of the function S defined by:

$$S(a_{i_l}, \lambda) = \sum_{l=1}^{L} \sum_{j=1}^{M} (V_{jl} - {}_lP_n)^2 + \lambda \left(\sum_{l=1}^{L} F_l \sum_{j=1}^{M} W_{jl} P_n - g\alpha \right) \qquad \ldots (3.16)$$

where V_{jl} represents the normal wind component at station j and level l, and λ is an arbitrary Langrangian multiplier. The bracketed part of the second term on the right hand side expresses the integral in Eq. (3.14) as a finite integration of the value of the polynomial approximation at any station j and level l. The integration weights F_l (vertical) and W_j (horizontal) are determined by the particular finite integration used, which in this study was trapezoidal integration.

Gruber and O'Brien (1968) point out that the most appropriate least squares polynomial must be of sufficiently high degree that it provides a good approximation to the data, but not of such a high degree that the data is fitted too closely and the "noise" retained.

Further details of the solution of Eq. 3.16 are given in Appendix A2. The method was applied to one of the theoretical wind profiles with superimposed random error suggested by Gruber and O'Brien and also to actual mean monthly data. The divergence and vertical velocity at each level using actual and adjusted data are shown in Fig. 3.4(a) for January 1974. In this case a fifth degree polynomial (i.e. N = 6) was used at all levels.

The results obtained with the synthetic and actual data are similar to those of Gruber and O'Brien (1968) when N = M - 1 (their Fig. 6), namely, that a small adjustment of the same sign is made to the divergence at each level. It was found that when the horizontal spacing of stations and the vertical spacing of the pressure levels is uniform an equal adjustment to the divergence is made at all levels by uniform change to the normal wind components at all the stations.

When a polynomial of fourth degree (i.e. N = M - 2) was used it was found that for uniform horizontal spacings the adjustments to each level are the same as for N = M - 1, but the adjustment to the individual winds is not even. The changes to the individual winds tend to alternate in sign, and the magnitude of the changes at a given station depend on which station was chosen as the origin for the x co-ordinate. If the horizontal spacing of the stations is not uniform, then the adjustments may even alternate in sign in the vertical.

For lower degree polynomials the adjustments made were even larger and also varied in sign.

As the adjustments do not seem to be made on a physically realistic basis when N<M-1 it seems that the method outlined is suitable only for N = M -1. In this case, however, there is no need to solve the set of linear equations (Eq. 3.16) for each occasion as it was found that the outward normal wind component at each station and level was adjusted by the amount ΔV_{jl} given by:

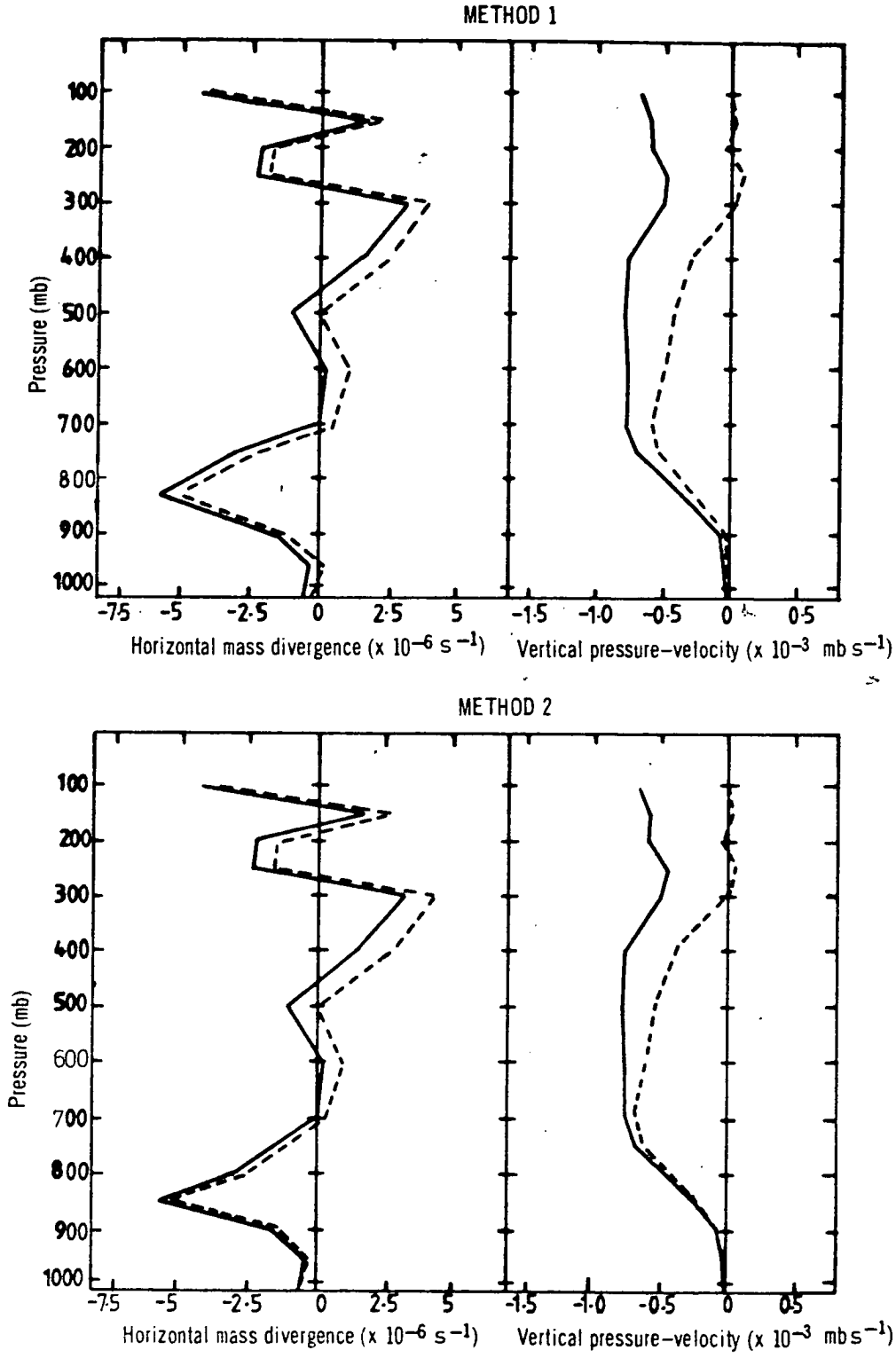

Fig. 3.4 Mean horizontal mass divergence and vertical pressure–velocity for January 1974 showing actual data (solid line) and values adjusted for mass balance (dashed line) using the two methods described in the text.

$$\Delta V_{j1} = -\left(F_{1}/\sum_{i=1}^{L} F_i^2\right) \left(W_j/\sum_{k=1}^{M} W_k^2\right) D \qquad \ldots (3.17)$$

where D is the difference between the observed and required mass divergence. For uniform vertical and horizontal spacings (F_1 and W_j) the ΔV_{j1} are uniform. As the directions of the outward normals are known, ΔV_{j1} can be added vectorically to the original wind vectors to obtain a set of adjusted wind observations that satisfy the mass divergence constraint. The procedure involves much less computation time than the solution of large matrices required by the initial statement of the technique, and makes its application on a daily basis feasible.

O'Brien (1970) suggests that because the errors in wind measurements increase with height, a uniform adjustment of the divergence estimates may not be the best form of correction. For observations at a single station with uniform vertical spacing he suggests an adjustment ΔD to the divergence at each level given by

$$\Delta D = -2kD/K(K+1) \qquad \ldots (3.18)$$

where k is the number of the level, ranging from 0 to K, and D is the difference between the required and observed vertically integrated divergence. O'Brien gives examples of the use of this form of adjustment in synoptic case studies.

The procedure could equally well be applied over a region with D referring to error in divergence over the region instead of at a single station. The general form of adjustment to the normal wind component would become:

$$\Delta V_{j1} = -\left(W_j/\sum_{k=1}^{M} W_k^2\right) \left(F_1 \left(P_o - P_1\right) D/\sum_{i=1}^{L} \left(F_i^2 (P_o - P_i)\right)\right) \qquad \ldots (3.19)$$

where P_1 is the pressure at level 1 and P_o is the surface pressure. Adjustments of this form (denoted as Method 2) for January 1974 are displayed in Fig. 3.4.

Both methods were tested in the evaluation of energy fluxes. It was found that the first method gave better results but details of comparison are deferred until Section 3.3.

A third form of adjustment is used by Behr and Speth (1977). They assume that the error in mass divergence is distributed uniformly round the perimeter of the atmospheric box and linearly distributed according to pressure increments in the vertical. However, this method was not attempted in the present study.

3.3 Results

3.3.1 Satellite Radiation Observations

From the mesh used by NOAA, grid points were selected so that the area sampled approximated the region of interest for this study. The grid points used and the area represented are shown in Fig. 3.5. It had originally been intended to calculate flux divergence measurements over two sub-areas to the north and south of the line Mildura-Wagga Wagga. Although this plan was not followed through due to limitations in the upper air data, satellite radiation data were extracted to represent these two sub-areas of the total area, denoted by AB. The grid-points used for each sub-area are also shown in Fig. 3.5.

Time series of the monthly mean absorbed short-wave, outgoing long wave, and net radiation at the top of the atmosphere for the three year period from June 1974 to May 1977 are shown in Fig. 3.6 for each sub-area. Values for AB are approximately the average of the values for A and B, and are given in Table 3.7. The outgoing long wave values are the average of the day-time and night-time measurements. Also shown in Fig. 3.6 are averages for each month based on all the data available (almost four complete years). As mentioned previously, due to

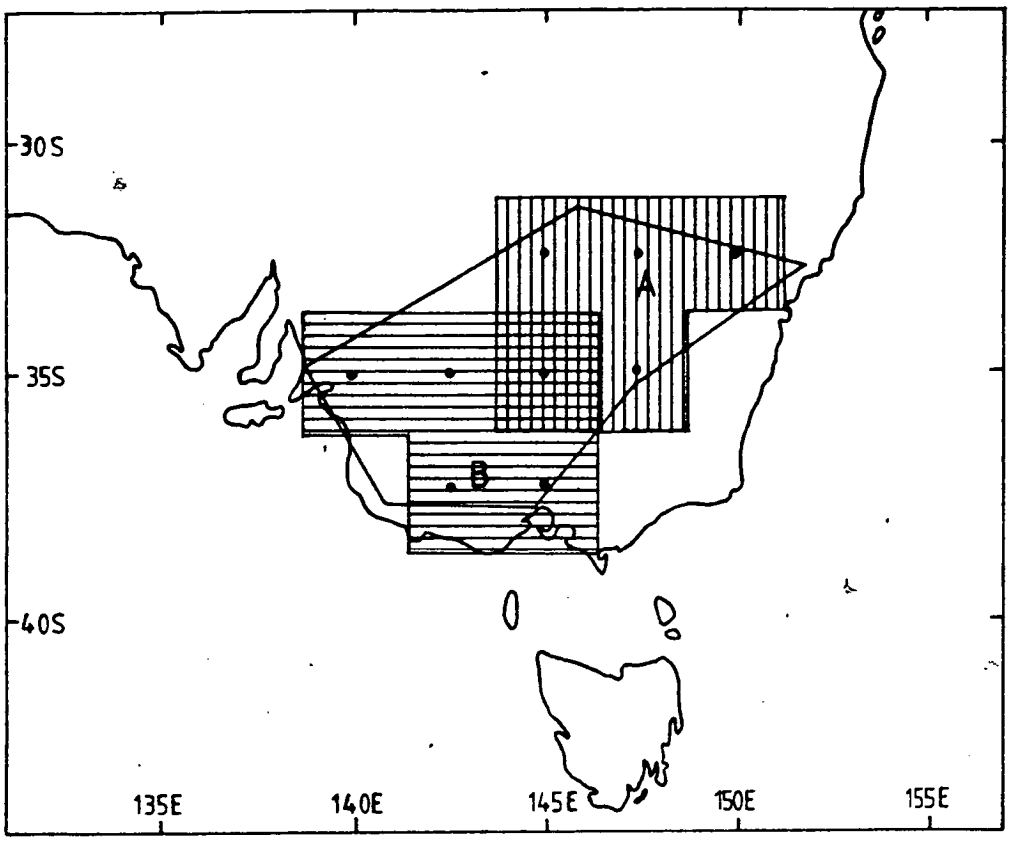

Fig. 3.5 Areas represented by the satellite data used in the study. Grid points for which satellite data were extracted are shown by dots. Sub-area A is shown by vertical hatching and sub-area B by horizontal hatching. Area AB was the total area covered by A and B. Also shown is the hexagon joining the six radiosonde stations.

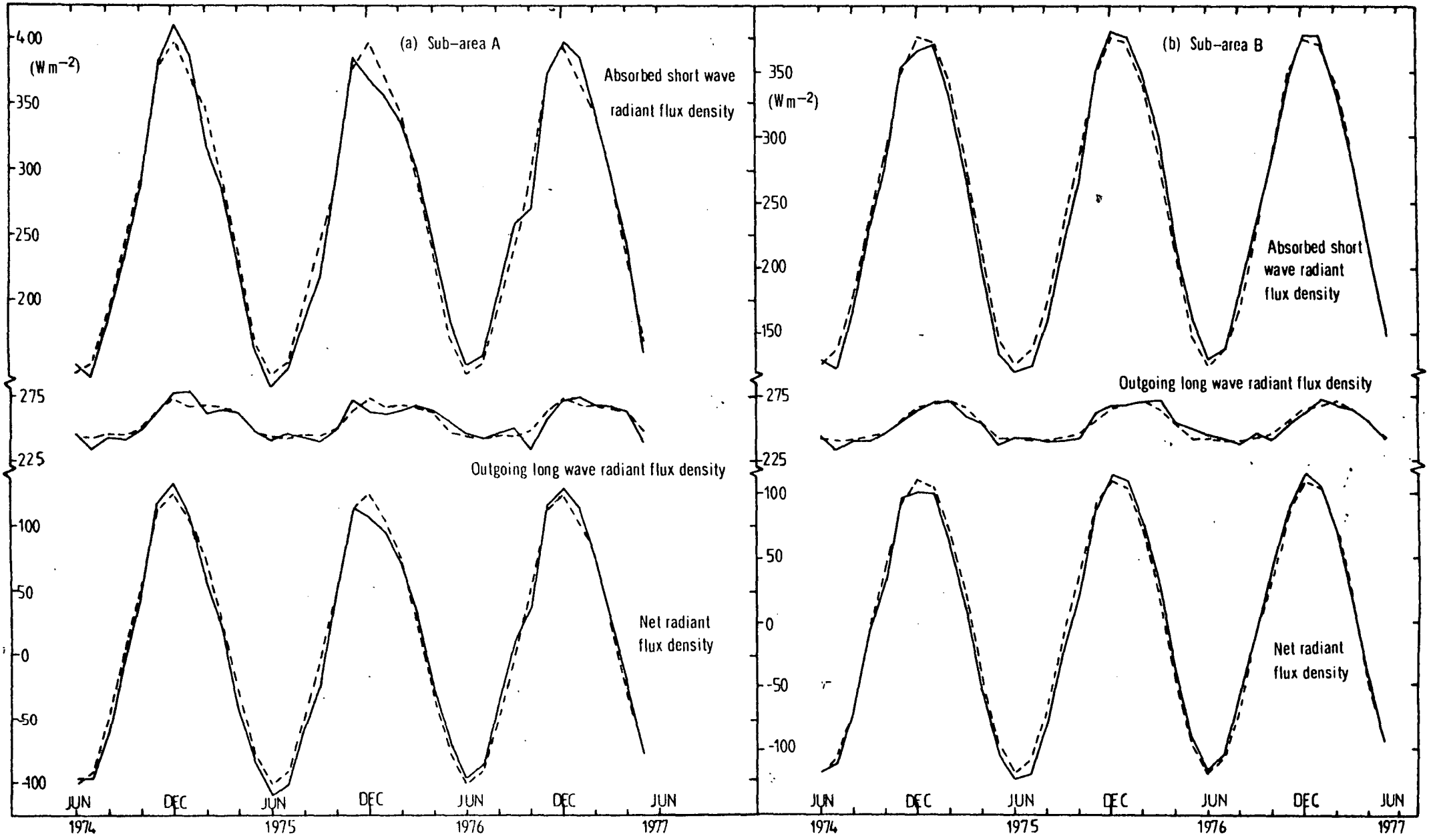

Fig. 3.6 NOAA satellite estimates of monthly average radiative flux density at the top of the atmosphere over the period June 1974 to May 1977 for (a) the northern sub-area A and (b) the southern sub-area B. Units are Wm^{-2}. Dashed lines represent the average for each month based on the 4 years of data available.

instrument malfunction the absorbed short wave radiation values for the period December 1975 to September 1976 may be systematically high by as much as five per cent (assuming a decrease of three per cent in the global average albedo of about 30 per cent). This may explain the high values of net radiation for 1976, although the values for 1977 are even higher.

The available solar radiation varies from 190 W m^{-2} to 505 W m^{-2} for area A and from 175 to 507 W m^{-2} for B. Albedo values for A are generally less than for B resulting in a slightly higher maximum of absorbed short wave radiation in A (about 400 W m^{-2} compared with 375 W m^{-2} in B). The average minimum over A exceeds that of B by about 20 W m^{-2}, slightly more than the difference in available solar radiation.

The amplitude of the outgoing long wave radiation is only about ten per cent of the amplitude of absorbed solar radiation, and irregularities are relatively more significant.

The net radiation curve is determined mainly by the absorbed short-wave radiation due to the small amplitude of the long-wave radiation variations.

Departures from the four year average for each month appear relatively slight in all three quantities. In most cases anomalies in the absorbed solar radiation are accompanied by small anomalies in the outgoing long wave radiation of the same sign, which compensate in part for the short wave anomalies. So net radiation anomalies are usually in phase with anomalies in the absorbed solar radiation but slightly smaller in magnitude. The average anomaly for absorbed short wave radiation over A was 11 W m^{-2} compared with 7.5 W m^{-2} for B with extreme values being -29 W m^{-2} in A (December 1975) and -17 W m^{-2} in B (October 1975).

The extreme departures of outgoing long wave radiation from the monthly average were -13 W m^{-2} for A (October 1976) and 7 W m^{-2} for B (-7 W m^{-2} in July 1974 and +7 W m^{-2} in May 1976). The highest departures for net radiation were -20 W m^{-2} for A (September 1975) and -14 W m^{-2} for B (August 1975).

Table 3.7

Atmospheric energy budget terms for the study area, 1974-1976. The atmospheric energy flux divergence was calculated as a residual from the net radiant flux density and storage terms. Units are W m^{-2}.

	Net radiant flux density Q^*_{TA}			Ground Storage S_G	Atmospheric Storage S_A			Atmospheric Energy Flux Divergence		
Month	1974	1975	1976		1974	1975	1976	1974	1975	1976
Jan	-	102.4	100.3	4.7	6.9	7.8	3.1	-	89.9	92.5
Feb	-	58.3	71.9	1.7	-5.6	1.3	-2.6	-	55.3	72.8
Mar	-	14.8	27.4	-1.7	-7.7	-6.2	-10.5	-	22.7	39.6
Apr	-	-47.9	-31.1	-4.7	-12.2	-6.6	-7.7	-	-36.6	-18.7
May	-	-93.8	-80.2	-6.4	-10.1	-9.6	-8.1	-	-77.8	-65.7
Jun	-106.9	-116.2	-107.2	-6.4	-7.7	-4.8	-4.2	-92.8	-105.0	-96.6
Jul	-104.3	-109.8	-96.1	-4.7	-1.9	-1.8	-2.3	-97.7	-103.3	-89.1
Aug	-67.2	-72.3	-49.3	-1.7	3.9	5.7	-0.5	-69.4	-76.3	-47.1
Sep	-7.0	-22.7	-0.2	1.7	6.4	5.8	2.4	-15.1	-30.2	-4.3
Oct	34.7	34.9	39.0	4.7	4.8	4.0	1.9	25.2	26.2	32.4
Nov	105.8	100.8	100.2	6.4	4.0	11.8	6.9	95.4	82.6	86.9
Dec	115.4	110.1	122.1	6.4	4.4	6.4	9.1	104.6	97.3	106.6
Yr	-	-3.5	8.1	0	-1.2	1.1	-1.0	-	-4.6	9.1

The departures from average were consistently of one sign for extended periods. The net radiation was mainly below the four year monthly average from July 1974 to November 1975 in B and to February 1976 in A (except for the summer months of 1974-5 in the latter case). This was succeeded by a period of generally above average net radiation which lasted until January 1977 (except October and November 1976 in A).

The departures of the absorbed short and emitted long wave radiation from the four year average for each month ($\Delta Q \downarrow$ and $\Delta Q \uparrow$ respectively) were linearly regressed and good correlations found. The regression equations and correlation coefficients (r) for the areas A and B are:

Area A

$$\Delta Q \uparrow = 0.375 \ \Delta Q \downarrow \qquad r = 0.90 \qquad \ldots (3.20)$$

(Standard error of estimate: 2.6 W m^{-2},

standard error of regression coefficient: 0.03)

Area B

$$\Delta Q \uparrow = 0.295 \ \Delta Q \downarrow \qquad r = 0.72 \qquad \ldots (3.21)$$

(Standard error of estimate: 2.5 W m^{-2},

standard error of regression coefficient: 0.04)

Because of autoregression in the monthly data the number of degrees of freedom will be less than the number of observations. The method of normalised correlation coefficients described by Davis (1976) and Sciremammano (1979) was used to test the significance levels of the above correlation coefficients which were both found to be better than the 0.1 per cent level.

The predominant cause of interannual variations in the absorbed short wave radiation will be differences in cloud cover, so the results

suggest that cloud cover variations affect the short wave component more than the long wave. Similar results have been found on a global basis by Ohring and Clapp (1980) using the NOAA data.

Further information on the relative roles of the long and short wave radiation components can be presented in the form of Fig. 3.7. Here the four-year monthly averages of the absorbed short and emitted long wave radiant flux densities are plotted as a scatter diagram. The straight line ($Q\uparrow = Q\downarrow$) applicable to a situation of no energy transport or storage reveals the departures of observed values from a case of local radiative equilibrium. These mean curves display the annual cycle. Inter-annual variations are perturbations from these curves governed by the linear relationships of Equations 3.20 and 3.21. The annual cycle shows a hysteresis effect with differences between the warming and cooling phases.

The curve for the study area (AB) is markedly different from that representing the zonal average for 35^{0}S between late spring and autumn. It shows a more rapid increase of its effective temperature in spring, higher peaks in summer and a more rapid cooling to about the same level as the zonal average in winter and early spring. These differences can be attributed to the difference in the underlying surfaces - land in the case of the study area and mostly sea for the zonal average. Other interesting features of the curves are segments with negative slope (e.g. from December to February in the zonal average) implying an increase in the effective temperature for a decrease in the available short wave input. Also noticeable is the relative constancy of the long wave flux from winter to mid-spring despite the large increase in the absorbed short wave radiation. In these cases the energy flux divergences and storage terms must alter so as to counteract the changes in the short wave radiation.

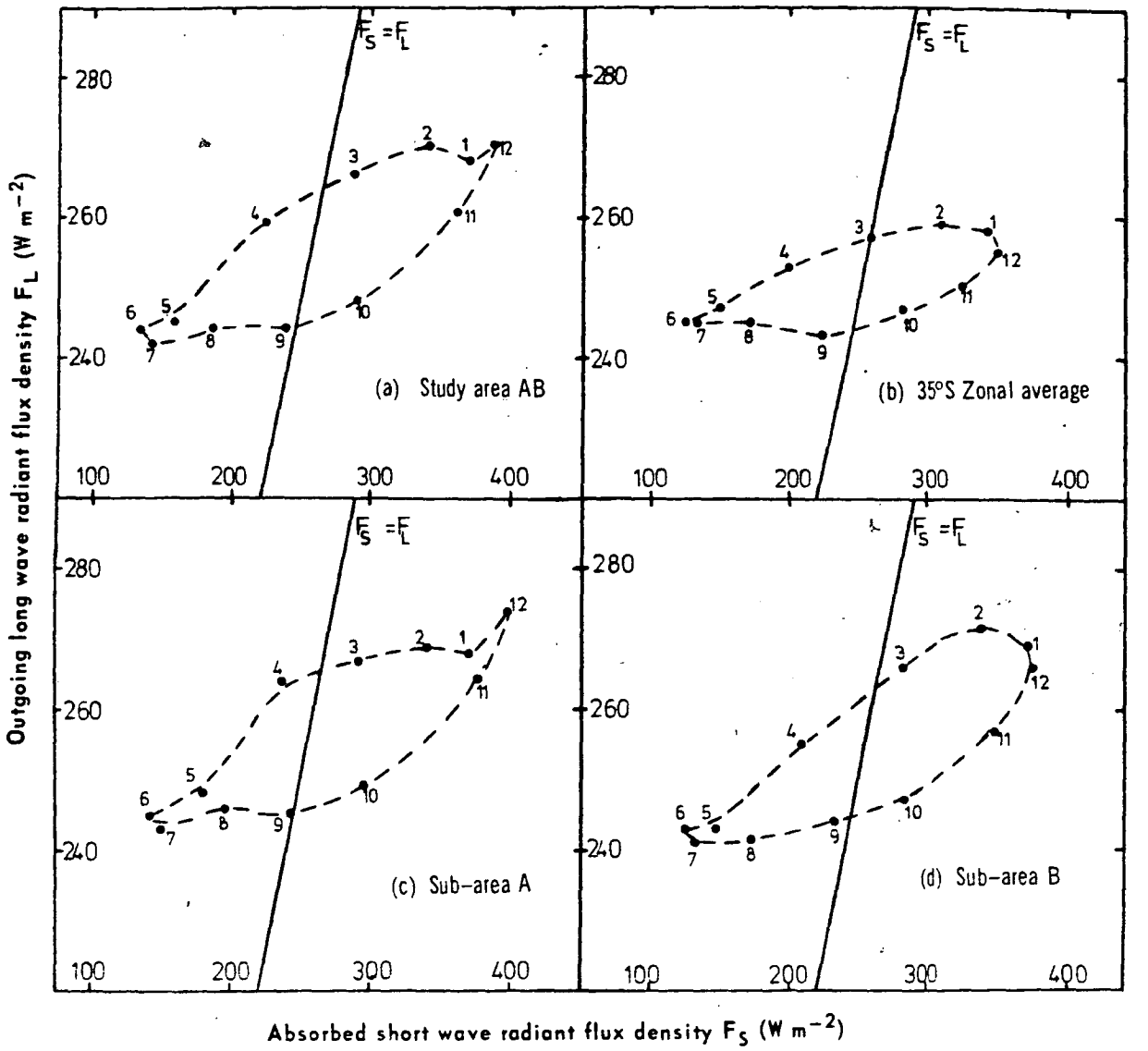

Fig. 3.7 Scatter diagram of monthly average absorbed short wave radiant flux density F_S and outgoing long wave radiant flux density F_L derived from NOAA satellite data. Units are Wm^{-2}. Numbers on the curves represent the number of the month (e.g. 1 January, ...).

Similar curves for the two sub-areas considered in the study (A, B) are also shown in Fig. 3.7. They reveal noticeable differences, particularly in summer and autumn when the long wave radiation for the northern area A drops away quickly from the December peak, presumably due to the southward movement of the inter-tropical convergence zone (ITCZ) and its associated cloudiness. The monthly average for January over A shows large inter-annual variations, a reflection of the erratic nature of the southward extent of the ITCZ. After this rapid drop the long wave radiation drops only slowly until late autumn when there is another steep fall to the mid-winter values. For sub-area B the long wave radiation increases until February and then drops away more slowly.

3.3.2 Atmospheric and Ground Storage

(a) Atmospheric Storage

The rate of energy storage in the atmosphere is given by the time derivative of the total energy of the atmospheric column, and is given by the first term on the right hand side of Eq. A1.11

$$S_A + S_Q = \frac{\partial}{\partial t} \int_{P_1}^{P_2} (V^2/_2 + CpT + Lq)\, dp/g \qquad \ldots (3.22)$$

Monthly mean values of atmospheric energy were found for the six radiosonde stations from daily 2300 GMT observations using trapezoidal integration between the daily surface pressure and 100 mb. The rate of energy storage for a given month was found from the difference in energy contents between the succeeding and preceding month, using an average of the six stations to represent the area AB. The data required for the two months December 1973 and January 1977 were obtained from monthly averages of upper air published by the Bureau of Meteorology, using the regression equations outlined in the previous section to determine the mean specific

humidity from the published median values. For kinetic energy, average December and January values for the 1974-1976 period were used.

The monthly rates of energy storage in the atmosphere from January 1974 to December 1976 are given in Table 3.7. The amplitude of this storage term is only about ten per cent of that for net radiation. However, in two of the years the rate of energy storage in the atmosphere became positive while the sign of net radiation was still strongly negative, and turned negative while the net radiation was strongly positive, implying that these energy changes were due to the flux divergence rather than the net radiation.

Time series of the total energy content and latent energy content between the surface and 100 mb for Laverton, Adelaide and Williamtown are presented in Fig. 3.8 along with long term averages for these stations calculated from data presented by Maher and Lee (1977). Long term means of kinetic energy were not available, so values averaged over the three years 1974-1976 only were used. The expected annual cycle dominates, with lowest values generally in July or August (although as late as October in Adelaide during 1976) and highest values in February. Inter-monthly variations, however, may be against the general seasonal trend. The latent energy cycle is in phase with the total energy cycle but also shows strong month-to-month variations.

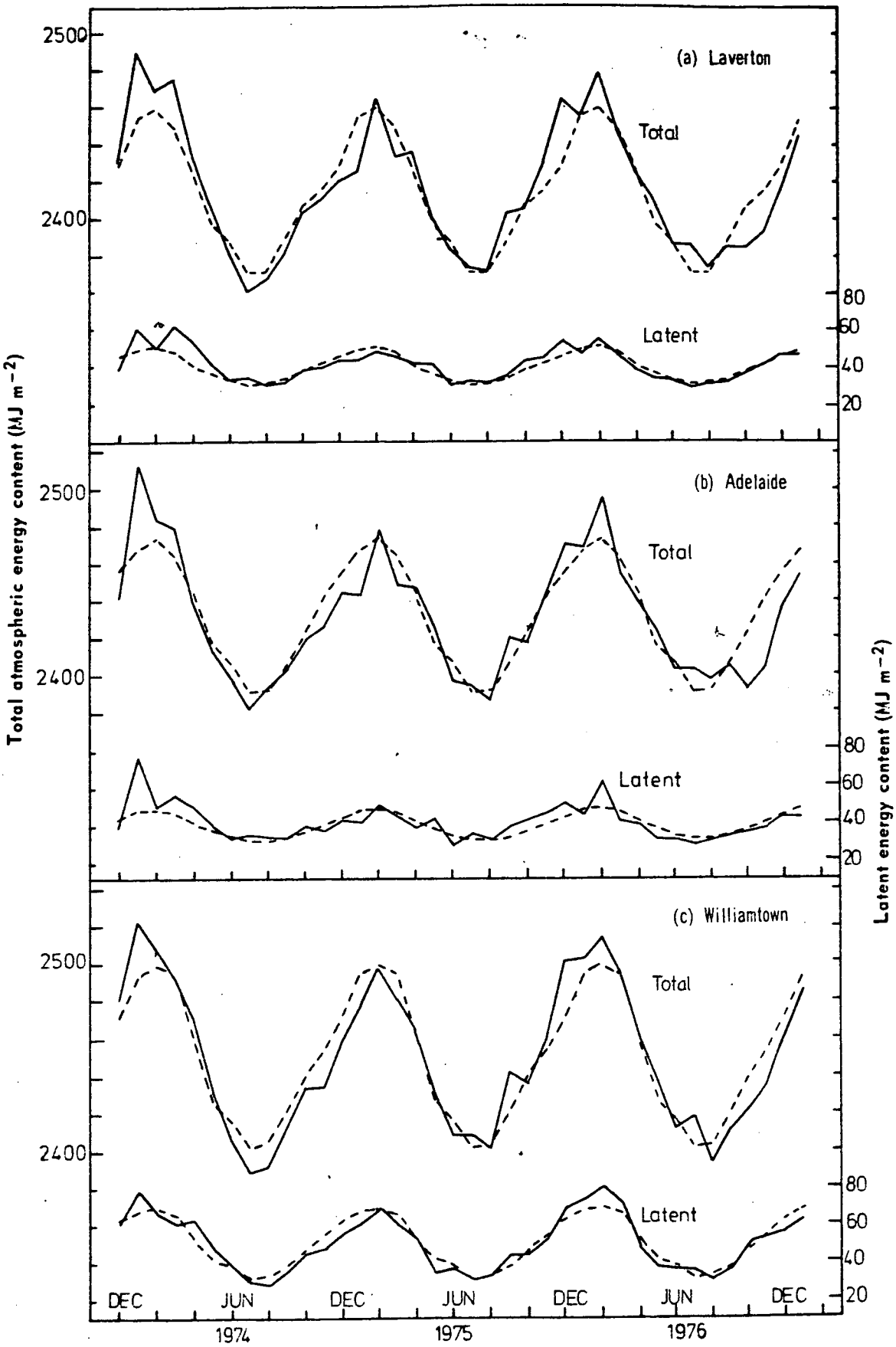

Fig. 3.8 Time series of the total atmospheric energy content (upper trace) and latent energy content (lower trace) for the period 1974–1976 at (a) Laverton, (b) Adelaide and (c) Williamtown based on 2300 GMT radiosonde observations from the surface to 100 mb. Dashed lines represent long term monthly averages calculated from Maher and Lee (1977). Units are MJ m^{-2}.

The long term average of total energy shows departures from a sinusoidal variation, a feature discussed by Oort (1971) in his Northern Hemisphere study. Between October and December the increase of total energy during the warming phase lags the variation at the surface due to marked cooling of the stratosphere. This effect is particularly noticeable at Laverton. The hump near June in the cooling phase corresponds to a period of marked warming at pressures below 250 mb associated with a lowering in the mean level of the tropopause.

The annual range of the long term averages of energy content for Laverton, Adelaide and Williamtown respectively are 89, 82 and 98 MJ m^{-2} for total energy and 20, 17 and 37 MJ m^{-2} for latent energy. The range of latent energy is about 20 per cent of the total range for Adelaide and Laverton, but near 40 per cent for Williamtown and Cobar, reflecting the greater role played by moisture in the energy balance at these equatorward stations.

(b) Ground Storage

The monthly average soil heat flux can be obtained by averaging Eq. 2.8 over a monthly period.

$$\text{i.e. } S_G(o,t) = \Delta T_o (2\pi\rho_s C_s \lambda/P)^{\frac{1}{2}} \sin(2\pi t/P + \pi/4) \quad \ldots(3.23)$$

An estimate of the surface amplitude ΔT_o and the date of maximum temperature are required. Because of the simplifications used in the derivation of this equation and uncertainties in estimates of the specific heat

of soil C_s, the rate of energy storage in the ground was determined from climatic averages of temperature rather than actual values over the period 1974 to 1976. Long term averages of the monthly mean temperature (Bureau of Meteorology, 1975) for the six stations shown in Fig. 3.1 were used to determine the average annual screen temperature amplitude. This was adjusted to a surface temperature amplitude by the factor 1.3 as described in Chapter 2. The monthly average screen temperatures showed an approximately sinusoidal variation through the year as required by the assumptions used in obtaining Eq. 3.23. The results are given in Table 3.7.

The amplitude of the ground storage cycle is 6.5 W m^{-2} and the terms are comparable with the atmospheric storage terms. A time derivative of the long term atmospheric energy curve (Fig. 3.8) shows that the rate of energy storage in the atmosphere leads that of ground storage by about one month in autumn, but that the two terms are approximately in phase during Spring.

3.3.3 *Energy Fluxes and Flux Divergence*

(a) Vertically Integrated Energy Fluxes

Vertical integrals from the surface to 100 mb of the combined sensible and latent energy flux for the six stations are shown in the form of a time series in Fig. 3.9. The total and eddy fluxes are both shown, in the form of a scalar magnitude and a direction. The three year averages for each month are given in Table 3.8.

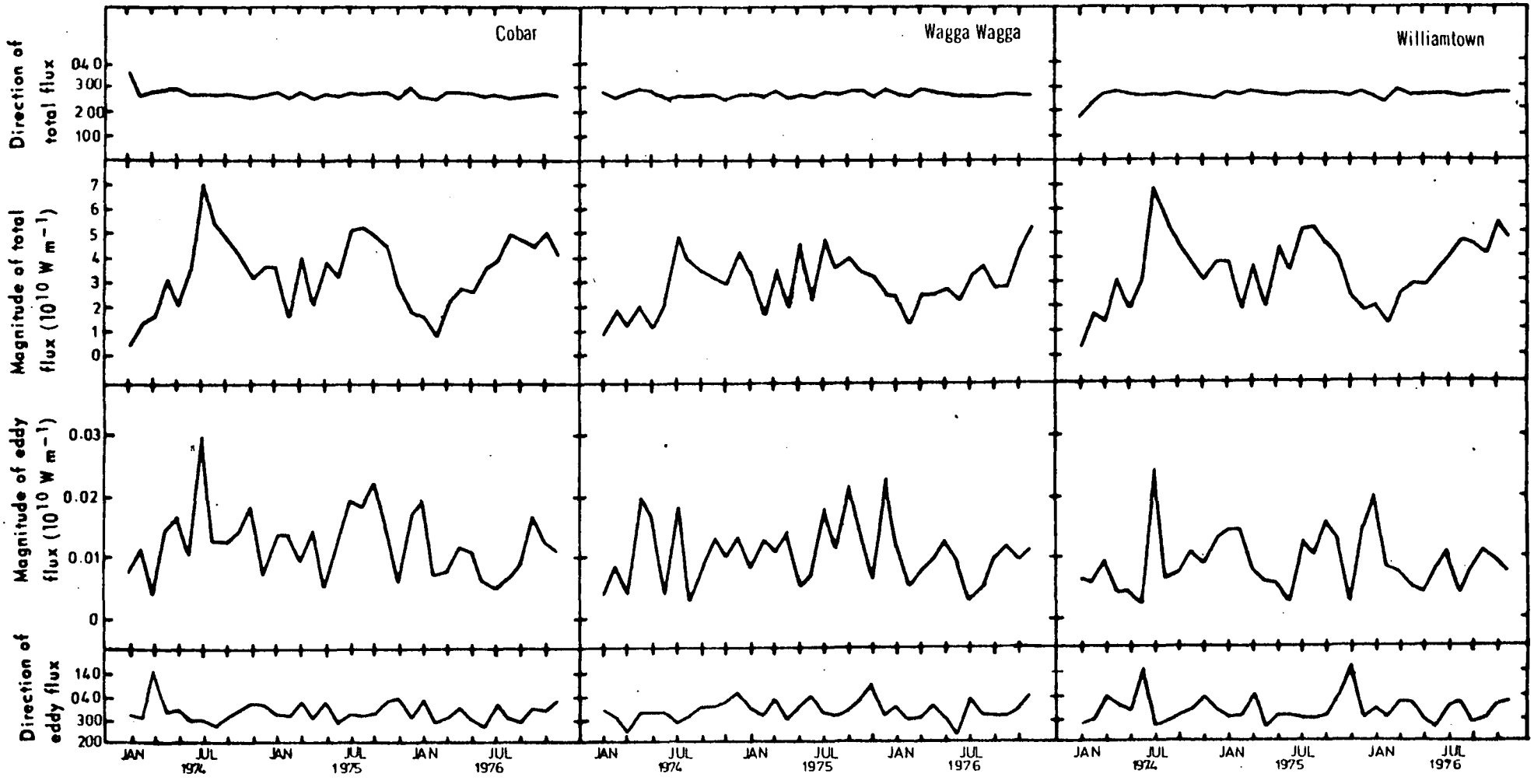

Fig. 3.9(a) Time series of the vertically integrated total and eddy flux magnitude and direction for the period January 1974 to December 1976 at Cobar, Wagga Wagga and Williamtown. Units of flux magnitude are 10^{10} W m^{-1}.

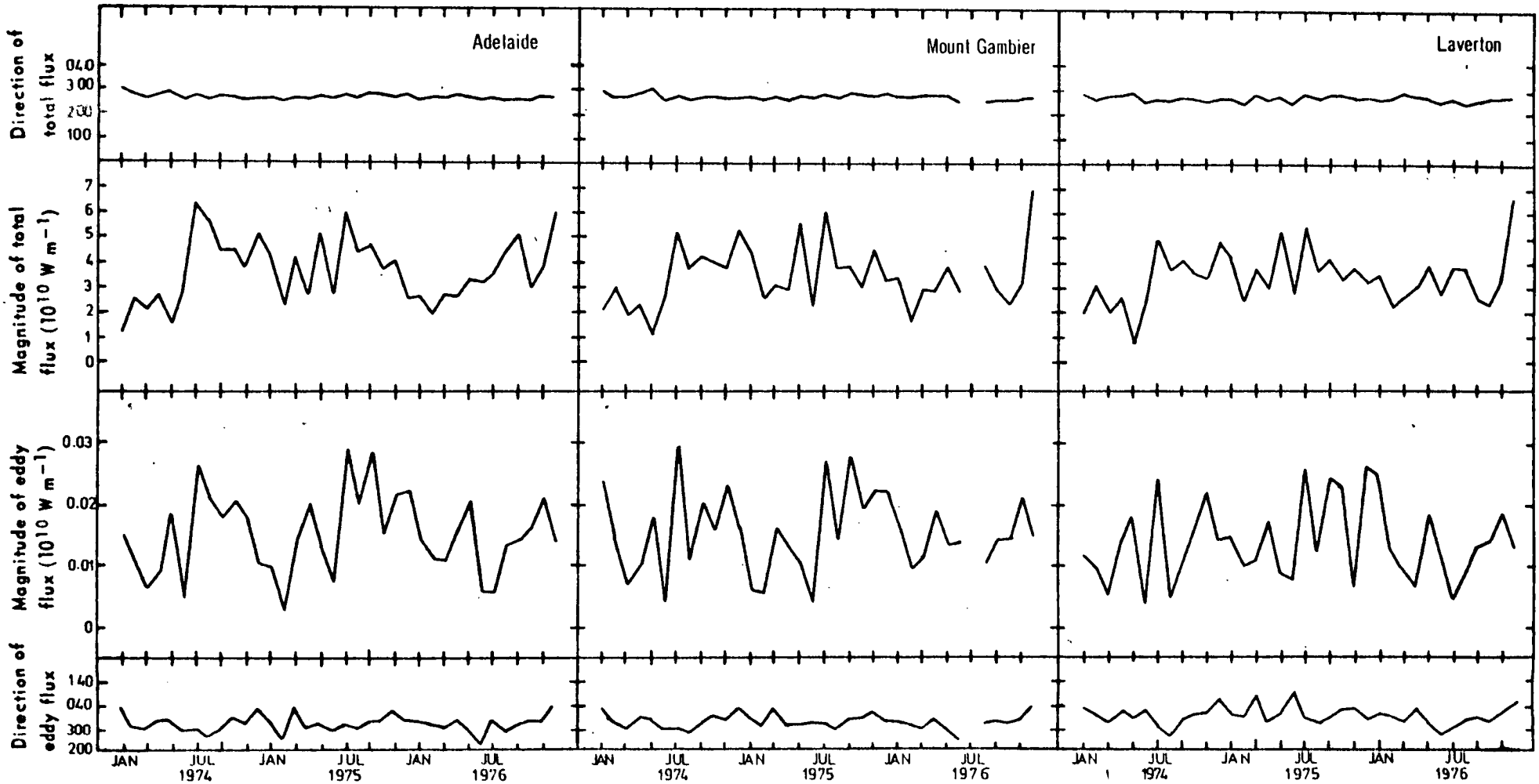

Fig. 3.9(b) Time series of the vertically integrated total and eddy flux magnitude and direction for the period January 1974 to December 1976 at Adelaide, Mount Gambier and Laverton. Units of flux magnitude are 10^{10} W m^{-1}.

Table 3.8

Monthly averages of Vertically Integrated Total and Eddy Flux (10^{10} W m^{-1}) for the three year period 1974-1976.

	Total Flux (10^{10} W m^{-1})						Eddy Flux (10^{10} W m^{-1})						Average of all Stations	
Month	Adelaide	Cobar	Williamtown	Wagga	Laverton	Mt Gambier	Adelaide	Cobar	Williamtown	Wagga	Laverton	Mt Gambier	Total	Eddy
January	2.7	2.0	2.0	2.2	3.2	3.3	0.013	0.014	0.014	0.008	0.018	0.016	2.6	0.014
February	2.2	1.3	1.5	1.6	2.5	2.3	0.008	0.011	0.010	0.009	0.011	0.010	1.9	0.010
March	3.1	2.7	2.5	2.4	2.8	3.0	0.010	0.007	0.009	0.008	0.009	0.012	2.7	0.009
April	2.7	2.7	2.6	2.2	2.8	2.7	0.015	0.014	0.005	0.015	0.013	0.014	2.6	0.013
May	3.3	2.9	3.1	2.9	3.3	3.5	0.018	0.011	0.005	0.012	0.016	0.014	3.2	0.013
June	2.9	3.5	3.3	2.3	2.5	2.5	0.006	0.010	0.005	0.007	0.008	0.007	2.8	0.007
July	5.3	5.4	5.3	4.3	4.9	5.6	0.020	0.018	0.017	0.013	0.019	0.028*	5.1	0.019
August	4.9	5.3	5.2	3.8	3.7	3.8	0.018	0.013	0.007	0.007	0.009	0.011	4.4	0.011
September	4.4	4.9	4.5	3.5	3.6	3.7	0.020	0.015	0.011	0.014	0.017	0.021	4.1	0.016
October	3.7	4.4	3.9	3.1	3.0	3.1	0.017	0.016	0.012	0.014	0.019	0.016	3.6	0.016
November	3.9	3.8	3.6	3.5	3.5	3.8	0.020	0.013	0.007	0.009	0.016	0.022	3.7	0.015
December	4.5	3.3	3.4	4.0	4.9	5.2	0.016	0.012	0.012	0.016	0.019	0.017	4.2	0.015
Annual	3.6	3.5	3.4	3.0	3.4	3.5	0.015	0.013	0.009	0.011	0.014	0.016	3.4	0.013

* Two years' data only

The greatest total flux occurs mostly in July with values in the second half of the year generally higher than those in the first half. This pattern can also be seen in the eddy flux, although the average September values are lower than some values in the first half of the year. In the time series an annual variation is only distinct at Cobar and Williamtown, and to a lesser extent at Adelaide. In the spatial average for the six stations the difference between June and July is quite striking. While July has the highest total and eddy flux, June has the lowest eddy flux and the fifth lowest total flux.

The eddy flux was generally less than one per cent of the total flux for each station, and as a percentage of the total flux showed little variation through the year or between stations although the lowest values generally occurred in the winter months, and the values for January at Cobar and Williamtown exceeded one per cent in 1974 and 1976. Ratios of the eddy to total flux averaged over the three years are given in Table 3.9.

The time series for each station reveal similar patterns. A strong peak in the total flux for July 1974 and July 1975 at Cobar, Williamtown and Adelaide is also evident at the other three stations, while troughs occurred at each station in March 1974 and February 1976.

Correlation coefficients (r) were calculated between the fluxes at two pairs of stations. For the total fluxes at Adelaide and Williamtown the correlation was

high ($r = 0.87$) but for the eddy fluxes, the correlation coefficient was only 0.25. For Laverton and Cobar the correlation coefficient for the eddy flux ($r = 0.74$) exceeded that for the total flux ($r = 0.55$) with both values lying between the Adelaide-Williamtown values.

The explanation for these correlations can be seen in the angles at which the fluxes are directed. The total flux is generally directed close to 270^0 (westerly) for all stations with little deviation, except when the flux has a very low value, such as at Williamtown in January 1974. Because the eddy flux is so small relative to the total flux, the mean flux is usually directed within half a degree of the total flux.

The direction of the eddy flux was much more variable. The average angles between the eddy and mean fluxes are listed in Table 3.10. The range used for the angles was from -180 to +180 degrees with the positive direction taken as clockwise from the mean to the eddy flux. The eddy flux is mostly directed at an angle of about $+60^0$ to the mean flux although negative angles did occur. In these cases either the eddy or mean flux was small. At least one station had a negative angle in each of the three June months considered. Table 3.10 shows that the angle was generally lowest in winter, and exceeded 90^0 on average in December. In the annual mean, the angle was lowest at Cobar (57^0) and highest at Mt Gambier (65^0).

The total and eddy fluxes are plotted in Fig. 3.10 as vectors for the mid-season months, and also for June in light of the difference in fluxes between June and July during the study period. The annual and inter-annual variations displayed are discussed further in Chapter 4.

Table 3.9

Monthly averages for the period 1974-1976 of the ratio of vertically integrated eddy flux to the vertically integrated total flux (expressed as a percentage).

Month	Adelaide	Cobar	Williamtown	Wagga	Laverton	Mt Gambier	Average
January	0.70	1.06	1.42	0.40	0.58	0.60	0.79
February	0.38	0.88	0.64	0.57	0.46	0.43	0.56
March	0.34	0.27	0.45	0.34	0.31	0.38	0.35
April	0.58	0.52	0.23	0.70	0.46	0.51	0.48
May	0.72	0.45	0.18	0.67	1.04	0.78	0.64
June	0.20	0.28	0.13	0.31	0.31	0.27	0.25
July	0.35	0.31	0.30	0.29	0.37	0.51*	0.35
August	0.38	0.23	0.13	0.18	0.24	0.29	0.24
September	0.46	0.29	0.24	0.39	0.48	0.57	0.41
October	0.48	0.35	0.30	0.43	0.61	0.56	0.45
November	0.52	0.35	0.19	0.26	0.47	0.60	0.40
December	0.45	0.46	0.45	0.49	0.45	0.40	0.45
Annual	0.46	0.45	0.39	0.42	0.48	0.49	0.45

* Based on two years' data only.

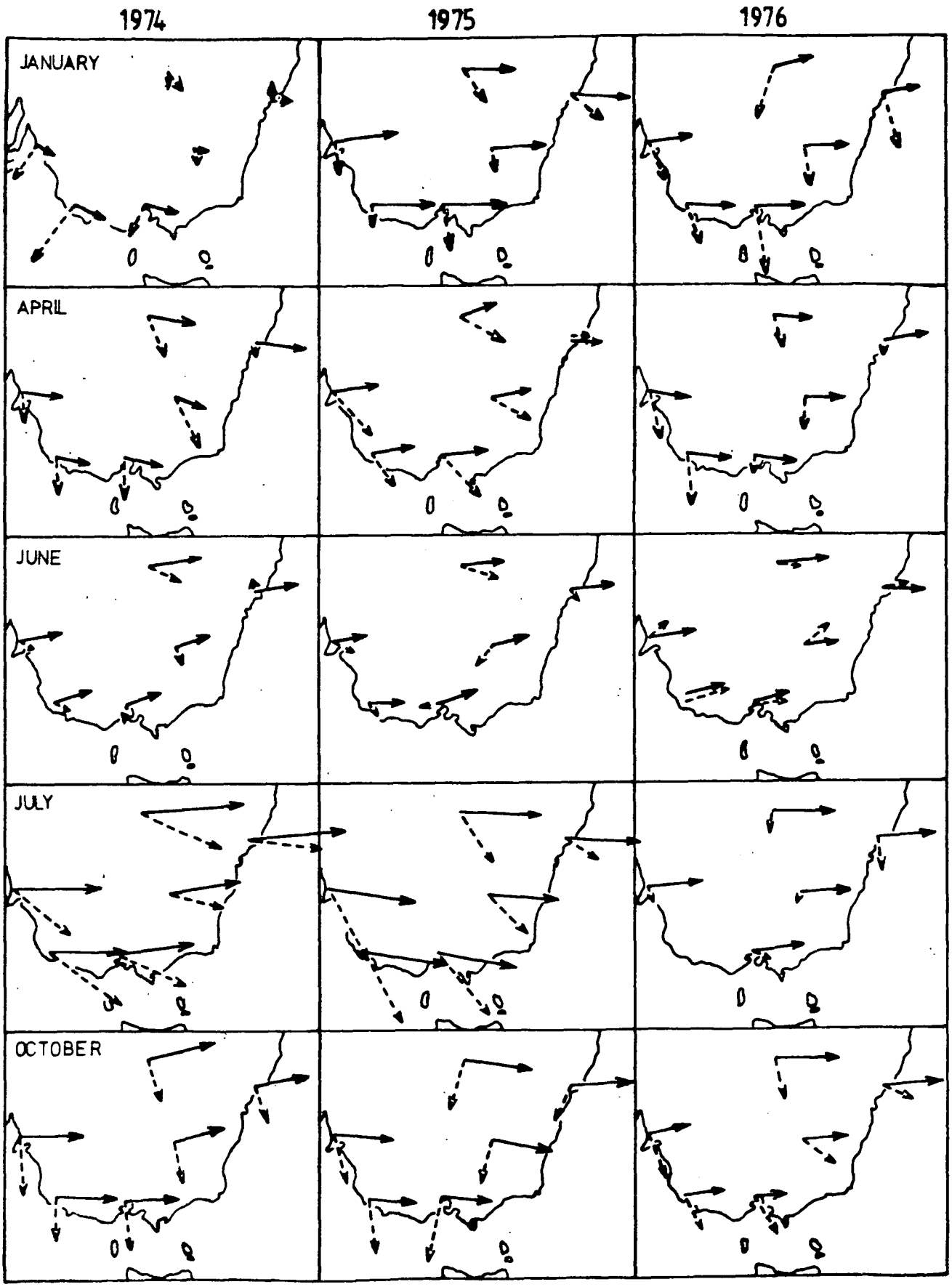

Fig. 3.10 Representation of the relative magnitudes and directions of the monthly average vertically integrated fluxes for January, April, June, July and October of the three years 1974 to 1976. Solid arrows represent the total flux and dashed arrows the eddy flux. Eddy fluxes have been magnified 150 times relative to the total flux.

Table 3.10

Monthly average angle (degrees) between the vertically integrated Mean and Eddy Fluxes (measured clockwise from the mean to the eddy vector) for the period 1974-76.

Month	Adelaide	Cobar	Williamtown	Wagga	Laverton	Mt Gambier	Average
January	84	53	76	73	85	82	76
February	36	54	65	49	79	61	57
March	77	6	109	32	75	64	61
April	63	62	62	55	74	72	65
May	51	70	53	59	50	41	54
June	18	24	-14	65	-14	41	20
July	54	61	43	64	33	43*	50
August	30	31	63	51	38	47	43
September	53	42	42	67	69	68	57
October	78	88	79	78	76	78	79
November	81	111	46	12	98	86	72
December	109	78	73	103	101	102	94
Annual	61	57	58	59	64	65	61

* Based on two years' data only.

(b) Vertical Profiles

Time series showing the vertical distribution of the i and j components of the total and eddy flux are shown in Fig. 3.11 for the three stations Laverton, Adelaide and Williamtown. These stations were chosen to represent a broad spatial range, and also on the basis of completeness of records. The total flux will be closely determined by the monthly mean i or j wind component as

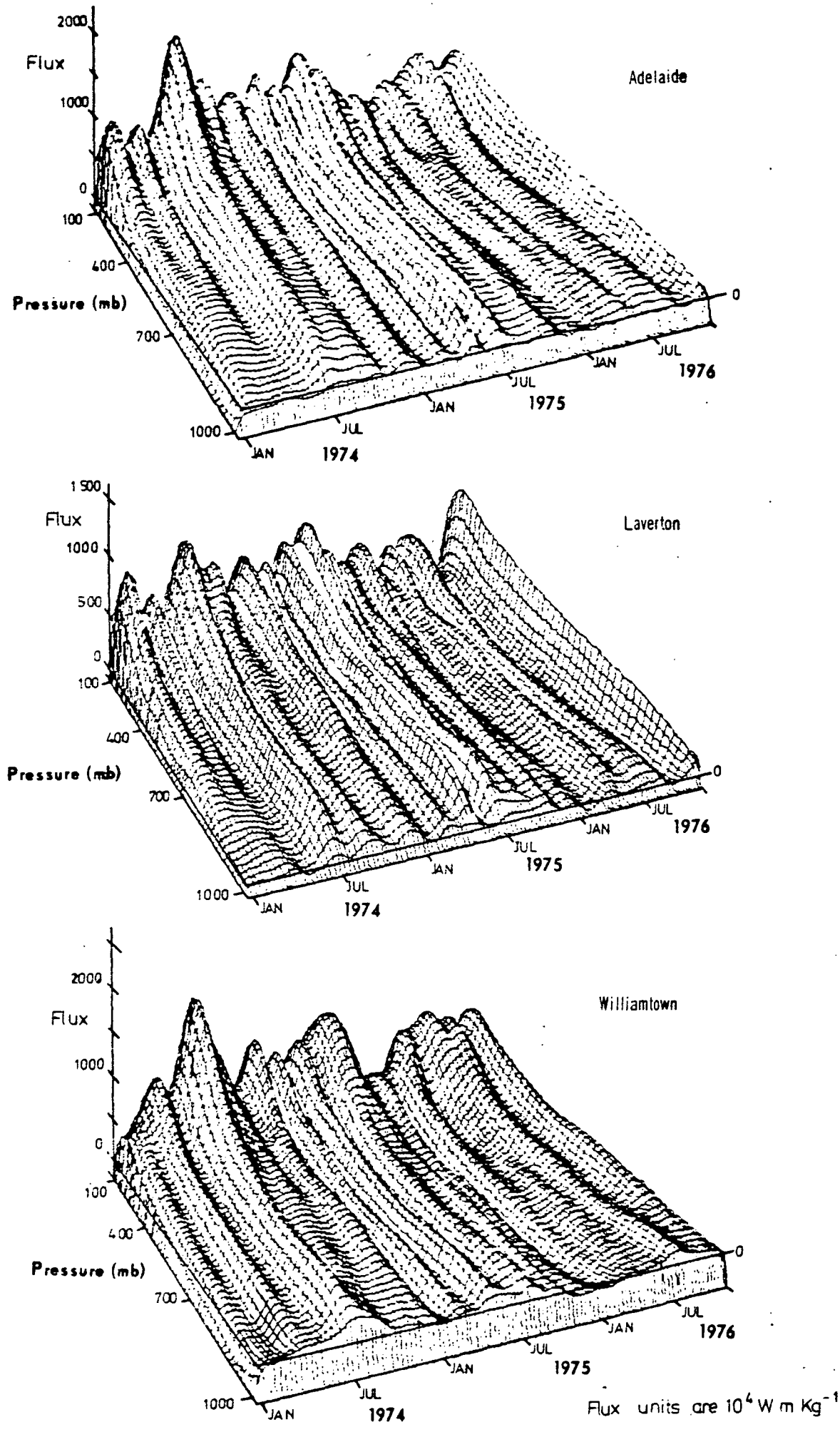

Fig. 3.11(a) Time series showing the vertical distribution of the total zonal flux.

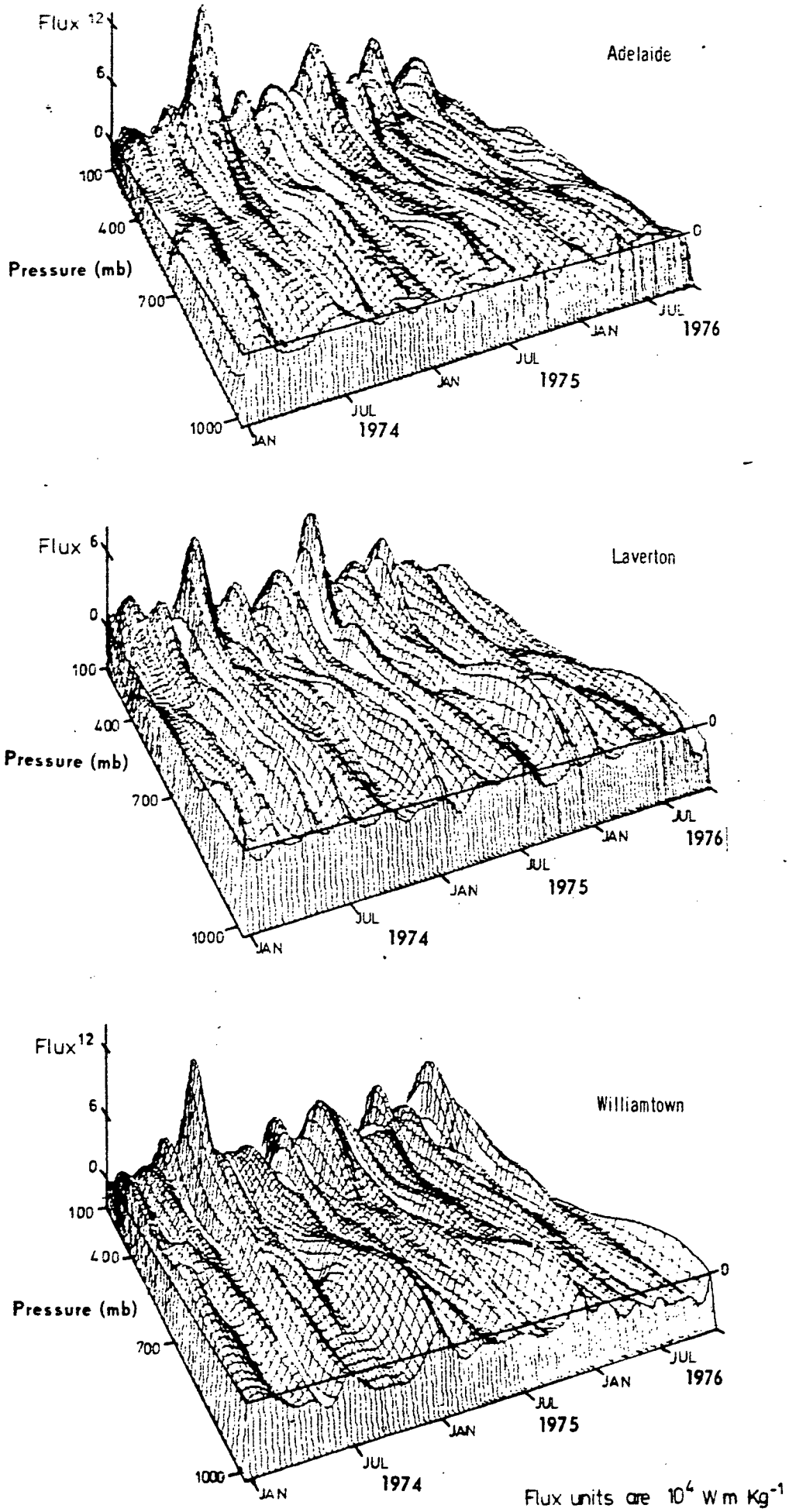

Fig. 3.11(b) Time series showing the vertical distribution of the eddy zonal flux.

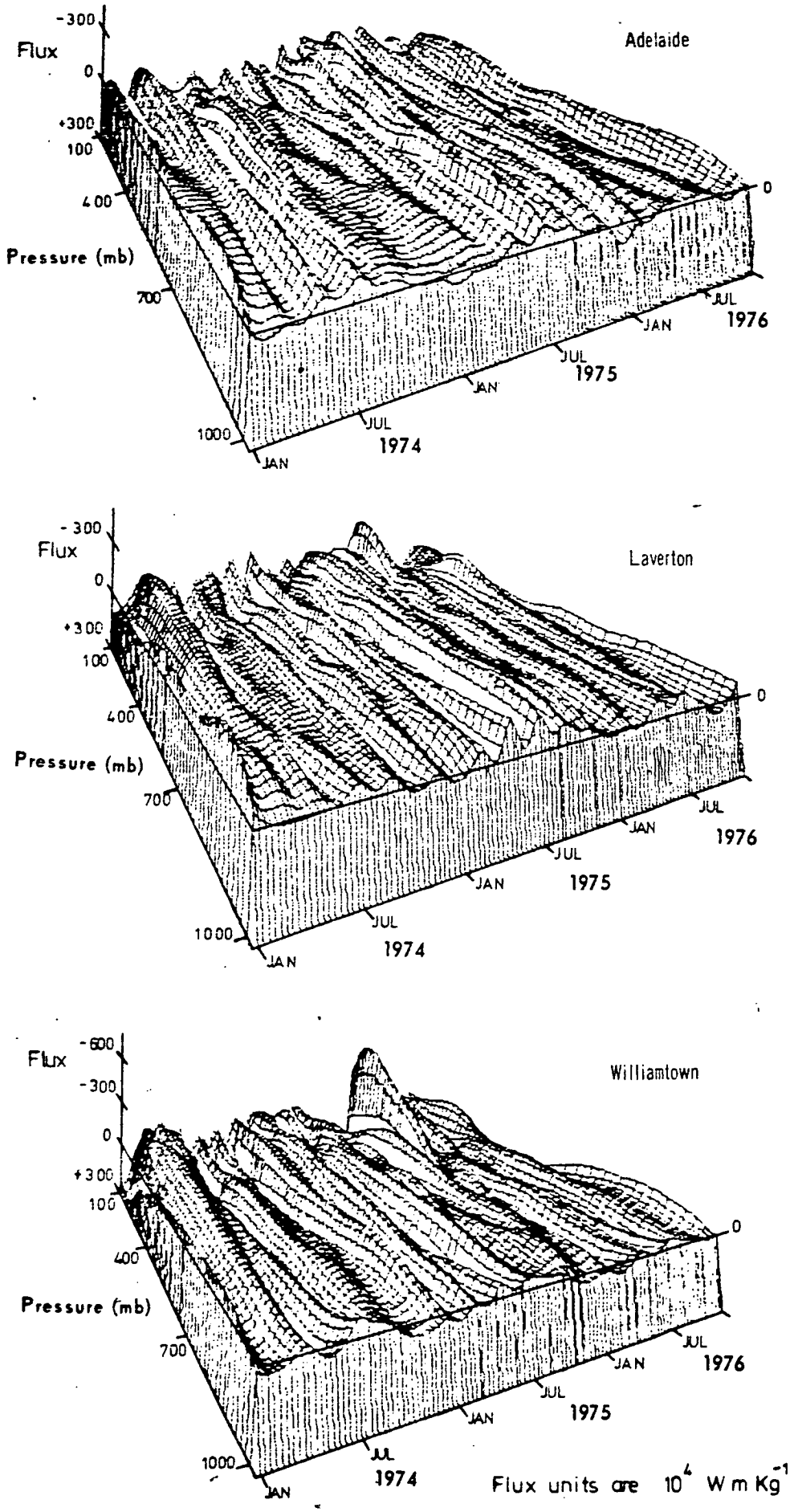

Fig. 3.11(c) Time series showing the vertical distribution of the total meridional flux (note that the direction of the flux axis has been reversed).

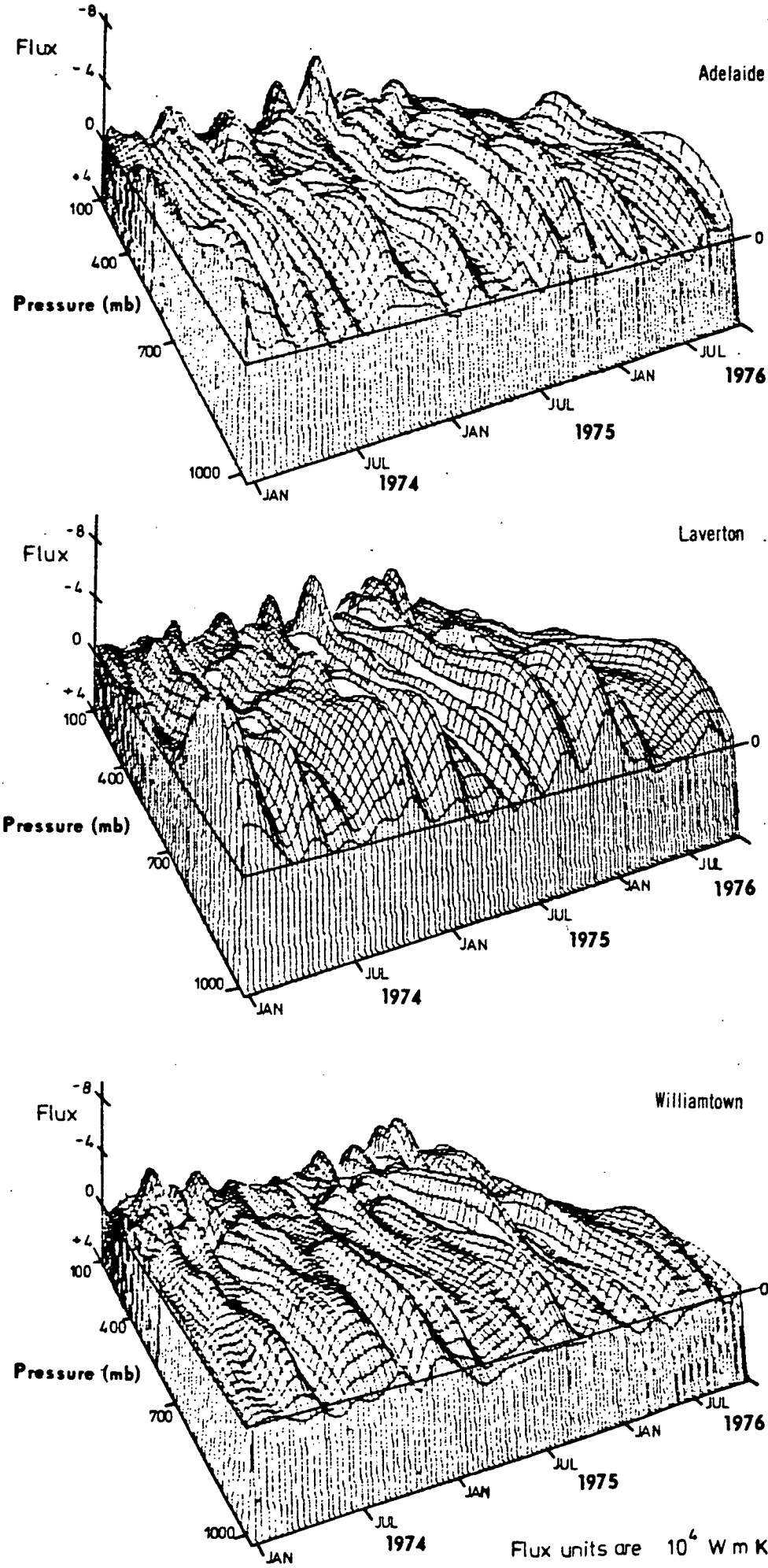

Fig. 3.11(d) Time series showing the vertical distribution of the eddy meridional flux (note that the direction of the flux axis has been reversed).

the total atmospheric energy varies only slowly with altitude. This is reflected in the high values of the total flux component, especially the i component, in the upper troposphere (e.g. the 100 mb layer centred on 200 mb). The i component of the flow is generally westerly, although easterly flow occurs at the 50 mb level, and also in the lower troposphere mainly during summer. In January 1974 the easterly flow extended to pressures below 500 mb at Williamtown with easterly flow up to the 700 mb level persisting until March. Easterly flow was well developed again in the 1975-1976 summer, whereas in the previous summer, easterly flow appeared only in February. The three figures for the i component show marked similarities, especially in the appearance of jet associated maxima near the 200 mb level. This is to be expected from the good correlation of the total flux discussed in the previous section.

Continuity between the three stations is not so evident in the cross sections of the j component of total flux. The highest values are less than those of the i component reflecting the predominant zonality of the winds over the region. There are alternations of direction temporally and also in the vertical. The highest value reached was a southerly flow at the 200 mb level at Williamtown in March 1976.

In contrast to the total flux, the zonal eddy flux shows alternations between easterly and westerly transport, although westerly flow predominates. The highest values occur in the upper troposphere, as for the total flux.

The maxima in the i component of eddy flux can be identified for each of the three stations, but there is no clear continuity of minor features between stations. The highest values for the three years occurred at the 300 mb level at each station, in July 1974 for Williamtown and Laverton and August 1974 for Adelaide.

The j component of the eddy flux is generally negative, i.e. directed southwards, although there is some northward transpórt, mainly in the upper troposphere. The meridional eddy flux shows a more uniform vertical distribution than the fluxes discussed above, although the largest values tend to occur at pressures exceeding 800 mb. This latter feature was noted for Laverton by NEA.

One feature noticeable in the eddy fluxes, particularly the i components at each of the stations, is a marked change from June to July in 1974 and 1975. The magnitude and usually the direction changed dramatically. The change was not so marked in 1976.

(c) Flux Divergence

The required energy flux divergences calculated as a residual from the net radiation and storage terms (Eq. 2.1) are given in Table 3.7. As the storage terms are generally small relative to the net radiation, the required flux divergence closely follows the net radiation.

Energy flux divergences calculated from the raw wind data revealed errors of several orders of magnitude. The errors were associated with physically unreal values of the mass flux divergence, indicating that corrections for mass balance were required, as discussed in Section 3.2. This was done for four months and these months were chosen to represent a variety of prevailing synoptic situations. However the selection was limited by the completeness of records, as data were required from each station at all levels for the calculation of mass flux divergence. No months had a complete set of records for all days at all levels, and interpolation of missing data was required. The number of observations available for the 500 and 100 mb levels are given for each station in Table 3.11. The interpolations were undertaken manually by considering time series at adjacent levels and nearby stations. For three of the stations, (Laverton, Adelaide and Williamtown) 1100 GMT radiosonde data were available, facilitating the interpolation. Upper wind data were also available at 0500, 1100 and 1700 GMT for all stations and these reports could be used to help fill gaps in the data.

The required mass divergence for a given day was calculated from the pressure difference between the succeeding and preceding day. Two processes were used as discussed in Section 3.2. The few months for which daily mass balance of the winds was attempted were February, April, July and August of 1975. The energy flux divergences before and after the mass balance adjustments are listed in Table 3.12 along with the required energy flux divergences as listed in Table 3.7.

The results show a dramatic improvement although the final values are still significantly in error. Merely ensuring a complete set of data reduced the error by an order of magnitude in three of the four months. Of the two methods used to adjust for mass balance, the first method (uniform correction in the vertical) consistently gives better results for these monthly averages. For a single flight the second method may be more useful. The values produced by the first method will be adopted for discussion.

Agreement between the derived and required energy flux divergence is best for February 1975, where the calculated flux divergence of 44 W m^{-2} differs by only 11 W m^{-2} from the required value. The discrepancy for August is disappointingly large, and much larger than that for July 1975. The agreement is worst for the months of July and August when there were most missing data.

Table 3.11

Number of Observations at the 500 and 100 mb levels in the months for which wind data were adjusted for mass balance.

Station	February 1975		April 1975		July 1975		August 1975	
	500	100	500	100	500	100	500	100
Adelaide	28	28	30	28	30	28	31	31
Cobar	28	26	30	28	31	25	30	21
Williamtown	28	28	28	25	31	30	31	30
Wagga Wagga	26	19	30	23	29	12*	29	14
Laverton	27	26	29	30	31	31	31	30
Mt Gambier	27	25	29	28	30	29	31	29

* 20 at 150 mb

Table 3.12

Energy flux divergence measurements ($W m^{-2}$) for four months in 1975 showing the effects of interpolating missing data and adjusting the winds for mass balance. The energy flux divergences of the zonal and meridional wind components (denoted i and j, respectively) are included in addition to results for the wind vector. Required flux divergences were extracted from Table 3.7. The mass balance techniques are discussed in the text.

	Total Flux divergence ($W m^{-2}$)			Eddy Flux divergence ($W m^{-2}$)			Mean Flux divergence ($W m^{-2}$)
	i	j	Vector	i	j	Vector	Vector
February 1975							
Required			55				
Raw data	-97	3912	3815	20	114	134	3681
Missing data interpolated	-3475	658	-2817	58	1	59	-2877
Mass balance 1	-2617	2661	44	54	-11	43	1
Mass balance 2	-2607	2697	90	55	-8	47	42
April 1975							
Required			-37				
Raw	-3831	-1930	-5761	23	-46	-23	-5737
Missing data interpolated	-5776	5032	-744	-41	35	-6	-737
Mass balance 1	-5543	5557	14	-39	34	-5	19
Mass balance 2	-5542	5566	24	-40	33	-7	31
July 1975							
Required			-103				
Raw	8080	3238	11319	-770	848	78	11240
Missing data interpolated	-8348	9047	699	2	36	38	661
Mass balance 1	-8606	8442	-164	6	44	50	-213
Mass balance 2	-8611	8429	-181	5	43	48	-229
August 1975							
Required			-76				
Raw	-5943	10066	4123	-62	80	18	4105
Missing data interpolated	-1372	1780	408	-71	-94	-165	573
Mass balance 1	-1563	1328	-235	-67	-92	-159	-76
Mass balance 2	-1565	1321	-244	-67	-89	-156	-89

The total and mean vector flux divergences are consistently a small difference between large zonal and meridional terms, although this pattern is less marked for August 1975. In each of the four months considered, there was energy convergence by the zonal component and divergence in the meridional term.

Eddy flux divergences in each of the four months are altered only slightly by the mass balance adjustments from the values obtained after interpolation to form a complete data set, while the adjustment for the divergence of the mean flux may be several orders of magnitude. This is particularly noticeable for February where the mean flux divergence is reduced from -2877 W m^{-2} to practically zero. The size of the adjustments made to the mean flux divergence and the fact that the latter is a small difference of two large terms derived from the i and j wind components, suggest that the mean energy flux divergence is poorly determined by the limited spatial and temporal sampling, whereas the eddy flux divergences may be realistic. It may be useful to accept the eddy flux divergence and infer the mean flux divergence from the difference between the observed and required divergences. In this case, the mass balance adjustments to the raw wind data would not be essential if the data were interpolated to form complete sets. This required mean flux divergence is given for the four months in Table 3.13 and, if realistic, indicates competing processes between mean and eddy flux divergence for July and August 1975.

Table 3.13

Estimates of the mean flux divergence (W m^{-2}) as a residual from the required energy flux divergence and the computed eddy flux divergence.

	February 1975	April 1975	July 1975	August 1975
Required Energy Flux divergence	55	-17	-103	-76
Computed Eddy Flux divergence	44	-5	49	-160
Residual Mean Flux divergence	11	-12	-152	84

The contributions of the various energy types (enthalpy, latent energy, etc) to the total flux divergence are discussed in Chapter 4.

An independent test of the latent energy flux divergence was made by attempting to estimate the terms of the water vapour budget (Eq. A1.15), using estimates of the precipitation and potential evaporation from Bureau of Meteorology surface data. As noted in Appendix A1 this approach is also subject to large errors. Monthly rainfall totals for the study were planimetered to derive an estimate of the areal average precipitation. To evaluate the areal evapotranspiration, estimates of open water evaporation were made from Bureau of Meteorology Class A Pan data by using the factors developed for two small lakes near the study area (Blue Lagoon and Lake Wyangan) by Hoy and Stephens (1979). These factors are 0.91, 0.87, 0.72 and 0.73 for February, April, July and August respectively. The open water evaporation was converted to an estimate of the potential evapotranspiration over vegetation using the simple crop factors of 0.8 for February, 0.7 for April and 0.6 for the winter months (Monteith, 1973).

Monthly station values were plotted and planimetered to obtain the areal average evaporation. Estimates of the small atmospheric moisture storage term were made from the changes in the latent energy component of the total atmospheric energy storage discussed in Section 3.3.2.

The results (Table 3.14) suggest that the measured latent energy flux divergences for July and August 1975 are of the wrong sign. In these months precipitation exceeded potential evapotranspiration, requiring moisture convergence, whereas the measured values show divergence. Precipitation over the region was close to average in July 1975 and well above average in August so that moisture convergence seems more plausible. It should be noted that these errors are still small components of the discrepancy in the total energy budget and, in fact, that a change to latent energy convergence would worsen the overall discrepancy for these two months.

Measured moisture divergences for February and April 1975 are in accord with the excess of potential evapotranspiration over precipitation. In February, where the overall energy budget discrepancy is small, inserting the measured flux divergence, storage and latent energy release due to precipitation in Eq. A1.15, suggests an actual evapotranspiration of only about half the potential rate. This seems feasible as the rainfall in this month and the preceding two months was below average over most of the study area, reducing the supply of soil moisture available for evapotranspiration. For April the actual evapotranspiration is about 70 per cent of the potential, if the measured moisture divergence is accepted.

Table 3.14

Terms in the moisture budget averaged over the study area for four months in 1975.

	February 1975	April 1975	July 1975	August 1975
Class A Pan evaporation - monthly total (mm)	230	114	67	71
Potential evapotranspiration over vegetation, ET (mm)	168	70	29	31
Monthly precipitation, R (mm)	25	16	45	48
ET - R (mm month^{-1})	143	54	-16	-17
ET - R (W m^{-2})	148	52	-15	-16
Moisture storage, S_Q (W m^{-2})	1	-2	0	1
Required latent energy flux divergence, ET - R - S_Q (W m^{-2})	147	54	-15	-17
Measured latent energy flux divergences (W m^{-2}):				
(a) raw data	-14	-30	-161	-57
(b) missing data interpolated	20	22	8	27
(c) after mass balancing	59	35	4	18

Table 3.14 also gives estimates of moisture divergence obtained before adjusting the winds for mass balance. The raw data, which had some missing observations, are very much in error, except perhaps in August. The mass balancing procedure gives the best results in each case. Even in water vapour budget studies it seems that a mass balancing procedure, as suggested by Rasmusson (1968), may be beneficial.

(d) Effect of Mass Balance Adjustment on Computed Fluxes

The effect of the mass balance procedure on the computed fluxes was considered by comparing the relative changes in the i and j components of the vertically integrated fluxes of the interpolated data sets before and after the adjustment for mass balance using the first method. This serves as a measure of the average correction made to the fluxes, although overestimating the changes where the flux components change sign in the vertical.

For the eastward component of the total and mean flux the change was mostly less than one per cent, with the largest change being two per cent. The changes made to the eastward eddy flux were also mostly less than one per cent, but one alteration was eleven per cent. This occurred on an occasion when the eddy flux was small, and changed sign several times in the vertical.

The northward component of the fluxes were modified to a greater extent. Although the changes were still mostly less than five per cent, there were several changes exceeding ten per cent, with the largest change being 29 per cent in the eddy flux at Adelaide for February 1975 and in the total flux for Laverton in August 1975. The vertical profiles of these fluxes before and after adjustment are

shown in Fig. 3.12. In both cases the vertically integrated flux was a small difference of oppositely directed fluxes, and neither the fluxes themselves nor the structure of the profile have been altered significantly by the mass balancing adjustments. The greater effect of the mass balancing on the meridional fluxes is attributed to this typical vertical profile. The zonal flux is generally more constant in sign throughout the atmosphere.

The effects on the vertically integrated vector fluxes were generally a change in magnitude by less than two per cent and a direction change of less than two degrees, as the largest relative changes were made to the generally small meridional components. For the case of February 1975 at Adelaide discussed above the effect on the vertically integrated eddy flux vector was a change of ten per cent in the magnitude and a rotation of five degrees. Because the energy flux divergence is a small term these small changes to the fluxes produce drastic changes to the computed energy flux divergence, but the discussion above on the fluxes is not invalidated.

3.3.4 *Sampling Errors*

(a) Missing Observations and Instrumental Errors

The effect of missing observations on the fluxes was investigated by comparing the fluxes calculated from the raw data with those where missing observations had been interpolated to form complete sets of data for a month. From the four months for which the data had been augmented, July 1975 at Wagga Wagga was selected as having the most missing observations. A comparison

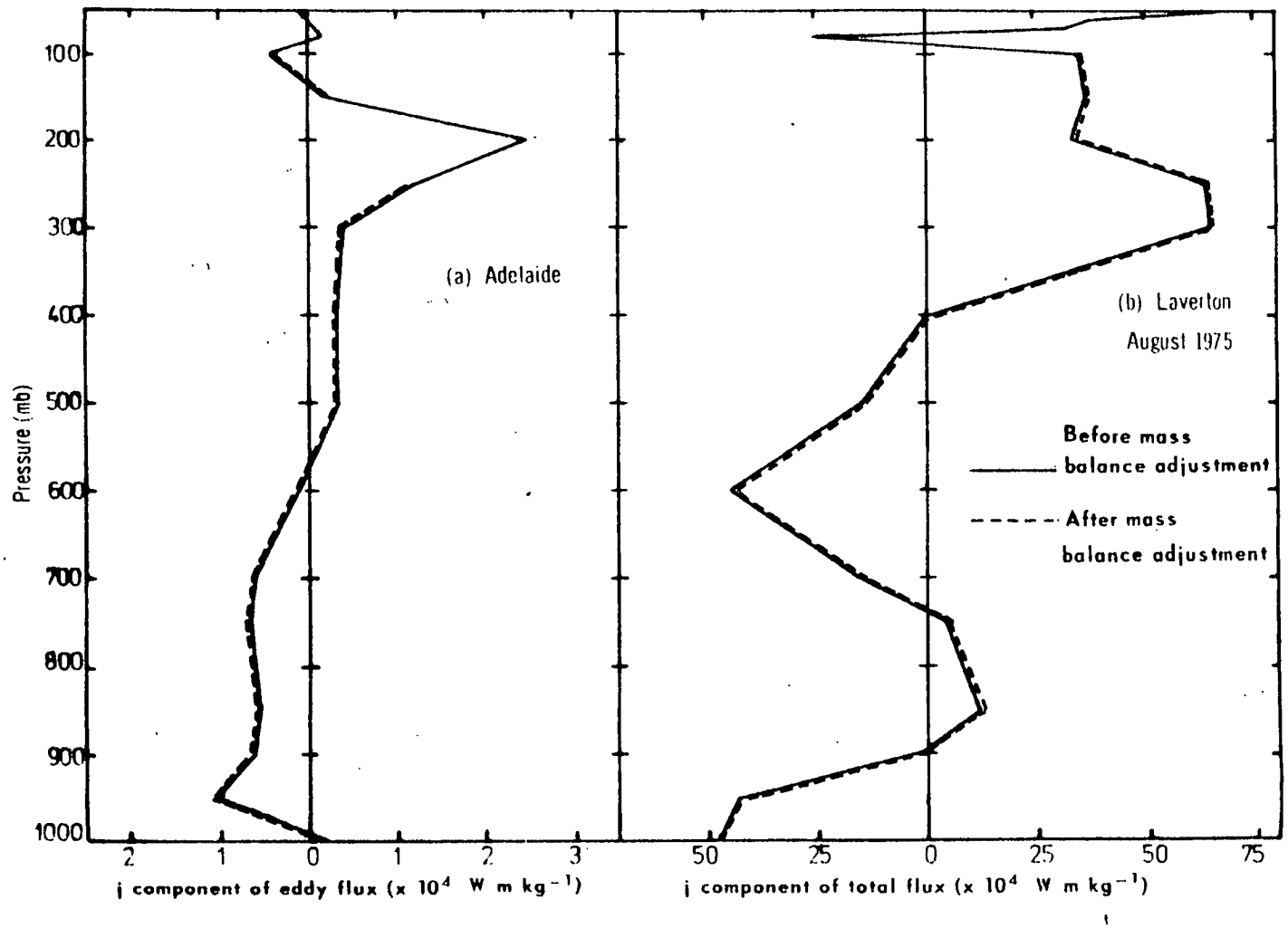

Fig. 3.12 Effect of the mass balance adjustments on (a) the j component of the eddy flux at Adelaide in February 1975, and (b) the j component of the total flux at Laverton in August 1975.

of the vertical profiles using the raw and augmented data is given in Fig. 3.13, with the number of observations available at each level in the raw data. Even one missing observation can cuase a significant difference in the calculated flux. The underestimation of the jet stream associated flux near the 200 mb level is in line with the findings of studies discussed in Section 3.2. The largest relative errors occur in the meridional total energy flux.

In the vertically integrated vector flux for the four months interpolation generally made only small differences, but for some stations the change in magnitude was as high as ten per cent for the total and mean flux and 30 per cent for the eddy flux. Direction changes were mostly less than two degrees although as high as seven degrees for the eddy flux. In the case of July 1975 at Wagga Wagga mentioned above, the changes to the vertically integrated fluxes are listed in Table 3.15.

The modifications made by the mass balance adjustment procedure were much less than the difference due to missing observations.

For the mean flux of the total energy E ($= gz + CpT + Lq + \frac{1}{2}V^2$) the instrumental errors will be dominated by errors in the wind observations as discussed in Section 3.1.2. The example given in that section, assuming the instrumental errors are random, suggests an error of about two per cent for the monthly mean zonal flux but about 20 per cent for the mean meridional flux where the average wind speed was of the same order of magnitude as the instrumental error.

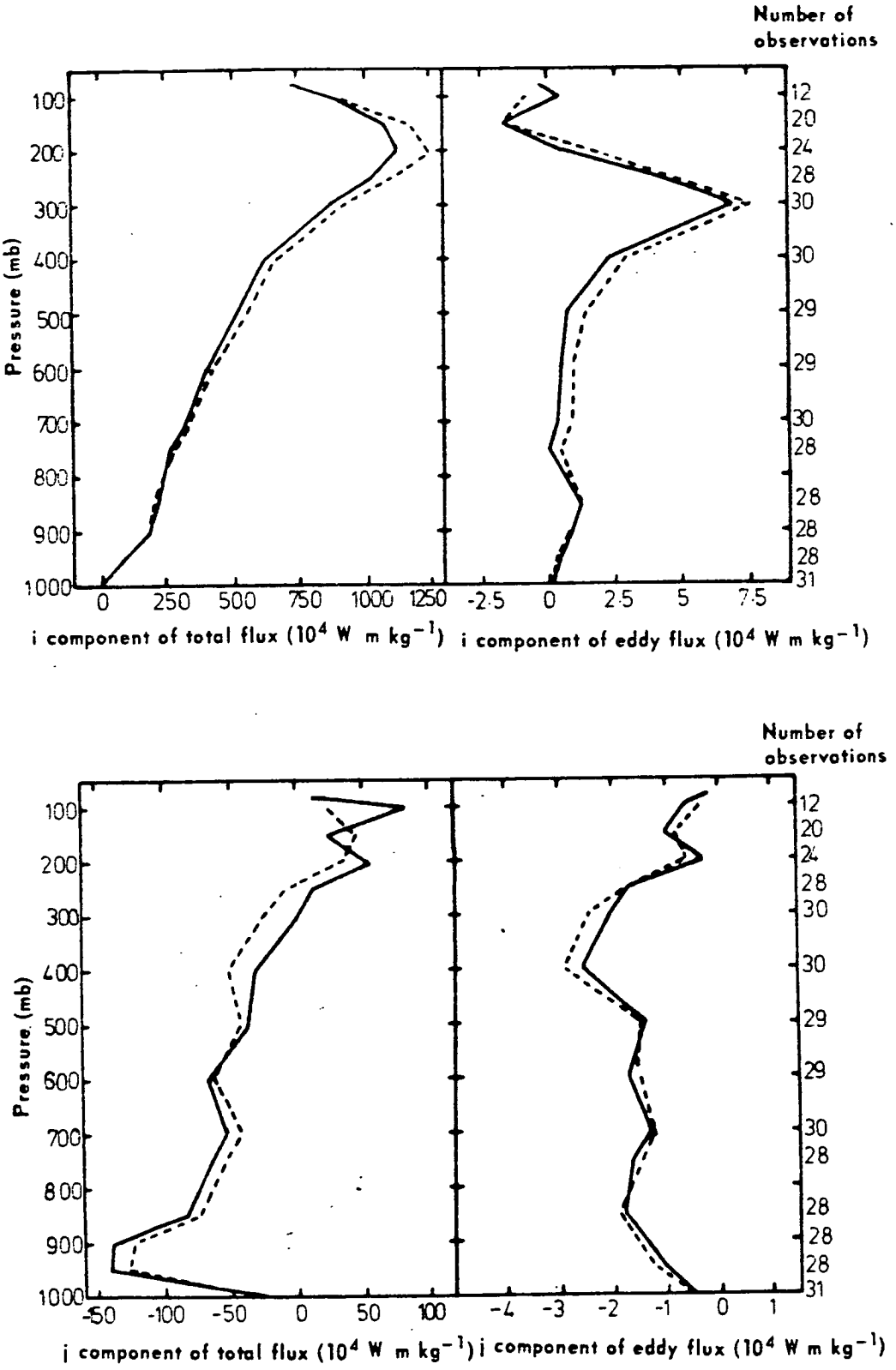

Fig. 3.13 Effects of missing data on the monthly average flux measurements at Wagga Wagga in July 1975. Values before (solid) and after (dashed) interpolating missing data are shown. The number of observations available at each level is shown on the right hand side.

For the eddy flux of the total energy, the latent energy flux will also be important at low levels, although the eddy fluxes of potential and kinetic energy are generally small. The error estimates in Section 3.1.2 suggest that the instrumental error in the monthly eddy fluxes could be between five and ten per cent.

For the vertically integrated fluxes these estimates for random instrumental error should be divided by about three as the data are summed over thirteen levels. This does not consider the other sources of error discussed in Section 3.1.2 that compound the purely instrumental errors. However, the profiles of Fig. 3.13 suggest that even a small number of missing observations can cause errors that exceed these observational errors.

(b) Temporal Sampling

Any consistent diurnal variations in the energy fluxes or radiation terms would not be sampled by the once daily satellite sampling or the use of only 2300 GMT upper air data. Diurnal variations in absorbed short wave radiation and outgoing long wave radiation could be studied using data from a geostationary satellite or a series of polar-orbiting satellites, but such data were not available for this study. Energy fluxes were calculated for the three stations at which 1100 GMT radiosonde and upper wind information was available. As the missing observations are crucial, as indicated in the previous section, the missing records were interpolated and a comparison made of these augmented 1100 and 2300 GMT data sets.

Table 3.16 gives the magnitude and direction of the vertically integrated fluxes at 2300 and 1100 GMT for February, July and August 1975. There are significant differences in the magnitude of the fluxes especially in February although for this month four complete 1100 GMT flights were missed at Adelaide and six at Laverton. The direction appears more consistent, especially for the total flux. The large change in the direction of the eddy flux for February at Adelaide occurs for a very low value of the eddy flux and may be partly due to the high number of missing observations.

However, the results in February suggest that the diurnal effect may be significant, especially in summer, and this raises doubts about the adequacy of using only once daily upper air observations. As they were not altered greatly by the mass balancing adjustments, the eddy flux divergences were re-calculated using an average of the 2300 and 1100 GMT fluxes where both were available, and 2300 GMT data otherwise. These divergences were compared with the values obtained using 2300 GMT data only (before mass balancing). The eddy flux divergences changed from 59 to 45 W m^{-2} in February 1975, 38 to 24 W m^{-2} in July but only from -165 to -167 W m^{-2} in August 1975. This may be an artificial test reflecting only the uncertainty in the eddy flux at each station, but it may also indicate that a once daily calculation is not sufficient, although when used with the mean flux divergences for 2300 GMT the disagreement between the estimated and required total flux divergences is accentuated rather than improved.

Table 3.15

Effects on the vertically integrated flux components at Wagga Wagga in July 1975 of interpolating missing data. Flux units are 10^{10}W m^{-1}. (Vertical profiles of the flux components are shown in Fig. 3.13).

Component	Raw data	Missing Observations Interpolated
i component of total flux	4.78	5.10
i component of eddy flux	0.012	0.016
j component of total flux	-0.37	-0.41
j component of eddy flux	-0.014	-0.015
Magnitude of total flux vector	4.79	5.11
Direction of total flux vector	274	274
Magnitude of eddy flux vector	0.019	0.021
Direction of eddy flux vector	319	313

(c) Spatial Sampling

Linear interpolation of the fluxes between adjacent stations is another possible source of error in the flux divergence calculations, especially where mountain ranges intervene between adjacent stations. The airflow over mountains, in particular the extent of blocking of the low level flow, is not well understood. The latent energy flux is likely to be most affected by the linear interpolation approximation due to its confinement to the lower layers. This problem, in the context of water vapour transport, has been discussed by Hutchings (1957). He considered the two extremes of

(i) linear variation between stations with all the flow below ridge level blocked, or

Table 3.16

Comparison of vertically integrated flux measurements for 1100 and 2300 GMT at Adelaide, Williamtown and Laverton. Missing data have been interpolated at both observation times. Flux units are 10^{10} W m^{-1}.

Time (GMT)	i component of flux total	i component of flux eddy	j component of flux total	j component of flux eddy	Total Flux Magnitude	Vector Direct'n	Eddy Flux Magnitude	Vector Direct'n
Adelaide February 1975								
1100	1.98	0.001	1.11	-0.003	2.27	241	0.003	350
2300	2.15	0.002	0.74	0.001	2.28	251	0.003	257
July 1975								
1100	5.85	0.020	-0.76	-0.023	5.90	278	0.030	319
2300	5.88	0.015	-0.90	-0.024	5.94	279	0.028	327
August 1975								
1100	4.22	0.018	0.56	-0.009	4.26	263	0.020	296
2300	4.35	0.017	0.55	-0.011	4.38	263	0.020	302
Williamtown February 1975								
1100	1.66	0.013	0.17	-0.015	1.67	264	0.020	319
2300	1.83	0.011	0.29	-0.010	1.85	261	0.015	312
July 1975								
1100	4.86	0.015	-0.08	-0.008	4.86	271	0.016	298
2300	5.10	0.011	-0.19	-0.007	5.11	272	0.013	305
August 1975								
1100	5.22	0.008	-0.17	-0.006	5.22	272	0.010	308
2300	5.21	0.009	-0.20	-0.006	5.21	272	0.010	304
Laverton February 1975								
1100	2.25	0.004	0.83	-0.006	2.40	250	0.007	329
2300	2.16	0.005	0.76	-0.009	2.29	251	0.010	333
July 1975								
1100	5.51	0.018	-1.11	-0.019	5.62	281	0.026	316
2300	5.54	0.017	-1.00	-0.021	5.63	280	0.027	321
August 1975								
1100	3.81	0.009	0.21	-0.008	3.81	267	0.013	312
2300	3.64	0.010	0.03	-0.008	3.64	270	0.013	310

(ii) the flow altered by the topography such that all the water vapour passes over or between the mountains.

This second case is equivalent to assuming that the mountains do not exist, and is described by a linear variation between stations. Hutchings concluded that this second option was more reasonable, although this would not be so for cases of orographically induced precipitation.

CHAPTER IV

DISCUSSION

Introduction

This chapter discusses the contribution of each energy type (enthalpy, latent energy, etc.) to the total flux and flux divergence, and the vertical profile of these terms. A brief investigation of the synoptic patterns that prevailed during the study period is included as an introduction to the discussion.

4.1 Synoptic situations and their relation to the measured energy fluxes

The relation of the energy fluxes to synoptic patterns has been the subject of several investigations. In a regional study for North America, Astling and Horn (1972) found that the type of synoptic disturbance played an important role in determining the poleward eddy flux of total energy with large amplitude troughs and closed lows (classified at the 500 mb level in their scheme) being most effective. The maximum transport occurs during the intensifying stage. Tucker (1979) found evidence that the poleward transient eddy transport of sensible energy in the southern hemisphere was carried out principally by individual low pressure systems and that the developing and mature stages of such systems were the most effective. He suggested that the observed latitudinal profile of the poleward transient eddy enthalpy flux may be due to the preponderance of different stages in the life cycle of such systems at different latitudes.

The daily (0900 EST) mean sea level isobaric analyses as published in the Bureau of Meteorology Monthly Weather Review series issued for each state, were classified according to the gradient wind direction over the study area, with a subsidiary classification into the curvature of the isobars. Four stream directions were used covering the quadrants centred on the cardinal points, with three further categories for situations where no single wind direction could be assigned. These covered (a) high

pressure systems or ridges, (b) troughs, low pressure systems or fronts with a marked wind change and (c) cols. The sub-classification for isobar curvature consisted of three categories - cyclonic, anticyclonic or indeterminate, the latter including both straight and mixed flow. Where fronts occurred without a marked wind change, the occurrence was included in the appropriate wind direction category. This scheme is similar in principle to the Lamb classification scheme as used by Murray and Lewis (1966).

The classification scheme could obviously be extended to include upper air patterns but was used as a simple index of the synoptic pattern over the study area. A step-wise multiple regression was applied to calculate the multiple correlation coefficient between the monthly totals in each category and the vertically integrated fluxes, and to assess the most useful predictors of the various fluxes. At each step in the regression program the next synoptic category to be entered is selected according to which will make the greatest reduction in the residual error sum of squares. This means that the variables are not necessarily selected in decreasing order of correlation with the dependant variable, due to correlations among the independent variables.

Histograms for each wind direction category on a monthly basis are shown in Fig. 4.1. Also shown are the combined totals of anticyclonic and cyclonic curvature.

The easterly and westerly categories show clear annual cycles with westerly winds common from late autumn to early spring, but rare in summer and early autumn, while the reverse pattern is displayed for easterly winds. The number of highs over the area was generally highest in winter, in line with the results of Karelsky (1961), while the frequency of lows was a minimum from about May to July.

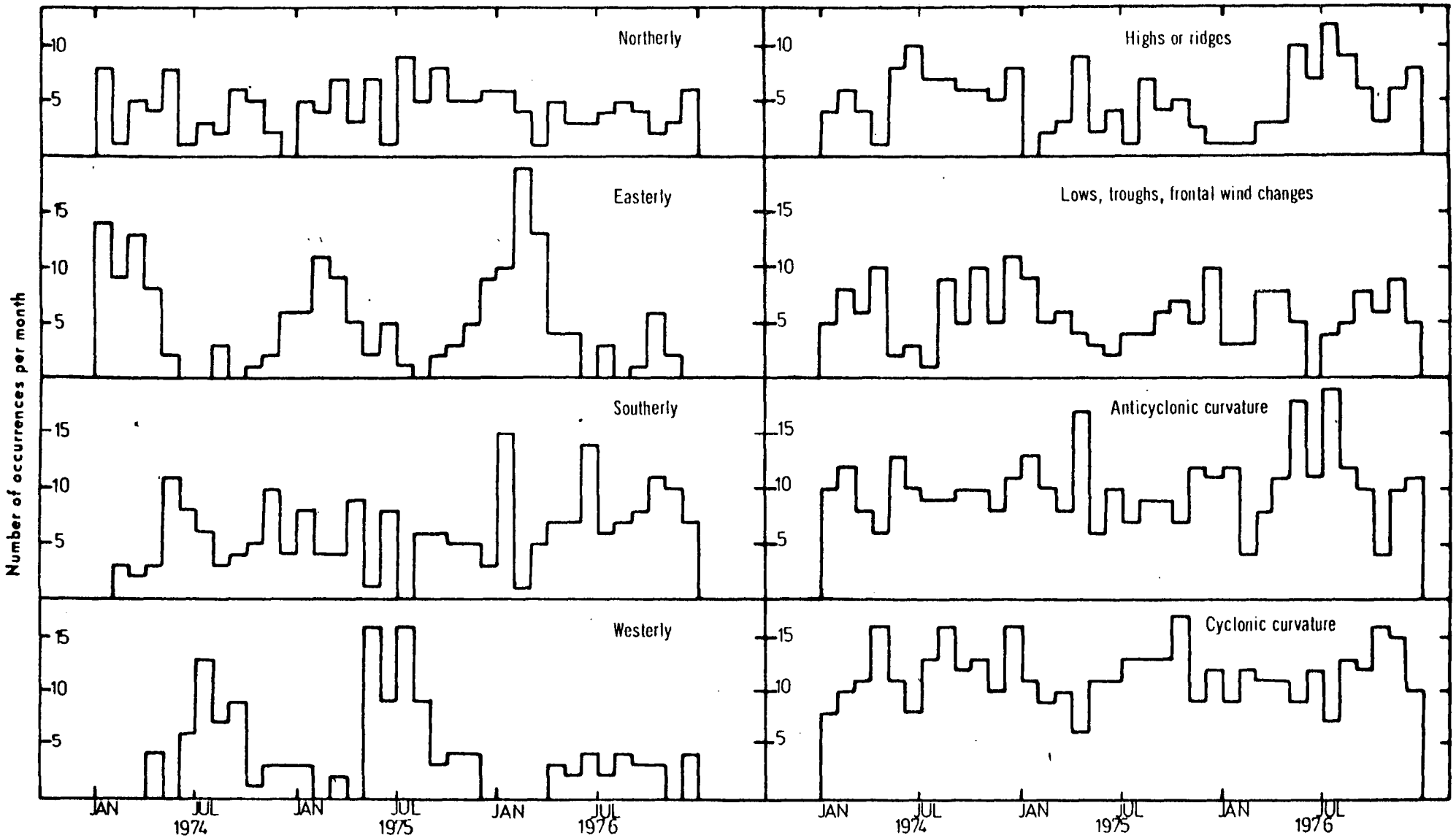

Fig. 4.1 Monthly totals in the wind direction and isobar curvature categories discussed in the text for the study area during the period 1974–76.

Some inter-annual variations can also be seen. The most noticeable is the relative absence of westerlies in 1976 which is apparently compensated for by an increase in the number of highs over the area. The period from April to August 1976 was very dry over most of the study area. Another marked feature is the high number of easterly situations from spring 1975 to autumn 1976, compared with the same period the previous year. Southerly situations were absent in January 1974 with a commensurate increase in northerly, easterly and high pressure centre occurrences.

Inspection of Fig. 3.9 shows that the major peaks in the frequency of westerlies also tend to be associated with peaks in the vertically integrated zonal total energy flux (e.g. July 1974, May 1975 and July 1975) while a low frequency of westerlies or frequent occurrence of easterlies tend to be associated with reduced zonal flux (e.g. May 1974 and most summer months).

Table 4.1

Multiple Correlation Coefficients (r) and Standard Errors of Estimate (SEE) between the vertically integrated fluxes and the synoptic categories. Units of standard error are 10^6 W m^{-1}.

Station	Zonal Total Flux		Zonal Eddy Flux		Meridional Total Flux		Meridional Eddy Flux	
	r	SEE	r	SEE	r	SEE	r	SEE
Adelaide	0.81	87	0.58	0.74	0.68	44	0.74	0.54
Cobar	0.89	80	0.52	0.70	0.69	47	0.73	0.46
Williamtown	0.89	80	0.48	0.63	0.64	44	0.56	0.44
Wagga	0.80	79	0.37	0.74	0.73	39	0.76	0.46
Laverton	0.71	94	0.43	0.76	0.76	43	0.70	0.59
Mt Gambier	0.76	98	0.59	0.68	0.74	39	0.70	0.60
Average	0.84	77	0.50	0.62	0.74	35	0.81	0.35

In the time cross-sections for the zonal total flux (Fig. 3.11) it can be seen that the peaks in the jet stream transport are also associated with greater transport in the lower troposphere, so that the surface wind regime is closely related to the vertically integrated flux. The correlation coefficients between the zonal total flux averaged over the six stations and the number of westerly and easterly occurrences in each month were 0.67 and -0.69 respectively. The significance levels of these correlation coefficients were tested using the method described in Section 3.3 and found to be at about the seven per cent level.

The correlation coefficients for the zonal fluxes at individual stations were of similar magnitude except at Laverton and Mt Gambier where significantly lower values were found (approximately 0.5) with a better correlation for westerlies than easterlies. The best correlation for easterlies occurred at Cobar ($r = -0.77$) and for westerlies at Williamtown ($r = 0.63$).

Correlations with the other categories were all much lower (less than 0.4). The step-wise multiple regression between the spatially averaged zonal total flux and all of the categories selected easterlies, southerlies, westerlies and lows as the first four variables and found a multiple regression coefficient of 0.84. The regression coefficients for easterlies and southerlies were negative. The multiple correlation coefficients for individual stations varied from 0.7 to 0.9 and are listed in Table 4.1.

The meridional total flux often changes sign in the vertical (see Fig. 3.11) and although there is good correspondence between the major peaks in the vertically integrated flux and high occurrence of northerlies (e.g. January and May 1974, July and September 1975) it is not so good for the southerly category. The correlation coefficients between the meridional total flux (averaged over the six stations) and the monthly totals of northerly and southerly situations were -0.58 and 0.34 respectively.

Using the method mentioned above, the correlation between the flux and the frequency of northerlies was found to have a significance level of one per cent, which was even more significant than the correlation between zonal total flux and easterlies due to less autocorrelation within the meridional data. The correlation with southerly occurrences, however, was less than with the number of highs ($r = 0.47$) and only slightly greater than with the number of easterlies ($r = -0.32$). For individual stations the correlation with the frequency of northerlies was highest at the three south coastal stations (the best being at Adelaide with $r = 0.63$) and worst at Williamtown ($r = 0.36$). At Williamtown and Wagga, the frequency of highs had a better correlation than the frequency of northerlies, but at all stations the correlation with southerlies was lower than for northerlies. The multiple correlation coefficient with all the categories was 0.74 and the first three variables entered into the regression were northerlies, easterlies and lows, all with negative regression coefficient. (Southern hemisphere polewards fluxes are treated as negative in the present sign convention).

The highest values of the zonal eddy flux are associated with the jet stream and dominant peaks in the vertical integral (e.g. July and August 1974) do not have any marked maximum near the surface. (See Fig. 3.11). The multiple correlation coefficient between the six station average flux and the synoptic indices is only 0.50 (although near 0.6 for individual station fluxes at Adelaide and Mt Gambier). The first variable selected was the frequency of westerlies with a partial correlation coefficient of 0.3 which is significant only at the 10 per cent level after allowing for autocorrelation. For individual stations, the correlations were of the same order, with westerlies being the best predictor except at Wagga and Laverton where the number of lows was more closely although inversely related.

For the areal average of meridional eddy flux the multiple correlation coefficient was 0.81 with northerlies being the first variable selected followed by the number with indeterminate curvature, southerlies and lows. Except for the second variable mentioned, the regression coefficients were negative. Except at Williamtown individual station values were slightly lower, but were at least 0.7 with northerlies the best predictor. At Williamtown the multiple correlation coefficient was only 0.56 and westerlies had the best partial correlation.

The areally averaged meridional eddy flux had a partial correlation coefficient of -0.49 with the monthly totals of northerlies. After allowing for autoregression, this is still significantly below the 0.5 per cent level, so that the frequency of northerlies does seem a useful indicator of the average meridional eddy flux. The correlations for individual stations were slightly lower but still generally better than -0.4. The number of highs was also well correlated with the eddy flux although not selected by the regression procedure due to a strong correlation between the frequencies of highs and northerlies. The correlation coefficient for southerlies was generally below 0.2 and even varied in sign among the stations. A major peak of southerly occurrences in June 1976 was associated with generally northward eddy transport, but other strong southerly peaks (e.g. May and November 1974) have strong southward transport.

There seem to be useful correlations between the simple synoptic index selected and the areally averaged zonal total and meridional eddy flux, and to a lesser extent the meridional total flux, but the linear regression of the surface categories for the zonal eddy flux is much less successful. The success of an index relating surface patterns to vertically integrated fluxes obviously depends on changes at the surface being consistently reflected through the depth of the atmosphere. The alternation of sign in the vertical profile of the zonal

eddy flux has been shown in previous studies for stations in the study region (e.g. NEA).

The high partial correlation coefficients between the frequency of northerlies and the meridional total and eddy fluxes are in line with a study for middle latitudes of the northern hemisphere by Miles (1976) who found that the polewards flux of enthalpy was more closely related to an index of the surface meridional circulation than to the surface zonal flow. He considered the total polewards flux averaged round 45^{0}N for which the mean meridional flux is secondary to the eddy flux, in contrast to the values for the study region where the converse is generally true.

The frequency of lows was among the first few variables selected by the multiple regression technique for the meridional total and eddy flux, although the correlation coefficient between the monthly values of eddy flux and the number of closed lows centred over or near the study area (within 500 kilometres) was quite low ($r = 0.23$). A study of individual synoptic features over the study region would produce more significant results.

4.2 Contribution of the various energy types to the overall flux and flux divergence

4.2.1 Total Flux

Values of the vertically integrated total fluxes for the mid-season months averaged over the six study stations and over the years 1974-1976 are presented in Table 4.2. The zonal components generally show only small variations from year to year and among the six stations whereas the meridional values vary even in sign both spatially and temporally, so that the average values for the meridional flux are significantly smaller than values in individual years and three years' data cannot be regarded as providing a stable average.

The total fluxes are dominated by the i component as indicated by the almost westerly direction of the flux vectors. The major contribution to the zonal total flux is from the persistent westerly flow over the region in the upper troposphere where water vapour content is low, so that the vertically integrated flux is dominated by the sensible energy flux. The enthalpy flux generally accounts for 70 to 75 per cent of the overall total with another 25 to 30 per cent in the geopotential flux. Kinetic and latent energy flux make up only about one per cent.

In the meridional component where the vertical distribution of the flux is more uniform, the latent energy term is relatively more important and is occasionally of comparable magnitude to the sensible energy fluxes. In January, when the overall flux is a small residual of counteracting fluxes, the latent energy flux even exceeds the combined flux.

The latent energy flux vector has a significant northerly component, especially in summer, while the other vectors are almost directly eastward.

4.2.2 Eddy Fluxes

Average values of the eddy fluxes and vector angle are also given in Table 4.2. In the eddy flux the enthalpy and geopotential do not have such large absolute magnitudes, and the distribution of the combined flux among the constituents is more even. The combined zonal eddy component is generally directed towards the east, but there is some counteraction between the values of individual terms, and also, except for kinetic energy, among the stations. All the constituent terms are significant with the geopotential term generally the smallest.

The meridional eddy transport is performed principally by the enthalpy and latent energy fluxes with the kinetic energy and geopotential fluxes usually accounting for less than 10 per cent.

Table 4.2

Mid-season Values of Vertically Integrated Fluxes averaged over the 6 study stations and the three years 1974-76 (10^8 W m^{-1}).

Month	Type	Total Flux			Eddy Flux		
		Zonal	Meridional	Angle	Zonal	Meridional	Angle
January	Kinetic	0.4	0	275	0.13	-0.04	287
	Enthalpy	178	-3.5	271	0.09	-0.65	352
	Potential	71	4.3	267	-0.18	0.01	093
	Latent	0.4	-1.2	341	0.17	-0.52	342
	Sum	250	-0.4	270	0.19	-1.20	351
April	Kinetic	0.3	-0.1	278	0.14	-0.05	290
	Enthalpy	187	-2.4	271	0.43	-0.63	326
	Potential	70	-1.2	271	-0.03	-0.03	045
	Latent	1.0	-0.4	291	-0.01	-0.32	001
	Sum	258	-4.1	271	0.53	-1.02	333
July	Kinetic	1.2	0	271	0.31	-0.05	279
	Enthalpy	373	5.5	269	0.75	-0.84	318
	Potential	127	5.6	267	0.02	0.07	196
	Latent	2.3	-0.5	282	0.17	-0.21	321
	Sum	503	10.7	269	1.25	-1.04	310
October	Kinetic	0.5	0	270	0.13	-0.02	279
	Enthalpy	261	8.4	268	0.05	-0.92	357
	Potential	89	4.3	267	0.02	-0.01	297
	Latent	1.8	-0.5	286	0.04	-0.47	355
	Sum	353	12.1	268	0.24	-1.42	350

In contrast to the other eddy fluxes the geopotential flux is often directed northwards. The average value for July is northward at all stations except Adelaide. The geopotential flux may exceed ten per cent of the total meridional eddy flux, but in such cases (e.g. Williamtown in April and July) it is usually directed northwards and offset by a relatively large component of the kinetic energy flux directed southwards. The relative contributions of the sensible and latent energy terms vary among the stations with the sensible energy having a lowest and the latent energy a highest percentage at the inland stations of Cobar and Wagga. The lowest proportion of latent energy flux occurs at the south coastal stations of Mt Gambier and Laverton. There is also a seasonal variation with the relative contribution of sensible energy being highest in winter and lowest in summer, and conversely for latent energy.

The overall eddy flux is directed approximately south-eastwards in April and July, but close to southwards in January and October. The kinetic energy flux is more westerly than the combined eddy flux, and the geopotential flux is variable in direction.

4.2.3 Flux Divergence

The contributions of the individual energy types to the total, mean and eddy flux divergence listed in Table 4.3 show much counteraction between the various terms. In the total flux divergence the terms of largest magnitude are the enthalpy and geopotential, but even the kinetic energy flux divergence is not negligible, despite its very small contribution to the total flux. In July and August the measured divergences of the kinetic energy flux are larger than those of latent energy.

For the four months considered there was consistent divergence of the enthalpy flux with geopotential flux convergence of greater magnitude, resulting in overall sensible energy convergence. The measured

latent energy terms showed divergence in each of the four months. This seems an unusual result for the winter months and was discussed in Section 3.3.

In the eddy flux divergence the enthalpy term is usually the largest, latent energy generally next, with the flux divergences of kinetic energy and geopotential of comparable magnitude. The combined eddy term of sensible energy showed divergence except in August, and hence is mostly opposed to the mean sensible energy term.

There is also counteraction between the mean and eddy latent energy terms, with the eddy flux showing convergence. Similar counteractions were noted in the studies for the Baltic and Mediterranean discussed in Chapter 2.

Table 4.3

Flux Divergence ($W\ m^{-2}$) of individual energy forms

Energy Form		February 1975	April 1975	July 1975	August 1975
Total Flux	Kinetic	-1	3	-13	-21
	Enthalpy	300	286	30	118
	Geopotential	-314	-310	-185	-350
	Latent	59	35	4	18
	Combined	44	14	-164	-235
Eddy Flux	Kinetic	1	9	8	-15
	Enthalpy	43	17	32	-105
	Geopotential	6	-6	19	5
	Latent	-6	-25	-10	-44
	Combined	43	-5	49	-160
Mean Flux	Kinetic	-2	-6	-21	-6
	Enthalpy	257	269	-2	223
	Geopotential	-319	-304	-204	-355
	Latent	65	59	14	62
	Combined	1	19	-213	-75

As noted in Chapter 3 for the overall energy flux, the mean fluxes of the individual energy types, but again not the eddy fluxes, show a pattern of convergence in the zonal and divergence in the meridional components, except the kinetic and latent energy fluxes in August 1975.

On a monthly basis the measured latent energy flux divergences as discussed in Section 3.3 have been supported for February and April by the moisture budget, but shown to be wrong even in sign for July and August. However, this is not crucial as the latent energy term is relatively unimportant during the winter months. In February, the combined sensible energy flux divergence is a small residual of the counteracting enthalpy and geopotential terms, so that most of the total flux divergence is due to the latent energy term, specifically the mean latent energy flux divergence, as the eddy latent energy term is small and convergent. The moisture budget depends on the relative magnitudes of precipitation and evapotranspiration, so that the overall atmospheric energy budget is strongly linked to surface conditions.

For the other months the overall terms can only be regarded as tentative due to the large discrepancy in the total budget. In April the combined sensible energy term is again smaller than the latent energy divergence, which in turn is smaller than the February value although the eddy term is larger. The sensible energy convergence is also due to the mean motion.

In July, the sensible energy terms, particularly geopotential energy, dominate. The total and mean latent energy terms are smaller than the kinetic energy terms, and the enthalpy terms are also smaller than other months.

For August, the geopotential is the smallest of the eddy terms and the largest of the mean terms. The eddy and mean sensible energy terms are of the same sign in contrast to the other months, while the latent energy term has strong counteraction between the mean and eddy terms.

4.3 *Vertical Profiles of Flux and Flux Divergence*

Vertical profiles of the overall energy flux components have been discussed in Chapter 3. Profiles for individual energy components at stations in or near the study area are given by NEA and for moisture transports by Hutchings (1961), so only the main features will be mentioned here.

The total transport consisting of the mean winds weighted by the absolute energy values is dominated by the sensible energy. As shown in Fig. 3.11 the zonal transport is strongly concentrated in the 200-300 mb layer, but the meridional component is more uniformly distributed with layers of alternating signs.

The meridional eddy enthalpy flux has a peak at about 850 mb in all seasons, which extends to near the surface in summer, especially for the south coastal area. A secondary peak is evident between about 200 and 150 mb especially in summer, with a tertiary peak at 400 mb most noticeable in spring. The corresponding zonal term has a positive peak at about 250 mb especially in winter, but the flux changes sign several times in the vertical.

For eddy latent energy the meridional component is generally directed polewards at all levels, reaching a peak at about the 750 mb level, but remaining significant at the 400 mb level. The zonal component is generally smaller with negative (westwards) flux near the surface and eastwards flux in upper layers.

Vertical profiles of the total and eddy flux divergences, including divergences of the zonal and meridional components, are shown in Fig. 4.2 for the four months which were adjusted for mass balance. One noticeable feature is the compensation between the zonal and meridional components through the whole vertical profile of the total flux divergence. As noted for the vertically integrated fluxes this is not so marked in August 1975. The total flux divergence profiles reflect the pattern of

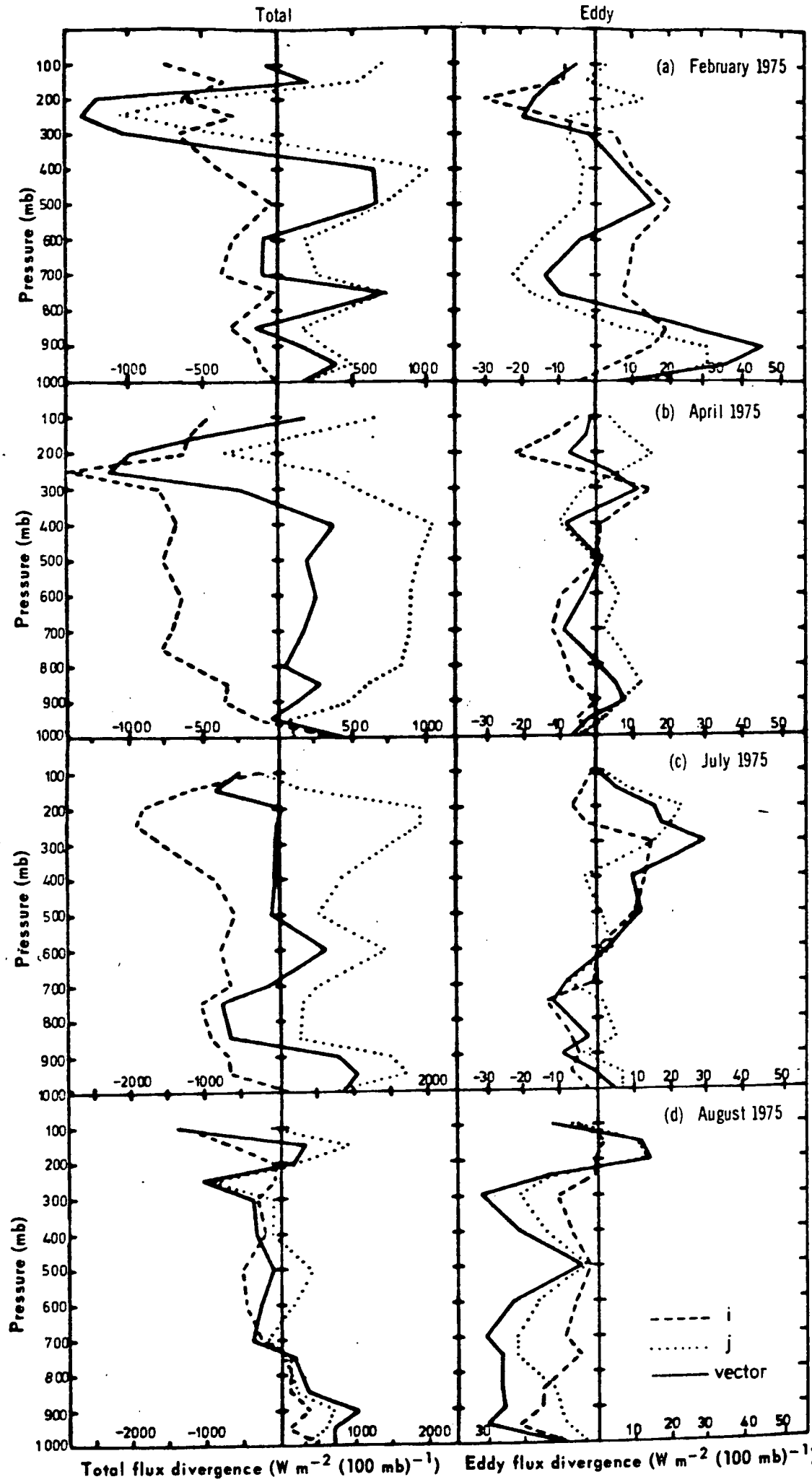

Fig. 4.2 Vertical profiles of atmospheric energy flux divergence showing the contributions of the i and j flux components. Units are W m^{-2} (100 mb)$^{-1}$.

mass flux divergence and the values at each level are dominated by the sensible energy. As discussed previously, though, all the terms are significant when vertically integrated, due to the compensating import and export in different layers. This also applies to the vector total and eddy terms where, at individual levels, the total flux divergence is an order of magnitude greater than the eddy term, but the vertical integrals of each are comparable.

Another noteworthy feature is the magnitude of the flux divergences at individual levels which can exceed 1000 W m^{-2} (100 mb)$^{-1}$ particularly at high levels. The zonal and meridional terms in July approach twice this value in the 200-300 mb layer.

For February 1975 the total flux divergence shows strong convergence averaging about 1200 W m^{-2} over the 200-300 mb layer with export at most other levels. Both the zonal and meridional components contribute to the convergence, while these terms are usually of opposite sign in other layers. In the eddy profile the zonal and meridional terms re-inforce in a layer between the surface and 850 mb but generally counteract otherwise. In the eddy layer near the surface the enthalpy and latent energy terms are roughly comparable, and of the same sign, but at higher levels the latent energy term is mainly convergent while the enthalpy term remains divergent. The mean latent energy flux was divergent at all levels and both the mean and eddy terms were still significant at 400 mb, the lowest pressure for which mixing ratio data were available.

The pattern that emerges is of many counteracting effects, but overall there is energy convergence in the upper layers (particularly by the mean flow) and divergence by all forms of energy at lower levels.

The April 1975 profile again shows strong counteraction between zonal convergence and meridional divergence except near the surface and at 200 mb, with the net effect being import of energy in the 150-300 mb layer and mostly export otherwise. The corresponding mass flux profile

for the month indicating mean downwards vertical motion is in line with the frequent occurrence of highs and anticyclonic isobaric curvature in this month. The eddy flux divergence terms are small in comparison with those of other months, and alternate in sign several times in the vertical with the meridional and zonal terms generally of opposite sign. The eddy latent energy term showed consistent convergence, with highest values between the surface and 850 mb. The vertical integral of the eddy flux divergence is small, so that the total flux divergence is dominated by the mean motion which imports sensible energy in the upper layers and exports sensible and latent energy in the middle and lower layers.

A noteworthy feature of the July profile is the low value of the total flux divergence in the upper troposphere, due to almost exact cancelling between the large zonal and meridional terms. In contrast to April the eddy profile shows a fairly regular structure with strong divergence in the upper layer over a less marked layer of convergence.

The August 1975 profile has total flux divergence near the surface with generally convergence in middle and upper layers, but no marked counteraction between the zonal and meridional components as in the other months considered. The eddy term is strongly convergent at most levels, in both zonal and meridional components, and in sensible and latent energy.

The large value of the total energy convergence at 100 mb in August (-1350 W m^{-2} $(100\ mb)^{-1}$) suggests that if the profile had been extended to lower pressures the vertically integrated flux divergence, which is a very small residual of opposing terms, could have been significantly affected. For example, an average of only half the 100 mb value for an extra 20 mb would have added an extra convergence of 135 W m^{-2} to the vertical integral. A contribution of this magnitude is roughly the discrepancy in the energy budget for August. The choice of the 100 mb level as the effective top of the atmosphere may have been a significant

source of error, as in this case the overall mass flux has been forced to be slightly more convergent than it would have been had the data been extended to pressures less than 100 mb. This also appears to be a problem to a lesser extent in other months, particularly July, and it may be more than a coincidence that the month in which the energy budget discrepancy is least (February) has the smallest total flux divergence at the 100 mb level.

The 200-100 mb layer does play a significant role in the vertically integrated flux divergence in each of the months considered. As the pressure of the tropopause level generally exceeds 200 mb, this suggests that interactions between the troposphere and lower stratosphere are significant in the atmospheric energy budget.

The results of the two dimensional model of Paltridge (1978) based on a postulate of maximising the rate of entropy production also suggest a pattern of zonal convergence and meridional divergence (his figures 9 and 10) although the absolute values of the fluxes in Paltridge's results are much smaller than observed as they represent fluxes based on energy budget considerations alone. According to Paltridge's hypothesis such a pattern would be due to the relative radiative regimes of south-east Australia and adjacent areas, particularly oceans.

4.4 *Comparison of Measured Fluxes and Flux Divergences with zonal averages*

The mean meridional fluxes for the study area were several orders of magnitude greater than the zonal average and varied greatly over the three years, even in sign, so that they cannot be realistically compared with the zonal average. Seasonal average values of the eddy enthalpy, geopotential and latent energy fluxes derived from the 1974 to 1976 data are shown for four of the stations in Table 4.4 along with zonal average values taken from NEA. As results for 40^0S were not available, the values for 40^0 N were used instead. The results of NEA include transient

and standing eddies, although the latter are small in the southern hemisphere (van Loon and Williams, 1977), and are averaged over five years, so that interannual variations would also contribute to the eddy term.

All the station values of the combined eddy flux in summer, and all except Williamtown in spring, are larger than the zonal average, but the reverse is true in winter with Williamtown only 32 per cent and Laverton only 39 per cent of the zonal average.

In the eddy enthalpy transport the station values generally exceed the zonal average except in winter. Values in summer are well above the zonal value, especially at Laverton, but the winter fluxes at Williamtown and Laverton are only about half the zonal average.

The eddy geopotential term is small both in the zonal average and at individual stations. While the zonal averages are all directed toward the north, some station values are polewards.

The eddy latent energy fluxes are close to the zonal values in summer and spring, significantly less in autumn, but well below in winter, especially at Laverton and Williamtown where the fluxes are only 20 and 16 per cent respectively of the zonal average.

It is difficult to draw conclusions as northern hemisphere data are used for most of the zonal averages, but the difference in the relation to the zonal average between summer and winter at Cobar probably reflects differences in the prevailing synoptic patterns. In winter the sub-tropical ridge lies over the area, and the frequency of high pressure systems is high (Karelsky, 1961), whereas in summer Cobar is in a prevailing easterly zone and on the fringe of the monsoonal area over northern Australia. The results do suggest that south-east Australia may be a preferred area for meridional eddy transport in spring and summer, but an area of below average transport in winter.

Due to the uncertainty in southern hemisphere atmospheric flux measurements, the computed values of flux divergence for the study area can only be compared with northern hemisphere values. The total flux divergence for February 1975 (a required value of 55 W m^{-2}) is greater than the summer value of 29 W m^{-2} for 35^0N (see Section 2.1). The required values for July and August 1975 are convergences of -103 and -76 W m^{-2} respectively but the zonal average for 35^0N is a slight divergence of 6 W m^{-2}. The flux divergence of the different energy forms for the study area are generally greater in magnitude than the zonal average, especially for summer. The 35^0N values do not show any counteraction between the enthalpy and geopotential mean flux divergences.

Considering the flux divergences of only the meridional components over the study area, shows that the eddy terms are generally about the same magnitude, although sometimes of opposite sign due to different counteractions with the mean flux. The mean sensible energy flux divergences are several orders of magnitude greater than the zonal average due to the strong compensation between zonal import and meridional export over the study area. The mean latent energy term is also larger than the zonal average, but not to the same extent.

The flux divergences for the individual energy terms over the study area are generally similar in magnitude to the estimates of Gallardo et al (1977) for the Mediterranean area, although interactions between the mean and eddy terms may be of opposite sense. The main exceptions are a lower total sensible energy convergence in winter over the Mediterranean, and a stronger sensible energy convergence in summer counteracted by a very strong latent energy export (127 W m^{-2}). This is a reflection of the difference in the underlying surface-totally land in one case and mainly water in the other.

The individual vector flux divergences over the study area do not reach the peak values experienced over the high latitude Baltic Sea and adjacent areas. Behr and Speth (1977) report values of mean enthalpy flux divergence exceeding 2000 W m^{-2}. Where this occurs, there is a strong counteraction by the eddy enthalpy and both geopotential terms, so that the combined sensible energy terms are of the same order of magnitude as for the study area.

Table 4.4

Comparison of Average Polewards Eddy Fluxes for the study region for the years 1974-76 with Zonal average values taken from NEA. The zonal averages used correspond to 30°S for Cobar (CO), 40°N for Laverton (LV) and the mean of the 30°S and 40°N values for Adelaide (AD) and Williamtown (WM). Units are 10^6 W m^{-1}.

Flux	Season	AD	Zone	CO	Zone	WM	Zone	LV	Zone
Eddy	Summer	-65	-24	-41	-22	-46	-24	-96	-25
Enthalpy	Autumn	-77	-46	-40	-27	-40	-46	-67	-65
	Winter	-65	-78	-48	-47	-34	-78	-55	-109
	Spring	-118	-60	-75	-38	-48	-60	-109	-82
	Annual	-81	-52	-51	-33	-42	-52	-82	-70
Eddy	Summer	2	1	-1	1	-1	1	4	2
Geopotential	Autumn	-5	2	1	3	6	2	2	2
	Winter	9	5	9	6	4	5	5	5
	Spring	-6	4	1	6	7	4	-7	2
	Annual	0	3	3	4	4	3	1	3
Eddy	Summer	-36	-36	-49	-35	-37	-36	-46	-36
Latent	Autumn	-25	-42	-31	-38	-9	-42	-25	-46
Energy	Winter	-15	-43	-22	-36	-7	-43	-10	-51
	Spring	-45	-40	-48	-36	-27	-40	-43	-44
	Annual	-30	-40	-37	-36	-20	-40	-31	-44
Total	Summer	-98	-58	-91	-56	-83	-58	-138	-60
Eddy	Autumn	-108	-85	-71	-61	-43	-85	-90	-109
	Winter	-70	-117	-61	-78	-37	-117	-61	-155
	Spring	-168	-97	-121	-68	-68	-97	-160	-125
	Annual	-111	-89	-86	-66	-58	89	-112	-112

CHAPTER V

CONCLUSIONS

This study was aimed at examining the atmospheric energy fluxes and the energy budget on a regional scale and attempting to relate these to the prevailing synoptic patterns. Summaries of the technique employed and the results obtained are given below.

5.1 Technique

The study combined satellite, radiosonde and some surface meteorological data in an evaluation of the terms of the atmospheric energy budget for the region. Although strict closure of all the terms was not obtained the adjustment of the wind data for mass balance made it possible to draw some conclusions regarding energy transfers within the region. Adjustments which were evenly divided in the vertical in proportion to the pressure interval gave better results than a scheme which made greater adjustments at upper levels (i.e. lower pressures). Gross errors are introduced to the flux divergence estimates by missing data, and a coherent set of data seems essential. Missing data also cause significant errors in the flux measurements, particularly the meridional and eddy terms. Given a coherent data base, only small adjustments are made to the eddy flux divergence by the mass balancing procedure, and its application to the monthly mean winds only may still give satisfactory results with a considerable saving in computation. The latent energy flux divergences are also altered significantly by the adjustments for mass balance, suggesting that even in moisture budget studies such a procedure is warranted.

The NOAA Heat Budget Archive derived from the operational satellites provided valuable information on the net radiant flux density which would otherwise have had to be obtained from radiative transfer models. Some minor problems with the data are the uncertainty in the long wave flux measurements and the limited temporal sampling. This latter factor may

account for differences between NOAA and Nimbus-3 estimates of ocean-land contrasts in the radiative fields.

The techniques employed in this study could be refined by including data from other observation times. This would involve much interpolation as only three of the six stations have radiosonde data at 1100 GMT. The wind data from other observation times at least could be used with interpolated values of temperature, geopotential and specific humidity. The location of the study area could also be moved inland to exclude the mountain range that lies along the east of the study area. The possibility that pressure levels below 100 mb may be significant in the overall energy budget, suggests that the vertical range of observations should be extended, even at the cost of more interpolation due to an inevitable increase in the frequency of missing observations.

5.2 *Results obtained*

The overall energy budget for the study area is seen to be a complex interplay of the different energy forms, their zonal and meridional components and their mean and eddy resolutions. In particular there is counteraction in the total energy flux divergence between generally zonal convergence and meridional divergence reflecting the pattern of mean mass flux over the area. All the energy forms, even kinetic energy, are significant in the overall budget.

For most of the terms there is also compensation in the vertical, with the overall divergence a small residual of opposing terms, especially for the mean flux divergence. Because of this it seems that levels above the tropopause, and even pressure levels below 100 mb in some cases, are significant.

The measured fluxes, except the zonal eddy term, showed good correlations with a simple index of the surface synoptic pattern, formed

as a multiple linear regression of the number of occurrences per month of specified air stream direction and curvature categories.

Satellite radiation measurements revealed interesting differences of the radiative regime between the study area and the zonal average and also within the study area. The differences with respect to the zonal average reflect the differences in the predominant underlying surface. For the study region anomalies of individual monthly values from the four-year mean showed a good correlation between the short wave and long wave terms, with the former generally larger in magnitude, so that the anomalies of net radiation are inversely related to variations in cloudiness. Because it is a very small residual, little information on the atmospheric energy flux divergence is provided by the net radiation at the top of the atmosphere, apart from an estimate of its overall magnitude.

5.3 *Possible Extensions of the study*

The study could logically be extended temporally and spatially to provide results for a larger area over longer periods, but also for shorter durations to investigate individual synoptic systems. The current availability of frequent geostationary satellite data enables net radiant fluxes to be evaluated even for time scales of the order of one day. Further investigations of the moisture budget could be made, although their usefulness in estimating areal evapotranspiration on the regional scale appear limited with the present density of upper air stations.

ACKNOWLEDGEMENTS

I gratefully acknowledge the guidance and suggestions provided by my two supervisors at the University of Tasmania, Dr M. Nunez (Geography Dept.) and Dr J.E. Humble (Physics Dept.). The topic for the thesis was originally suggested by Dr Nunez.

Without the support of the Bureau of Meteorology and the generous assistance of many individual officers, this thesis could not have been completed. Constructive suggestions by Dr W.K. Downey and Mr F. Woodcock on specific aspects were much appreciated. I am also indebted to the Public Service Board for the award of a Postgraduate Scholarship which allowed a period of full-time study.

Finally, I wish to thank my wife Christina, for her patient support and encouragement during the course of study. She produced two offspring during the gestation period of this one thesis.

REFERENCES

Abel, P.G. and Gruber, A. 1979. An improved model for the calculation of long-wave flux at 11 μm. NOAA Tech. Mem. NESS 106 (24 pp).

Astling, E.G. and Horn, L.H. 1972. Atmospheric energy transport over North America for three winter months. Mon. Weath. Rev., 100 491-502.

Baese, K. and Liebing, H. 1977. An investigation of the atmospheric heat and moisture balance in the Baltic Sea region: Part III. Preliminary results of a determination of evaporation minus precipitation (April, May, June 1976 in the frame of the International Hydrological Programme). Met. Rdsch., 30, 185-92.

Behr, H.D. and Speth, P. 1977. An investigation of the atmospheric heat and moisture balance in the Baltic Sea region: Part II. Heat balance. Met. Rdsch., 30, 99-111.

Berson, F.A. 1961. Circulation and energy balance in a tropical monsoon. Tellus, 13, 472-85.

Bureau of Meteorology 1968. The Laverton Serial Sounding Experiment. Met. Summary, Bur. Met., Melbourne (65 pp).

Bureau of Meteorology 1975. Climatic Averages, Australia (Metric edition), Bur. Met., Melbourne.

Davis, R.E. 1976. Predictability of sea surface temperature and sea level pressure anomalies of the North Pacific. J. Phys. Oceanogr. 6, 249-66.

Dopplick, T.G. 1974. Radiative heating in the atmosphere. Chapter 6 of Newell et al (1974, op. cit.).

Ellis, J.S., Vonder Haar T.H., Levitus S. and Oort, A.H. 1978. The annual variation in the global heat balance of the earth. J. geophys. Res., 83, 1958-62.

Gallardo F.S., Puigcerver M. and Alonso S. 1977. The energy budget of the western Mediterranean: a preliminary assessment. Rev. Geofisica, 36, 90-110.

Gray, T.I. 1978. Personal Communication.

Gruber, A. and O'Brien J.J. 1968. An objective analysis of wind data for energy budget studies. Jnl appl. Met., 7, 333-38.

Gruber, A. 1970. The energy budget over the Florida Peninsula when a convective regime dominates. Jnl appl. Met., 9, 401-16.

Gruber, A. 1977. Determination of the earth-atmosphere radiation budget from NOAA satellite data. NOAA Tech. Rep. NESS 76 (28 pp).

Haltiner, G.J. 1971. Numerical Weather Prediction. (John Wiley and Sons Inc. : New York.) 317 pp.

Hastenrath, S.L. 1966. On the general circulation and energy budget in the area of the Central American Seas. J. Atmos. Sci., 23, 694-711.

Holopainen, E.O. 1977. Energy balance of the earth. Aust. Met. Mag., 25, 89-103.

Hoy, R.D. and Stephens S.K. 1979. Field study of lake evaporation - analysis of data from phase 2 storages and summary of phase 1 and phase 2. Aust. Water Res. Council, Tech. Paper No. 41, A.W.R.C., Canberra (177 pp).

Hutchings, J.W. 1957. Water vapour flux divergence over southern England. Q. JI R. Met. Soc., 83, 30-48.

Hutchings, J.W. 1961. Water-vapour transfer over the Australian continent. J. Met., 18, 615-34.

Jacobowitz, H., Smith, W.L., Howell, H.B., Nagle, F.W. and Hickey, J.R. 1979. The first 18 months of planetary radiation budget measurements from the Nimbus 6 ERB experiment. J. Atmos. Sci., 36, 501-7.

Karelsky, S. 1961. Monthly and seasonal anticyclonicity and cyclonicity in the Australian region - 15 years (1946-1960). Met. Study No. 13, Bur. Met., Melbourne.

Levitus, S. and Oort, A.H. 1977. Global analysis of oceanographic data. Bull. Am. met. Soc., 58, 1270-84.

Lorensz, E.N. 1967. The Nature and Theory of the General Circulation of the Atmosphere. WMO Publ No. 218, T.P. 115 (World Meteorological Organization : Geneva, Switzerland) 161 pp.

Maher, J.V. and Lee, D.M. 1977. Upper air statistics, Australia, surface to 5 mb, 1957 to 1975. Met. Summary, Bur. Met., Melbourne.

Mak, M. 1978. On the observed momentum flux by standing eddies. J. Atmos. Sci., 35, 340-46.

Miles, M.K. 1976. The relation of the poleward flux of sensible heat during the winter half year to some zonal and meridional indices of the circulation. Q. Jl. R met. Soc., 102, 743-48.

Monteith, J.L. 1973. Principles of Environmental Physics. (Edward Arnold : London.) 241 pp.

Murray, R. and Lewis, R.P.W. 1966. Some aspects of the synoptic climatology of the British Isles as measured by simple indices. Met. Mag., Lond., 95, 196-203.

Newell, R.E., Vincent, D.G., Dopplick, T.G., Ferruzza, D. and Kidson, J.W. 1969. The energy balance of the global atmosphere. In The Global Circulation of the Atmosphere, Corby, G.A. (ed.), R. Met. Soc., London (pp 42-90).

Newell, R.E., Kidson, J.W., Vincent, D.G. and Boer, G.J. 1972. The General Circulation of the Tropical Atmosphere and Interactions with Extratropical Latitudes : Vol. 1 (M.I.T. Press, Cambridge, Mass.) 258 pp.

Newell, R.E., Kidson, J.W., Vincent, D.G. and Boer, G.J. 1974. The General Circulation of the Tropical Atmosphere and Interactions with Extratropical Latitudes : Vol. 2. (M.I.T. Press. Cambridge, Mass.) 371 pp. (Denoted NEA in the text).

Newton, C.W. 1972. Southern hemisphere general circulation in relation to global energy and momentum balance requirements. Met. Monogr., 13, 215-40.

O'Brien, J.J. 1970. Alternative solutions to the classical vertical velocity problem, Jnl. Appl. Met., 9, 197-203.

Ohring, G. and Clapp P. 1980. The effect of changes in cloud amount on the net radiation at the top of the atmosphere. J. Atmos. Sci., 37, 447-54.

Oke, T.R. 1978. Boundary Layer Climates. (Methuen : London) 372 pp.

Oort, A.H. 1971. The observed annual cycle in the meridional transport of atmospheric energy. J. Atmos. Sci., 28, 325-39.

Oort, A.H. and Rasmusson, E.M. 1971. Atmospheric circulation statistics. NOAA Professional Paper No. 5. (U.S. Government Printing Office, Washington, D.C.) 323 pp. (Denoted OR in the text.)

Oort, A.H. and Vonder Haar, T.H. 1976. On the annual cycle in the ocean-atmosphere heat balance over the northern hemisphere. J. Phys. Oceanogr., 6, 781-800

Oort, A.H. 1978. Adequacy of the rawinsonde network for global circulation studies tested through numerical model output. Mon. Weath. Rev., 106, 174-95.

Paltridge, G.W. 1978. The steady-state format of global climate. Q. Jl. R. met. Soc., 104, 927-45.

Pierrehumbert, C.L. 1972. Precipitable water statistics, Australia. Monthly statistics of precipitable water between surface and 400 mb at 2300 GMT 1958-1969. Met. Summary, Bur. Met., Melbourne.

Priestley, C.H.B. and Troup, A.J. 1964. Strong winds in the global flux of momentum. J. Atmos. Sci., 21, 459-60.

Raschke, E. and Bandeen, W.R. 1970. The radiation balance of the planet earth from radiation measurements of the satellite Nimbus 2, Jnl. appl. Met, 9, 215-38.

Raschke, E., Vonder Haar, T.H., Bandeen, W.R. and Pasternak, M. 1973. The annual radiation balance of the earth-atmosphere system during 1969-70 from Nimbus 3 measurements. J. Atmos. Sci., 30, 341-64.

Rasmusson, E.M. 1967. Atmospheric water vapour transport and the water balance of North America: Part I. Characteristics of the water vapour flux field. Mon. Weath. Rev., 95, 403-26.

Rasmusson, E.M. 1968. Atmospheric water vapour transport and the water balance of North America : Part II. Large-scale water balance investigations. Mon. Weath. Rev., 96, 720-34.

Rasmusson, E.M. 1972. Seasonal variation of tropical humidity parameters. Chapter 5 of Newell et al (1972, op. cit.).

Rasmusson, E.M. 1977. Hydrological Application of Atmospheric Vapour-Flux Analyses. Operational Hydrology Rep. No. 11, WMO-No. 476 (World Meteorological Organization : Geneva, Switzerland) 50 pp.

Riehl, H. and Malkus, J.S. 1958. On the heat balance in the equatorial trough zones. Geophysica, 6, 503-38.

Rosen, R.D., Salstein, D.A. and Peixoto, J.P. 1979. Variability in the annual fields of large-scale atmospheric water vapour transport. Mon. Weath. Rev., 107, 26-37.

Rust, B.W. and Burrus, W.R. 1979. Mathematical Programming and the Numerical Solution of Linear Equations. (Elsevier : New York) 218 pp.

Sasamori, T., London, J. and Hoyt, D.V. 1972. Radiation budget of the southern hemisphere. Met. Monogr., 13, 9-22.

Sciremammano, F. 1979. A suggestion for the presentation of correlations and their significance levels. J. Phys. Oceanogr., 9, 1273-6.

Sellers, W.D. 1965. Physical Climatology. (Uni of Chicago Press : Chicago and London) 272 pp.

Sellers, W.D. 1973. A new global climatic model. Jnl. appl. Met., 12, 241-54.

Smith, W.L., Hickey, J., Howell, H.B., Jacobowitz, H., Hilleary, D.T. and Drummond, A.J. 1977. Applied Optics 16, 306-18.

Spillane, K.T. 1969. Reliability of wind data determined by 277 radar in Australia Met. Study No. 18, Bur. Met., Melbourne.

Starr, V.P. 1951. Applications of energy principles to the general circulation, in Compendium of Meteorology, Malone, T.F. (ed.), (Amer. Met. Soc:, Boston, Mass.) pp. 568-74.

Trenberth, K.E. 1979. Mean annual poleward energy transports by the oceans in the southern hemisphere. Dyn. Atmos. Oceans, 4, 57-64.

Tucker, G.B. 1979. Transient synoptic systems as mechanisms for meridional transport : an observational study in the southern hemisphere. Q. Jl. R. Met. Soc., 105, 657-72.

Van Loon, H. and Williams, J. 1977. The connection between trends of mean temperature and circulation at the surface : Part IV. Comparison of the surface changes in the northern hemisphere with the upper air and with the Antarctic in winter. Mon. Weath. Rev., 105, 636-47.

Vonder Haar, T.H. and Suomi, V.E. 1971. Measurements of the earth's radiation budget from satellites during a five-year period. Part I : Extended time and space means. J. Atmos. Sci., 28, 304-14.

Vonder Haar, T.H. 1972. Natural variation of the radiation budget of the earth-atmosphere system as measured from satellites. Preprints for Conf. on Atmos. Radiation, Amer. Met. Soc., Fort Collins, Colo., Aug 7-9, 1972.

Winston, J.S. 1967. Planetary scale characteristics of monthly mean longwave radiation and albedo and some year to year variations. Mon. Weath. Rev., 95, 235-56.

Winston, J.S. and Taylor, V.R. 1967. Atlas of World maps of longwave radiation and albedo for seasons and months based on measurements from TIROS IV and TIROS VII. ESSA Tech. Rep. NESC 43 (32 pp).

Winston, J.S. and Krueger, A.F. 1977. Diagnosis of the satellite-observed radiative heating in relation to the summer monsoon. Pure and Appl. Geophys., 115, 1131-44.

Winston, J.S., Gruber, A., Gray, T.I., Varnadore, M.S., Earnest, C.L. and Mannello, L.P. 1979. Earth-atmosphere radiation budget analyses derived from NOAA satellite data June 1974 - February 1978 (2 Vols). NOAA-NESS, U.S. Dept. Commerce, Washington, D.C.

Yates, H.W. 1977. Measurement of the earth radiation balance as an instrument design problem. Applied Optics, 16, 297-99.

Young, H.D. 1965. Statistical Treatment of Experimental Data. (McGraw-Hill : New York) 172 pp.

APPENDIX A1

ENERGY BUDGET EQUATIONS FOR THE ATMOSPHERE

Following Haltiner (1971) the equation for the sum of kinetic energy K and geopotential energy Φ per unit mass of the atmosphere in (x, y, p, t) co-ordinates can be derived from the vector equation of motion:

$$\partial K/\partial t + \nabla \cdot (K\underline{V} + \Phi\underline{V}) = \omega \, {}^{\partial\Phi}/_{\partial p} + \underline{V}.\underline{D} \qquad \ldots (A1.1)$$

where p represents pressure, $\underline{V}$ velocity, $\omega = {}^{dp}/_{dt}$ is the vertical pressure-velocity and $\underline{V}.\underline{D}$. is the frictional dissipation.

The thermodynamic equation for an air parcel is

$$Q_D = c_p dT/dt - \alpha dp/dt \qquad \ldots (A1.2)$$

where Q_D is the rate of energy added non-adiabatically, c_p is the specific heat at constant pressure and α is the specific volume.

From Eq. A1.2 the following equation for the enthalpy I = Cp T is derived:

$$\partial I/\partial t + \nabla \cdot (I\underline{V}) = \alpha\omega + Q_D \qquad \ldots (A1.3)$$

adding equations A1.1 and A1.3 gives

$$\partial (K + I)/\partial t + \nabla \cdot (K + I + \Phi) \, \underline{V} = Q_D + \underline{V}.\underline{D}. \qquad \ldots (A1.4)$$

as ${}^{\partial\Phi}/_{\partial p} = -\alpha$ by the hydrostatic assumption.

Eq. A1.4 states that the rate of change of kinetic energy and enthalpy is controlled by non-adiabatic heating Q_D, frictional dissipation ($\underline{V}.\underline{D}$) and the total energy flux divergence. The flux divergence of

enthalpy can be considered as a divergence of internal energy flux and work done adiabatically by the pressure forces on the walls of the atmospheric volume (e.g. Starr, 1951).

The value of c_p for dry air under normal atmospheric conditions is 996 J Kg^{-1} K^{-1} and the corresponding value for moist air C_{pm} is given by:

$$c_{pm} \simeq c_p \ (1+0.00081q) \qquad \ldots (A1.5)$$

where q is the specific humidity of water vapour measured in grams of water vapour per kilogram of dry air. The highest values of q experienced under normal conditions are of the order of 20 g Kg^{-1} so that the correction due to moisture content is generally less than two per cent throughout the atmosphere.

Frictional forces are only significant in the bottom 100 mb and are generally accepted as being small relative to the other terms. The practice adopted in other energy budget studies (e.g. Hastenrath 1966, Gruber 1970, Newell et al. 1974) of neglecting this term will be followed.

The divergence operator in Eq. A1.4 can be separated into a two-dimensional divergence ∇_2 in the constant pressure surface and a component normal to this plane

$$\nabla \cdot \underline{A} = \nabla_2 \cdot \underline{A_2} + \partial A_p / \partial p \qquad \ldots (A1.6)$$

where $\underline{A}$ is an arbitrary vector, with component $\underline{A_2}$ in the constant pressure surface and A_p normal to it.

Integrating Eq. A1.4 vertically from level 1 to level 2 obtains an expression for the energy balance over a cross-sectional area dA:

$$\int_{z_1}^{z_2} Q_D \, \rho dz dA = \int_{p_2}^{p_1} Q_D \, dp/g dA$$

$$= \int_{p_2}^{p_1} \partial/\partial t \, (V^2/2 + c_p T) \, dp/g dA$$

$$+ \int_{p_2}^{p_1} \nabla_2 . (V^2/2 + gz + c_p T) \, \underline{V}_2 \, dp/g dA$$

$$+ \int_{p_2}^{p_1} \partial/\partial p \, \omega \, (V^2/2 + gz + c_p T) \, dp/g dA \qquad \ldots (A1.7)$$

As the vertical velocity is generally small relative to the total velocity, $\underline{V}_2 \simeq \underline{V}$. Using the Gauss divergence theorem to expand the second term on the right hand side

$$\int_{z_1}^{z_2} Q_D \, \rho dz dA = \partial/\partial t \int_{p_2}^{p_1} (V^2/2 + c_p T) \, dp/g dA$$

$$+ \int_{p_2}^{p_1} \oint_\sigma (V^2/2 + gz + c_p T) \, \underline{V} . \underline{n} \, ds \, dp/g$$

$$+ ((V^2/2 + gz + c_p T)\omega/g)_1 \, dA$$

$$- ((V^2/2 + gz + c_p T)\omega/g)_2 \, dA \qquad \ldots (A1.8)$$

where σ is a closed line of segments ds bounding the area of interest, with $\underline{n}$ the unit normal vector to the line element (positive outwards).

The non-adiabatic energy sources are the net radiation through the top (Q_2^*) and bottom (Q_1^*) of the column and the heat released by condensation in the column. It is assumed that the latter term can be measured by the precipitation rate measured at the ground.

Thus $$\int_{p_2}^{p_1} Q_D \, dp/g \, dA = Q_2^* - Q_1^* + Q_R \qquad \ldots (A1.9)$$

where Q^* is positive in the downward direction and Q_R represents the rate of energy supplied by rainfall.

The equation corresponding to Eq. A1.8 for the latent energy budget is

$$\int_{p_2}^{p_1} \oint_{\sigma} Lq\underline{V}.\underline{n}\, ds\, dp/g + {}^{\partial}/_{\partial t} \int_{p_2}^{p_i} Lq\, dp/g\, dA$$

$$+ (Lq\omega/g)_1\, dA - (Lq\omega/g)_2\, dA + Q_R = 0 \qquad \ldots (A1.10)$$

This equation is only approximate as it neglects heat of fusion in ice formation or sublimation, and the transport of liquid water in the atmosphere.

Substituting Eq. A1.10 and A1.9 in A1.8 gives

$$Q_2^* - Q_1^* = {}^{\partial}/_{\partial t} \int_{p_2}^{p_1} (V^2/2 + c_pT + Lq)\, dp/g\, dA$$

$$+ \int_{p_2}^{p_1} \oint (V^2/2 + gz + c_pT + Lq)\, \underline{V}.\underline{n}\, ds\, dp/g$$

$$+ ((V^2/2+gz+c_pT+Lq)^{\omega}/g)_1\, dA - ((V^2/2+gz+c_pT+Lq)\omega/g)_2 dA \qquad \ldots (A1.11)$$

When the integration extends from the surface to the top of the atmosphere, the last term on the right hand side is zero, and the second last term is equal in magnitude but of opposite sign to the sum of sensible and latent energy transfers from the surface to the air, Q_H and Q_E respectively. Q_E is measured by the evapotranspiration rate (assuming dew is negligible, an assumption generally valid except perhaps in deserts).

The first term on the right hand side represents the storage of energy in the atmosphere, with the c_pT term including both internal energy (c_VT) and potential energy. Errors due to a restricted vertical integration are discussed by Oort (1971). The second term denotes the divergence of the energy flux. Using essentially the notation of Oke (1978) Eq. A1.11 can be expressed as

$$Q^*_{TA} - Q^*_{BA} = \nabla.(F_H + F_Q) + S_H + S_Q - (Q_H + Q_E) \quad \ldots (A1.12)$$

where the subscripts TA and BA denote the top of the atmosphere and surface (bottom of the atmosphere) respectively. F_H and F_Q denote the vertically integrated fluxes of sensible energy (enthalpy, potential energy and kinetic energy) and latent energy. S_H and S_Q represent therate of energy storage in the atmosphere as sensible (S_H) and latent energy (S_Q).

The divergence operator refers to two dimensions only. For the net radiation at the surface

$$Q^*_{BA} = Q_H + Q_E + S_G + S_O + \nabla \cdot \underline{F}_O \quad \ldots (A1.13)$$

where S_G and S_O refer to the rate of energy storage in the ground (S_G) and ocean respectively, and $\nabla \cdot \underline{F}_O$ represents the divergence of the sensible energy flux in the ocean.

This equation is again an approximation as it neglects terms such as snow melt, sensible energy transfer by precipitation, expenditure of energy for photosynthesis and heat flux from the earth's interior.

Adding Eq. A1.13 to Eq. A1.12 gives

$$Q^*_{TA} = \nabla .(F_H + F_Q + F_O) + S_H + S_Q + S_G + S_O \quad \ldots (A1.14)$$

This equation states that the net radiant flux at the top of the atmosphere either flows out of the column as sensible or latent energy, or is stored in the air, ground or ocean. The measurement of $\nabla \cdot F_Q$ is subject to errors due to inaccuracies in the humidity sensing elements of conventional radiosondes. An alternative form of Eq. A1.14 can be obtained by expressing Eq. A1.10 in the form

$$S_Q + \nabla \cdot F_Q - Q_E + Q_R = 0 \qquad \ldots (A1.15)$$

Substituting in Eq. A1.14 gives

$$Q^*_{TA} + Q_R - Q_E = \nabla \cdot (F_H + F_O) + S_H + S_G + S_O \qquad \ldots (A1.16)$$

This alternative method has difficulties of its own, particularly the measurement of precipitation over data sparse areas and the difficulty of measuring <u>actual</u> rather than <u>potential</u> evapotranspiration even where conventional data exist.

Throughout the present study the energy equations in the form of Eq. A1.14 were used. As the area being studied covered land only, the terms $\nabla \cdot F_O$ and S_O were zero, so that the energy equation can be written:

$$Q^*_{TA} = \nabla \cdot F_A + S_A + S_G \qquad \ldots (A1.17)$$

combining the atmospheric sensible and latent energy terms into F_A and S_A.

For studies over areas that include large bodies of water equations in the form of A1.12 are usually more convenient, with Q_H and Q_E estimated using empirical transfer functions and $Q^*_{TA} - Q^*_{BA}$, the net atmospheric

radiative flux, from radiation models possibly supplemented with satellite data.

Behr and Speth (1977) consider only the sensible energy budget. The form of equation used can be found by subtracting Eq. A1.10 from Eq. A1.12. Then

$$Q^{*}_{TA} - Q^{*}_{BA} = \nabla \cdot F_H + S_H - Q_R - Q_H \qquad \ldots (A1.18)$$

A constant value of L = 2500J g^{-1} was used throughout this study. Newton (1972) points out that in this case the sensible energy carried by the water vapour should not be taken into account, i.e., c_p should be constant and not increase with water vapour content as in Eq. A1.5. An increase of sensible energy with increasing temperature compensates for the decrease in L with increasing temperature. However, the procedure used will not introduce significant errors.

Heat storage in land

Sellers (1965) uses the classical theory of heat transfer in a homogeneous medium under the action of a sinusoidal temperature variation to show that the rate of heat flux at the surface at time t is given by:

$$S_G\,(o,t) = \Delta\, To\, (2\pi\rho_s\, C_s\, \lambda/P)^{\frac{1}{2}} \sin\,(2\pi t/P + \pi/4) \qquad \ldots (2.8)$$

where Δ To is the amplitude of the surface temperature wave, P is the period of oscillation, λ is the thermal conductivity, C_s is the specific heat and ρ_s is the density of the soil. For the annual cycle the time of maximum heat flux precedes the time of maximum surface temperature by 1½ months.

Sellers quotes studies that suggest a value of 1.3 for the ratio of the amplitude of the temperature wave at the soil surface to that of screen temperature measurements at a height of 2 metres. Values of ρ_s, C_s and λ depend on the type of soil and the soil moisture content. The thermal conductivity increases with increasing soil moisture content, showing a rapid increase at low moisture contents, but only a gradual increase for medium and high soil moisture. The heat capacity of $\rho_s \ C_s$ also increases with increasing soil moisture content, but with a smaller relative variation. The range of $(\rho_s \ C_s \ \lambda)^{\frac{1}{2}}$ is restricted by moisture contents generally experienced in the field, and Sellers (1973) uses a value of 0.0017 J m^{-2} K^{-1} $S^{-\frac{1}{2}}$ as a global average.

APPENDIX A2

FURTHER DETAILS ON PROCEDURES FOR THE MASS BALANCE ADJUSTMENT

The polynomial fitted to winds at each level was expressed in Eq. 3.15 as

$$ {}^{l}P_{n}(x_j) = \sum_{i=1}^{n(l)} a_{il}\, x_j^{n-1} \qquad \ldots (A2.1) $$

It is required to choose the coefficients a_{il} so as to minimise in a least squares sense, the difference between the observed data and its polynomial approximation under the constraint of Eq. 3.14. Such problems are treated in numerical analysis text books such as Rust and Burrus (1972).

The terms of Eq. A2.1 can be written in matrix notation as

$$ \underline{W} = P\underline{A} \qquad \ldots (A2.2) $$

where P is a matrix whose terms are powers of x_j having M^{*} x L rows and NL columns where $NL = \sum_{l=1}^{L} n(l)$. $\underline{A}$ is a vector of the coefficients a_{il}.

The function S to be minimised is then given by

$$ S = (\underline{V} - P\underline{A})^{T} (\underline{V} - P\underline{A}) \qquad \ldots (A2.3) $$

where $\underline{V}$ is the vector of observed winds and the suffix T denotes the transpose of the matrix.

The equation of constraint can be expressed as

$$ H\underline{A} = \underline{\alpha} \qquad \ldots (A2.4) $$

A set of Lagrangian undertermined multipliers is introduced and the new function to be minimised is

$$ S = (\underline{V} - P\underline{A})^{T} (\underline{V} - P\underline{A}) + (H\underline{A} - \underline{\alpha})^{T} \underline{\lambda} \qquad \ldots (A2.5) $$

This is equivalent to Eq. 3.16 although a little more general in that there can be more than one constraint. In the mass balance problem, there is only one equation of constraint, making $\underline{\alpha}$ a constant and requiring only a single undetermined multiplier.

At the minimum of S, all the partial derivatives with respect to the independent variables $\underline{A}$ and $\underline{\alpha}$ are zero.

i.e. $$\partial S/\partial \underline{A} = -2P^T\underline{V} + 2P^TP\underline{A} + H^T\underline{\lambda} = 0 \qquad \ldots (A2.6)$$

$$\partial S/\partial \underline{\lambda} = H\underline{A} - \underline{\alpha} = 0 \qquad \ldots (A2.7)$$

Writing $\underline{\lambda} = 2\underline{\mu}$, the final equations expressed in matrix notation are

$$\begin{pmatrix} P^TP & H^T \\ H & 0 \end{pmatrix} \begin{pmatrix} \underline{A} \\ \underline{\mu} \end{pmatrix} = \begin{pmatrix} P^T\underline{V} \\ \underline{\alpha} \end{pmatrix} \qquad \ldots (A2.8)$$

This is a linear set of equations of the form $B\underline{X} = \underline{Y}$. The matrix B is square and symmetric, depending only on the spacing of the stations and the degree of the approximating polynomial at each level. The vector $\underline{Y}$ on the right hand side is derived from the observed wind data and the required constant α. Numerical techniques can be used to solve for the vector $\underline{X}$, which yields the vector of coefficients $\underline{A}$. This can then be substituted in Eq. A2.2 to derive the adjusted wind components.

The procedure requires significant computer time as even for 6 stations with 10 levels, B is a 61 x 61 matrix if N=M-1 at each level.

To prevent the matrices being ill-conditioned the components of the matrix all need to be of approximately the same order of magnitude. It was found necessary to normalise the horizontal and vertical weighting coefficients W_j and F_1 in Eq. 3.16.

Gruber and O'Brien (1968) suggest that if the data at a given level are regarded as reliable, then that level can be retained unaltered by making the polynomial of degree M at that level. This was attempted, but the matrix proved algorithmically singular if this was done even for one level.

The result quoted in Eq. 3.17 is suggested by the result found by O'Brien (1970) who used the same approach to determine the values of vertical velocity derived from an input field of observed divergences subject to the constraint of zero mass balance over a large region as in the above problem. The values of vertical velocity at any location were regarded as independent. O'Brien showed analytically for the case of uniform horizontal and vertical spacing that to satisfy the constraint, least squares minimisation required a uniform adjustment at each level and each station. For non-uniform spacing the result of Eq. 3.17 is obtained. This suggests that when N=M-1, giving N unknowns a_{il} and N equations at each level, there are enough degrees of freedom for the values at each station to be independent, and that the problem then becomes equivalent to that treated by O'Brien.